INFORMATION TO USERS

This manuscript has been reproduced from the microfilm master. UMI films the text directly from the original or copy submitted. Thus, some thesis and dissertation copies are in typewriter face, while others may be from any type of computer printer.

The quality of this reproduction is dependent upon the quality of the copy submitted. Broken or indistinct print, colored or poor quality illustrations and photographs, print bleedthrough, substandard margins, and improper alignment can adversely affect reproduction.

In the unlikely event that the author did not send UMI a complete manuscript and there are missing pages, these will be noted. Also, if unauthorized copyright material had to be removed, a note will indicate the deletion.

Oversize materials (e.g., maps, drawings, charts) are reproduced by sectioning the original, beginning at the upper left-hand corner and continuing from left to right in equal sections with small overlaps. Each original is also photographed in one exposure and is included in reduced form at the back of the book.

Photographs included in the original manuscript have been reproduced xerographically in this copy. Higher quality 6" x 9" black and white photographic prints are available for any photographs or illustrations appearing in this copy for an additional charge. Contact UMI directly to order.

UMI

A Bell & Howell Information Company
300 North Zeeb Road, Ann Arbor MI 48106-1346 USA
313/761-4700 800/521-0600

Selective Vulnerability and Mechanism of Degeneration in a Mouse Model of Amyotrophic Lateral Sclerosis

by

Brett M. Morrison

A dissertation submitted to the Graduate Faculty in Biomedical Sciences in partial fulfillment of the requirements for the degree of Doctor of Philosophy, The City University of New York

1998

This manuscript has been read and accepted for the Graduate Faculty in Biomedical Sciences in satisfaction of the dissertation requirement for the degree of Doctor of Philosophy

4/20/98
Date

Mariann Blum, Ph.D.
Chair of Examining Committee

4/27/98
Date

Terry A. Krulwich, Ph.D.
Executive Officer

John H. Morrison, Ph.D.

George W. Huntley, Ph.D.

Robert A. Lazzarini, Ph.D.

John Q. Trojanowski, M.D., Ph.D.

Supervisory Committee

The City University of New York

Abstract

Selective Vulnerability and Mechanism of Degeneration in a Mouse Model of Amyotrophic Lateral Sclerosis

by

Brett M. Morrison

Advisor: John H. Morrison, Ph.D.

Transgenic mice with a mutation in the superoxide dismutase (SOD-1) gene, corresponding to a mutation observed in familial amyotrophic lateral sclerosis (ALS), display progressive loss of motor function and provide a valuable model of ALS. Several mechanisms of degeneration have been proposed, including alterations of neurofilament and increased intracellular calcium related to excitotoxicity. We hypothesize that a neurochemical profile exists that renders specific subpopulations of neurons vulnerable to these degenerative mechanisms, and that this vulnerability profile will shed light on these mechanisms.

SOD-1 transgenic mice develop loss of motor neurons and interneurons, somatic accumulations of neurofilament, and astrocytosis in the spinal cord coincident with the onset of symptoms. The neuron loss is less than 50% in endstage SOD-1 transgenic mice, and we were interested in whether specific proteins localize preferentially to vulnerable or non-vulnerable neurons. Two proteins hypothesized to play a role in the pathogenesis of ALS are calbindin and neurofilament. We found that calbindin-immunoreactive neurons do not degenerate in SOD-1 transgenic mice, suggesting that elevated intracellular calcium, perhaps secondary to excitotoxicity, may be a component of the mechanism of ALS degeneration. In contrast to calbindin, neurofilament is present within a vulnerable pop-

ulation of neurons, and the magnitude of both motor neuron and interneuron loss is predicted by the percentage of these neuronal populations that contain neurofilament. These results suggest that the neurochemical profile (i.e., presence of neurofilament and absence of calbindin) of a neuron is a more dominant determinant of vulnerability than connectivity.

The absence of GluR2 from AMPA receptors on motor neurons may contribute to their excitotoxic degeneration, as AMPA receptors that lack GluR2 are calcium-permeable. We determined, however, that there is no correlation between vulnerability and the presence or absence of GluR2 in the spinal cord. In addition, we also found that the cellular and synaptic distribution of GluR2 is unaltered in SOD-1 transgenic mice. Therefore, GluR2 does not appear to be a determinant of cellular vulnerability, nor does the disruption of GluR2 appear to be a component of the mechanism of degeneration in this model of ALS.

Acknowledgments

This thesis could not have been completed without the assistance of numerous individuals. The ones named here are only the tip of the iceberg, and for all those not mentioned, thank you for your support and assistance. Special thanks to:

Dr. John Morrison (one last time, "no relation"). I couldn't have designed a mentor more suited to my style. You somehow manage to provide great support and guidance, while allowing me the scientific freedom to define my own research path. You have always treated me more as a peer than a student, and your advice and guidance on matters both scientific and personal have allowed me to mature as a scientist.

Dr. Mariann Blum, collaborator and Western blot tutor, who provided me with a lab away from lab, and never seemed to tire of my requests for advice. I learned a great deal in your lab and thank you for the experience.

Drs. John Trojanowski, Robert Lazzarini, George Huntley, Patrick Hof, Jim Roberts, Arthur Cederbaum, Dennis Healy, and Marilyn McGinnis for serving on my various committees and giving freely of their time and advice.

Dr. Jon Gordon for creating and maintaining the SOD-1 transgenic mice, without which there would be no thesis.

The past and present members of the Morrison and Blum laboratories, Fishberg Research Center, and Neurobiology of Aging for making my graduate school experience not only educational, but enjoyable as well. Specifically, thanks to Dr. Adam Gazzaley for numerous insightful lunch conversations and for providing me a glimpse of the path ahead, and to Bill Janssen for his expertise in electron microscopy and his infinite supply of amusing stories. Also, I thank Phil Mulieri, Angela Ho, Michelle Adams, Jen Coleman, and John Tullai for their support and friendship.

My family for providing me with a foundation of love and support that has made all my successes possible.

My wife Kristy, who has assisted me in more ways than I have the words (or the space) to describe. Whether I needed encouragement, a sounding board for ideas, or a friend with whom to celebrate, you were always up to the task. For this and so much more, thank you.

Table of Contents

List of Tables

List of Figures

List of Abbreviations

ALS	amyotrophic lateral sclerosis
AMPA	α-amino-3-hydroxy-5-methyl-4-isoxazole propionic acid
CB	calbindin
CR	calretinin
DMPO	5,5'-dimethyl-1-pyrroline *N*-oxide
ER	endoplasmic reticulum
GABA	gamma-aminobutyric acid
GFAP	glial fibrillary acidic protein
KARS	lysyl-tRNA synthetase
KSP	lysine-serine-proline
MB	maleate buffer
NFP	neurofilament protein
NFP-H	neurofilament protein-heavy chain
NFP-L	neurofilament protein-light chain
NFP-M	neurofilament protein-medium chain
NGS	normal goat serum
NMDA	N-methyl-D-aspartate
PBN	N-*tert*-butyl-α–phenylnitrone
PBS	phosphate buffered saline
PV	parvalbumin
SOD-1	Cu^{2+}/Zn^{2+} superoxide dismutase
TBS	tris buffered saline
TRAP	translocon-associated protein delta
UA	uranyl acetate

Chapter One

Introduction

ALS is a common neurologic disease with an annual incidence rate of approximately 1 in 100,000 (Adams et al., 1997). There are both sporadic and familial forms of the disease, with familial ALS accounting for approximately 5% of cases. The symptoms and pathology of patients with the familial form of ALS are identical to those of patients with the sporadic form, which suggests that the mechanisms of neurodegeneration for sporadic and familial ALS share common components. The early symptoms of ALS are muscle atrophy, weakness, and fasciculations. The disease progresses over an average of five years, leading to paralysis and premature death (Tandan, 1994; Adams et al., 1997). Pathologically, ALS is characterized by extensive loss of spinal, brainstem, and cortical motor neurons, corticospinal tract degeneration, somatic and axonal inclusions of aberrant neurofilament proteins, reactive astrocytosis, and atrophy of ventral roots (Hirano et al., 1967; Hirano, 1991; Leigh and Swash, 1991). The genetic linkage of mutations in the Cu^{2+}/Zn^{2+} superoxide dismutase (SOD-1) gene with the development of familial ALS revealed the first factor causally related to the disease (Rosen et al., 1993), and provided investigators with a starting point for hypotheses about the mechanisms of degeneration in ALS.

SOD-1 and SOD-1 Transgenic Mice

SOD-1 is a protein which is highly expressed in virtually all cells of the body, and is present within the cytoplasm of both neuronal and non-neuronal cells in the central nervous system (Pardo et al., 1995). The main enzymatic function of SOD-1 is the clearance of superoxide radical through the following chemical reaction:

$$2O_2^{\bullet -} + 2H^+ \rightarrow H_2O_2 + O_2$$

The reaction is catalyzed by the Cu^{2+} in the active site of the protein (Fridovich, 1974). Superoxide radical is a reactive intermediate formed from the reduction of O_2, and must

be cleared to prevent it from oxidizing proteins or peroxidizing lipids (Halliwell et al., 1992; Olanow and Arendash, 1994). A change in the enzymatic function of SOD-1 could therefore have devastating effects on the cellular environment.

Following the genetic linkage of mutations in the SOD-1 gene with the development of familial ALS (Rosen et al., 1993), alterations in the enzymatic function of SOD-1 were hypothesized to be involved in the pathogenesis of ALS. Since the initial report of mutant SOD-1, approximately 50 mutations of the SOD-1 gene, most of which result in the substitution of one amino acid, have been found in patients with familial ALS; and together, these mutations account for approximately 20% of all familial ALS cases (Siddique and Deng, 1996). The mutant forms of SOD-1 have several properties that differ from wild-type SOD-1. Many, but not all, mutations have reduced SOD-1 enzymatic activity (Borchelt et al., 1994; Nishida et al., 1994; Tsuda et al., 1994; Fujii et al., 1995), and all examined SOD-1 mutants are less stable than wild-type SOD-1, with half-lives ranging from 25 to 66% of the wild-type SOD-1 half-life (Borchelt et al., 1994). The combination of reduced specific activity and reduced SOD-1 protein, due to reduced half-life, likely explains the consistently lower SOD-1 enzymatic activity in red blood cells from ALS patients with mutations in SOD-1 (Deng et al., 1993). Interestingly, however, the SOD-1 mutants are not totally inactive. Many SOD-1 mutants retain full specific activity, including the G37R (Borchelt et al., 1994) and G85R (Fujii et al., 1995) SOD-1 mutants, and yet still cause disease in both humans and transgenic mice. In addition, virtually all SOD-1 mutants can rescue yeast lacking SOD-1 and return them to a wild-type phenotype (Nishida et al., 1994; Rabizadeh et al., 1995). The altered function of mutant SOD-1 is obviously complex; and to investigate these mutations *in vivo*, transgenic mice have been engineered that express several of the mutant forms of SOD-1 implicated in human ALS (Gurney et al., 1994; Ripps et al., 1995; Wong et al., 1995; Bruijn et al., 1997b).

Three transgenic mice that have mutations in the human SOD-1 gene [*i.e.*, G37R

(Wong et al., 1995), G93A (Gurney et al., 1994), and G85R (Bruijn et al., 1997b) substitutions] and one with a mutation in the mouse gene, G86R (Ripps et al., 1995), have been produced to date. All of the SOD-1 transgenic mice are normal at birth, but begin to develop motor dysfunction at 3 to 9 months of age, which progresses rapidly from limb weakness to total paralysis and premature death. The age of onset of these symptoms appears to correlate with the level of mutant SOD-1 expressed, as high expressors have an earlier onset of symptoms than low expressors (Wong et al., 1995; Bruijn et al., 1997b; Dal Canto and Gurney, 1997). Pathologically, all SOD-1 transgenic mice have spinal motor neuron degeneration and alterations in cytoskeletal components. Particular SOD-1 transgenic mice have other important pathologic changes, and a detailed comparison of the behavioral and pathologic alterations in the SOD-1 transgenic mice is presented in chapter five.

In order to minimize the anatomical differences between mouse and human, and study a system that clearly demonstrated pathologic degeneration in SOD-1 transgenic mice, we have focused our research on determining the factors that contribute to the selective vulnerability and mechanisms of degeneration of spinal cord neurons. The mechanism of degeneration initiated by mutated SOD-1 is unknown, but clues may be provided both by mechanisms of ALS degeneration that were proposed before the linkage of mutant SOD-1 with familial ALS and by biochemical investigations of the mutant forms of SOD-1. These mechanisms include the disruption of neurofilament, excitotoxicity, and unshielding of the copper ion in mutant SOD-1.

Disruption of Neurofilament

Neurofilaments are a class of neuron-specific intermediate filaments, whose major function appears to be to provide support and structure for axons (Shaw, 1991). Neurofilaments can be composed of the three neurofilament protein (NFP) subunits, as

well as α-internexin, peripherin, and nestin (Lee and Cleveland, 1996). The NFP subunits are named for their relative molecular weights: light (NFP-L), medium (NFP-M), and heavy (NFP-H), and these subunits appear to assemble as heteropolymers of NFP-L and either NFP-M or -H to form neurofilaments (Lee et al., 1993). In contrast, α-internexin can assemble into homopolymers. The assembly characteristics of peripherin and nestin have not been adequately investigated. Each NFP subunit, as well as α-internexin, peripherin, and nestin subunits, is composed of three domains: an amino-terminus head, a central rod, and a carboxy-terminus tail. The central rod domain appears to be the site at which subunits interact to form mature 10 nm neurofibrils. The tail domain is also an important modulator of NFP function, as the tail domains of NFP-M and NFP-H subunits contain multiple Lys-Ser-Pro (KSP) repeats that are sites of phosphorylation by serine / threonine kinases (Lee et al., 1988; Miyasaka et al., 1993; Shetty et al., 1993). These tail domains appear to project radially from the mature neurofibril, modulating both the spacing between adjacent neurofibrils and the interactions with other proteins (Miyasaka et al., 1993). Phosphorylation of the tail domains of NFP-M and NFP-H appears to cause greater spacing, while dephosphorylation leads to tighter packing (Matus, 1988; Nixon and Sihag, 1991). NFP is expressed in its nonphosphorylated form, which is found primarily in somata and proximal dendrites (Sternberger and Sternberger, 1983; Lee et al., 1987), and becomes phosphorylated as it is transported into the axon. Phosphorylated NFP is therefore found primarily in the axon of healthy neurons (Sternberger and Sternberger, 1983; Lee et al., 1987; Dahl et al., 1988; Matus, 1988). The role of NFP in neuronal physiology has been investigated by studying animals that are naturally deficient in NFP [*i.e.*, *quiverer* quail (Yamasaki et al., 1992; Ohara et al., 1993)]. Reduced expression of all NFP subunits, as occurs in the *quiverer* quail mutant, leads to a reduction in the caliber of neuronal axons. This atrophy of axons reduces the velocity of electrical transduction down the axon, adversely affecting neurotransmission (Sakaguchi et al., 1993). In addition, motor neuron axons in the rat spinal cord with less NFP have smaller

axon diameters and axotomy caused a reduction in both the quantity of NFP and the diameter of axons (Hoffman et al., 1984; Hoffman et al., 1985; Hoffman et al., 1987). These results provide further support for the hypothesized role of NFP in determining axon diameter. Rather than stemming from its role in normal physiology, however, much of the interest in NFP has arisen because of alterations of NFP found in neurodegenerative disorders.

From the earliest silver stains (Switzer, 1993), NFP has been implicated in neurodegenerative diseases, including Alzheimer's disease, Pick's disease, Parkinson's disease, and especially ALS (Leigh et al., 1989; Griffin et al., 1991; Trojanowski et al., 1993). The pathologic changes of these diseases all involve the accumulation of NFP as inclusions in the somata, dendrites, or axons, although the specific regional distribution and appearance of these inclusions differ. These inclusions can take the form of neurofibrillary tangles in Alzheimer's disease (Vickers et al., 1992; Trojanowski et al., 1993; Hof and Morrison, 1994), Lewy bodies in Parkinson's disease (Trojanowski et al., 1993), or Pick bodies in Pick's disease (Perry et al., 1987a; Ulrich et al., 1987). Specifically, the NFP pathology of ALS is characterized by accumulations of phosphorylated NFP in somata and by spheroids, which are large axonal swellings that contain NFP (Manetto et al., 1988; Munoz et al., 1988; Mizusawa et al., 1989; Troost et al., 1992). As discussed previously, phosphorylated NFP is present primarily in the axons of healthy neurons. Therefore, the accumulation of phosphorylated NFP in somata suggests a disruption in the processing and/or transport of NFP in ALS patients. Moreover, in studies of the neocortex of patients with Alzheimer's disease (Hof et al., 1990) and the retina in a primate model of glaucoma (Vickers et al., 1995b), neurons containing high amounts of somatic nonphosphorylated NFP were found to have increased vulnerability compared to neurons that were not immunoreactive for nonphosphorylated NFP. These studies suggest that disruption of NFP is a unifying feature of several neurodegenerative diseases, and may play an important role in the mechanism of degeneration of several different neuron populations.

The most direct evidence that alterations in NFP can cause pathologic changes and degeneration in neurons comes from transgenic mice with alterations in genes encoding NFP. Transgenic mice that overexpress mouse NFP-L (Xu et al., 1993) or human NFP-H (Côté et al., 1993), as well as transgenic mice that express a mutant form of NFP-L (Lee et al., 1994), display motor neuron pathology, and are excellent models of ALS. Several other NFP transgenic mice have CNS pathology, but do not accurately model ALS because motor neurons do not preferentially degenerate (Eyer and Peterson, 1994; Vickers et al., 1994; Vickers et al., 1995a; Tu et al., 1997). Of the three NFP mutations that induce motor neuron dysfunction in transgenic mice, two are caused by an increase in a NFP subunit [*i.e.*, mouse NFP-L (Xu et al., 1993) and human NFP-H (Côté et al., 1993)], and one by a mutation in NFP-L that was designed to disrupt the assembly of NFP fibrils (Lee et al., 1994). All of these genetic alterations of NFP lead to hypoactive mice with severe muscle atrophy and intracellular inclusions composed of the modified NFP subunit and other NFP subunits. The severity of pathology and the mechanisms by which these alterations in NFP lead to motor dysfunction may be quite dissimilar, however. In both of the mice with overexpression of NFP, the stoichiometry between NFP subunits is altered, either increasing or decreasing the ratio of NFP-L to NFP-H. This altered stoichiometry is likely the cause of NFP inclusions, since somatic and axonal NFP inclusions are also caused by the overexpressing mouse NFP-H (Marszalek et al., 1996) or by increasing the ratio of NFP-H to NFP-L in a cell culture of dorsal root ganglion neurons (Straube-West et al., 1996). Reduced rates of axonal transport may be responsible for the NFP inclusions, as Collard et al. (1995) found reduced rates of axonal transport in mice overexpressing the human NFP-H gene. Pathologic accumulations of NFP appears to be the NFP alteration that is least toxic to motor neurons, however, since transgenic mice that overexpress mouse NFP-H display NFP accumulations without any other signs of motor neuron dysfunction (Marszalek et al., 1996). In contrast, transgenic mice overexpressing mouse NFP-L and human NFP-H display a moderate level of motor neuron dysfunction

(Côté et al., 1993; Xu et al., 1993).

Mouse NFP-L and human NFP-H overexpressor transgenic mice also have NFP inclusions, which are likely caused by the alteration in subunit stoichiometry; but in addition, they show behavioral deficits in motor function, muscle atrophy, and motor axon degeneration. The additional toxicity in these transgenic mice may not be caused by the same mechanism as the inclusions. In the case of transgenic mice overexpressing human NFP-H, some property of the human NFP-H, perhaps the increased number of KSP phosphorylation sites, is likely the cause of the increased toxicity in these mice as compared to mice overexpressing mouse NFP-H. The increased phosphorylation state of human NFP-H may lead to abnormal binding of human NFP-H to transport machinery or abnormal spacing of NFP in mouse axons. The mechanism by which overexpression of mouse NFP-L leads to increased toxicity as compared to overexpressed mouse NFP-H is unclear. One possible explanation is that NFP-L forms the core of the NFP fibril, and alterations in this subunit may be particularly damaging to the organization of NFP within neurons.

The most neurotoxic alteration in NFP that has been modeled in transgenic mice is the assembly disrupting mutation of NFP-L (Lee et al., 1994). This is the only NFP transgenic that has loss of motor neurons and reactive astrocytosis. These mutations in NFP-L cause NFP inclusions without disturbing the stoichiometry of the NFP subunits, as all subunits show reduced expression. Rather than altering the ratio of the three NFP subunits, these mutations may alter the ratio of free NFP subunits to subunits associated with a neurofibril. The exact mechanism by which this mutation in NFP-L leads to motor neuron damage is unknown, but investigating this mechanism should be a priority because of the similarity in pathologic profiles between this transgenic mouse and patients with ALS.

These results in transgenic mice suggest that NFP alterations may be mechanistically involved in the motor neuron degeneration of at least a subset of ALS patients, perhaps through disruption of axonal transport, and not merely a hallmark of its pathology. This is also supported by the report of point mutations and deletions in the carboxy-ter-

minus of the NFP-H gene in some patients with sporadic ALS (Figlewicz et al., 1994). Other investigators looking for these disruptions have been unsuccessful (Rooke et al., 1996; Vechio et al., 1996), but if true, these mutations provide a direct link between alterations in NFP and ALS. We hypothesize that disruptions of NFP are a component of the pathology in SOD-1 transgenic mice. In addition, if NFP is an important component of the mechanism of degeneration in SOD-1 transgenic mice, then neurons that contain detectable levels of NFP should be preferentially vulnerable to degeneration.

Excitotoxicity

Excitotoxicity has been implicated as a mechanism of degeneration in numerous neurodegenerative disorders (Meldrum and Garthwaite, 1990). In general, excitotoxicity appears to result from over-activation of glutamate receptors, including both NMDA (Choi et al., 1988) and non-NMDA (Weiss and Choi, 1991) receptors, in response to glutamate or other excitatory amino acids. This over-activation results in an influx of sodium initially, which causes cell swelling, and then calcium, which appears to be necessary for neurodegeneration (Choi, 1987). Increased intracellular calcium activates many of the cell's degradative enzymes, including phospholipases that break down cell membranes, proteases that break down cytoskeletal and membrane proteins, and endonucleases that cleave chromatin into fragments, any of which could be responsible for excitotoxic degeneration [See (Orrenius et al., 1992) for review]. Observations of increased glutamate levels in plasma (Plaitakis and Caroscio, 1987) and cerebrospinal fluid (Rothstein et al., 1989), and decreased glutamate in the spinal cord parenchyma (Perry et al., 1987b; Plaitakis et al., 1988) of patients with ALS provided the first indication that alterations in glutamate transmission and metabolism may be mechanistically involved in ALS neurodegeneration. The mechanism for these shifts in the distribution of glutamate appears to involve changes in glutamate transporters, which are critical for removing excess glu-

tamate from excitatory synapses. ALS patients have a decrease in both glutamate transporter activity and the amount of a specific glial glutamate transporter, GLT-1, in affected areas of the nervous system like motor cortex and the spinal cord, but not in unaffected areas like the hippocampus and caudate nucleus (Rothstein et al., 1992; Rothstein et al., 1995). Reducing glutamate transporter activity, either by pharmacological antagonists (Rothstein et al., 1993) or anti-sense oligonucleotides (Rothstein et al., 1996), in a spinal cord slice preparation or *in vivo* leads to elevated extracellular glutamate and selective degeneration of spinal motor neurons. This modification of glutamate transporters could account for the observed alterations in glutamate metabolism reported in ALS patients.

Whether or not a particular neuron degenerates following increased synaptic glutamate may depend upon several factors including the potential for binding or sequestering free intracellular calcium, and also the specific glutamate receptors present in excitatory synapses. Cytoplasmic calcium is reduced by transport out of the cell, sequestration within cell organelles including the endoplasmic reticulum, mitochondria, and nucleus, or binding to cytoplasmic proteins (see Carafoli, 1987, and Blaustein, 1988 for reviews). We investigate the third of these mechanisms for reducing free calcium in the cytoplasm, the binding of calcium to cytoplasmic proteins. While many proteins can bind calcium to some extent, the EF-hand family of calcium-binding proteins appears to play the most significant role in buffering calcium in neurons (see Baimbridge et al., 1992 for review). The EF family of calcium-binding proteins can be divided into two large groups, "trigger" and "buffer" proteins. Although they may have some buffering capacities, the major function of trigger calcium-binding proteins is the initiation of other cellular events, including muscle contraction, cell signalling and second messenger cascades. This group of calcium-binding proteins include calmodulin, troponin-C, myosin light chain, and S-100. For the purpose of buffering calcium, the buffer proteins, which include calbindin (CB), calretinin (CR), and parvalbumin (PV), would appear to be more important. Based on their capacity to buffer calcium (Lledo et al., 1992; Chard et al., 1993) and unique distribution in the

nervous system (Hendry et al., 1989; Antal et al., 1990; Celio, 1990; Résibois and Rogers, 1992; Ren and Ruda, 1994), these proteins have been implicated in the specific cellular patterns of vulnerability to excitotoxic events. For the most part, CB, CR, and PV define separate populations of neurons, frequently interneurons, and are usually colocalized with gamma-aminobutyric acid (GABA) (Hendry et al., 1989). In neocortex, for example, CB localizes primarily to double bouquet cells, CR to bipolar cells, and PV to basket and chandelier cells (Andressen et al., 1993). All of these morphologically-defined cells are GABAergic interneurons, and in the vast majority of cases, these calcium-binding proteins do not colocalize with each other. In respect to buffering capacity, calcium-binding proteins have been shown to attenuate elevated intracellular Ca^{2+} (Lledo et al., 1992; Chard et al., 1993) and protect cells against toxicity resulting from elevated Ca^{2+} induced by glutamate receptor agonists, calcium ionophores, or serum from ALS patients in neuronal cultures (Mattson et al., 1991; Lukas and Jones, 1994; Ho et al., 1996). The ability to reduce intracellular calcium has been shown to result not only from their capacity to buffer intracellular Ca^{2+}, but also from their ability to reduce calcium flux through voltage-dependent calcium channels (Lledo et al., 1992). Because calcium-binding proteins appear to define neuron populations that are resistant to neurodegeneration in both AD (Ferrer et al., 1991; Hof et al., 1991; Hof and Morrison, 1991; Fonseca et al., 1993; Hof et al., 1993; Fonseca and Soriano, 1995) and ALS (Alexianu et al., 1994), we hypothesize that, as is the case for neocortical neurons in AD, the selective distribution of calcium-binding proteins in the ventral horn of the spinal cord will be an important correlate of resistance to degeneration in SOD-1 transgenic mice.

In addition to the presence or absence of calcium-binding proteins, specific neurons in the spinal cord may be selectively vulnerable to excitotoxicity and ALS degeneration due to their unique combination of glutamate receptors. Glutamate receptors fall into two general categories: ionotropic and metabatropic. Ionotropic GluRs have been divided into three pharmacologically defined and functionally distinct classes: α-amino-

3-hydroxy-5-methyl-4-isoxazole propionic acid/low-affinity kainate (AMPA), high-affinity kainate (kainate), and *N*-methyl-D-aspartate (NMDA) receptors. Recent studies have implicated AMPA and/or kainate receptors, but not NMDA receptors, in the excitotoxic mechanism of degeneration in ALS. First, neurodegeneration following inhibition of glutamate transporters is attenuated by antagonists to non-NMDA glutamate receptors, but not by antagonists to NMDA receptors (Rothstein et al., 1993). Second, motor neurons *in vivo* (Ikonomidou et al., 1996) and *in vitro* (Carriedo et al., 1996) are preferentially vulnerable to kainate toxicity, which would activate both AMPA and kainate receptors, but not NMDA toxicity. Non-NMDA glutamate receptors appear to be pentamers, composed of some combination of GluR1-4 for AMPA receptors and GluR5-7 and KA-1 and -2 for kainate receptors (Hollmann et al., 1989; Boulter et al., 1990; Keinanen et al., 1990; Brose et al., 1994). Certain subunit transcripts are subject to RNA editing, a mechanism which strongly influences properties such as Ca^{2+} permeability and rectification characteristics, with GluR2 almost completely edited to the arginine codon at the Q/R site (Sommer et al., 1991; Puchalski et al., 1994). When present in the AMPA receptor, edited GluR2 dominates the Ca^{2+} permeability and current-voltage characteristics, and as such, AMPA receptors that contain GluR2 do not flux Ca^{2+} (Geiger et al., 1995).

Given the importance of Ca^{2+} flux in the excitotoxic mechanism of neurodegeneration, many investigators have proposed that motor neurons are selectively vulnerable to excitotoxicity, and perhaps also in ALS, due to a lack of GluR2. Support for this hypothesis comes almost exclusively from spinal cord culture experiments. In response to kainate administration, *in vitro* motor neurons appear to be permeable to cobalt, a reflection of Ca^{2+} flux, and undergo degeneration (Carriedo et al., 1996). In addition, a recently presented abstract concluded that *in vitro* motor neurons lack GluR2 immunoreactivity (Bar-Peled et al., 1997). These *in vitro* studies contradict a number of studies that have demonstrated that motor neurons *in situ* contain GluR2 mRNA (Sato et al., 1993; Tolle et al., 1993; Jakowec et al., 1995a; Jakowec et al., 1995b; Tolle et al., 1995; Temkin

et al., 1997). The recent development of a GluR2-specific monoclonal antibody allows a definitive answer as to the presence or absence of GluR2 from motor neurons. We hypothesize that the distribution of GluR2 in the mouse spinal cord may correlate with the neurons that are resistant to degeneration in SOD-1 transgenic mice, and that there may by an alteration in the distribution or intensity of GluR2 immunoreactivity in SOD-1 transgenic mice.

Unshielding of Copper Ion

The biochemical disturbance resulting from the presence of the mutant SOD-1 protein is unknown. Initially, it was presumed that the mutations observed in ALS damaged cells by reduced clearance and subsequent accumulation of superoxide radical (Deng et al., 1993). However, as discussed previously, this does not appear to be the case. Rather, the mutated protein appears to have acquired a novel function, termed a gain-of-function mutation. Although the exact nature of this novel function is unknown, the locations of the mutations in SOD-1 suggest that unshielding of the copper ion may be involved (Deng et al., 1993; Wiedau-Pazos et al., 1996). Increased access of substrates to the copper would lead to increased catalysis of several reactions including oxidation of proteins by hydrogen peroxide and nitration of tyrosines by peroxynitrite (Beckman et al., 1993).

In the presence of hydrogen peroxide, wild-type SOD-1 catalyzes the formation of hydroxyl radical and the subsequent oxidation of proteins (Yim et al., 1990). This was determined *in vitro* by measuring the oxidation of 5,5'-dimethyl-1-pyrroline *N*-oxide (DMPO) and N-*tert*-butyl-α–phenylnitrone (PBN) by electron paramagnetic resonance. DMPO and PBN are spin traps, and the formation of DMPO-OH and PBN-OH in the presence of hydrogen peroxide and SOD-1 suggests that free hydroxyl radical can be produced by this reaction. The rate of this reaction with wild-type SOD-1 is quite slow, like-

ly due to the low affinity of wild-type SOD-1 for hydrogen peroxide. In contrast to wild-type SOD-1, mutant forms of SOD-1 (*i.e.*, G93A and A4V) have a greater affinity for hydrogen peroxide and catalyze the formation of DMPO-OH to a greater extent than wild-type SOD-1 (Wiedau-Pazos et al., 1996; Yim et al., 1996). Although the baseline peroxidase activity of wild-type SOD-1 is unaffected by copper chelation, the increased peroxidase activity of mutant SOD-1 is markedly attenuated by these chelators, suggesting that the copper ion in mutant SOD-1 is more exposed than in wild-type SOD-1. The spin trap DMPO is obviously not the intracellular target of this increased peroxidase activity. The actual target has not been determined, though the neurotransmitter glutamate has been shown to be altered by this reaction (Yim et al., 1996). Due to the importance of glutamate in the excitotoxic mechanism of degeneration, this putative alteration is extremely important and may provide an explanation for the similarities between the degeneration induced by mutations in SOD-1 and excitotoxic agents.

The second gain-of-function that has been demonstrated for mutant SOD-1 is increased nitration of tyrosines by peroxynitrite. Peroxynitrite ($ONOO^-$), which is a potent oxidant, is produced from nitric oxide ($^{\bullet}NO$) and superoxide ($O_2^{-\bullet}$) radicals, and breaks down into hydroxyl radical and $^{\bullet}NO_2$ (Beckman et al., 1992), which can nitrate phenols like tyrosine molecules in a reaction catalyzed by SOD-1 (Ischiropoulos et al., 1992; van der Vliet et al., 1995). Therefore, the degree to which certain proteins are nitrated is important as an indicator of both peroxynitrite breakdown and potential targets of this breakdown. Free nitrotyrosines can be measured by mass spectroscopy, while nitrotyrosines incorporated into proteins are evaluated by an antibody against nitrotyrosine. Utilizing these techniques, increased free nitrotyrosines have been reported in the spinal cord of ALS patients (Beal et al., 1997), G93A SOD-1 transgenic mice (Ferrante et al., 1997), and G37R SOD-1 transgenic mice (Bruijn et al., 1997a). In addition, increased immunoreactivity for nitrotyrosines have been observed in ALS patients (Abe et al., 1995; Beal et al., 1997) and G93A mice (Ferrante et al., 1997), but not in G37R SOD-1 trans-

genic mice (Bruijn et al., 1997a). At this time, however, no specific proteins have been demonstrated to have increased nitration of tyrosines in either ALS patients or SOD-1 transgenic mice. These *in vivo* results are supported by indirect *in vitro* evidence that mutant SOD-1 catalyzes the nitration of tyrosines to a greater extent than wild-type SOD-1 (Crow et al., 1997a). In this study, mutant SOD-1 is found to have reduced affinity for zinc, and therefore mutant forms of SOD-1 are more likely to lack zinc in the presence of zinc chelators. SOD-1 that lacks zinc catalyzes peroxynitrite-mediated tyrosine nitration to a greater extent than SOD-1 that contains a divalent cation in the zinc site. These investigators never directly demonstrate that mutant SOD-1 has an altered capacity for catalyzing the nitration of tyrosines, but only suggest this indirectly. Taken together, however, these studies suggest that mutant SOD-1 catalyzes the nitration of tyrosines in the presence of peroxynitrite to a greater extent than wild-type SOD-1, and this gain-of-function may be an important component of neurodegeneration in SOD-1 transgenic mice and ALS. If there is increased nitration of tyrosines, it is critical to determine which proteins accumulate nitrotyrosines and whether this alteration affects their function. Proteins that are particularly long-lived, like NFP and other components of the cytoskeleton (Shaw, 1991), may be particularly prone to accumulating nitrotyrosines over time. In fact, Crow et al. (1997b) has demonstrated that SOD-1 in the presence of peroxynitrite catalyzes the nitration of tyrosines on NFP-L, and that this nitration disrupts the assembly of NFP fibrils. Given the previously described importance of NFP in the pathology and perhaps the mechanism of ALS degeneration, these proteins are especially interesting targets for investigation.

Chapter Two

A Quantitative Immunocytochemical Analysis of the Spinal Cord in G86R Superoxide Dismutase Transgenic Mice: Neurochemical Correlates of Selective Vulnerability

Reprinted with permission from John Wiley and Sons

Morrison, B.M., J.W. Gordon, M.E. Ripps, and J.H. Morrison (1996) Quantitative immunocytochemical analysis of the spinal cord in G86R superoxide dismutase transgenic mice: neurochemical correlates of selective vulnerability. J. Comp. Neurol. *373*:619-631

Abstract

Transgenic mice with a G86R mutation in the mouse SOD-1 gene, corresponding to a mutation observed in familial ALS, display progressive loss of motor function and provide a valuable model of ALS. The pathology in the spinal cords of these mice was evaluated to determine whether there are chemically-identified populations of neurons that are either highly vulnerable or resistant to degeneration. Qualitatively, there were phosphorylated NFP-immunoreactive inclusions and a pronounced loss of motor neurons in the ventral horn of the spinal cord, without the presence of vacuoles, which have been reported in other SOD-1 transgenic mice. Neuron counts from SOD-1 and control spinal cords revealed that the percentage loss of NFP-, choline acetyltransferase (ChAT)-, and CR-immunoreactive neurons was greater than the percentage loss of total neurons, suggesting that these neuronal groups are particularly vulnerable in SOD-1 transgenic mice. In contrast, CB-containing neurons did not degenerate significantly, and represent a protected population of neurons. Quantitative double-labeling experiments suggested that the vulnerability of ChAT- and CR-immunoreactive neurons is primarily due to the presence of NFP within a subset of these neurons, which degenerated preferentially to ChAT- and CR-immunoreactive neurons that did not colocalize with NFP. Our findings suggest that NFP, which has been demonstrated previously to be mechanistically involved in motor neuron degeneration, may also be important in the mechanism of degeneration that is initiated by the SOD-1 mutation.

Introduction

ALS is a neurologic disease characterized by progressive upper and lower motor neuron degeneration frequently resulting in death within five years of onset (Leigh and Ray-Chaudhuri, 1994; Tandan, 1994). The genetic linkage of point mutations in the SOD-1 gene with familial ALS provided the first biochemical factor causally related to the disease (Rosen et al., 1993). Transgenic mice with SOD-1 mutations, corresponding to those observed in familial ALS (Gurney et al., 1994; Ripps et al., 1995; Wong et al., 1995), display a marked loss of motor neurons in the spinal cord and brainstem, argyrophilic dystrophic neurites, and progressive loss of motor function resulting in paralysis and premature death, consistent with reported findings in ALS patients (Hirano et al., 1967; Hirano, 1991; Leigh and Swash, 1991). The phenotypic and pathologic alterations observed in these mice occur despite normal or increased levels of SOD-1 enzymatic activity (Gurney et al., 1994; Ripps et al., 1995; Wong et al., 1995), suggesting that the mutations induce a novel function, not possessed by the wild-type protein. The mechanism of degeneration initiated by mutated SOD-1 is unknown, but clues may be provided by other proposed mechanisms of ALS neurodegeneration.

Two other mechanistic links to neurodegeneration that may be relevant to ALS involve NFP (Leigh et al., 1989; Griffin et al., 1991; Brady, 1993) and intracellular calcium (Krieger et al., 1994). NFP is an intermediate filament that consists of three subunits, heavy (H), medium (M), and light (L), and is important for maintaining axonal diameter and transport (Hoffman and Lasek, 1975; Hoffman et al., 1984; Trojanowski et al., 1986; Shaw, 1991). NFP is not present within all neurons (Fisher and Boycott, 1974; Sharp et al., 1982), and antibodies to NFP immunocytochemically label distinct neuronal populations (Campbell and Morrison, 1989; Vickers and Costa, 1992; Hof and Morrison, 1995), some of which are highly vulnerable to neurodegeneration (Morrison et al., 1987; Hof et

al., 1990). NFP exists in both phosphorylated and nonphosphorylated forms that have differential distributions within neurons, with phosphorylated NFP primarily present within axons and nonphosphorylated NFP present in somata and dendrites (Sternberger and Sternberger, 1983; Lee et al., 1987; Dahl et al., 1988; Matus, 1988). Although accumulation of phosphorylated NFP in somatic and axonal inclusions is a pathologic hallmark of ALS (Manetto et al., 1988; Munoz et al., 1988; Mizusawa et al., 1989; Troost et al., 1992) and has been observed in SOD-1 transgenic mice (Wong et al., 1995; Tu et al., 1996), the most direct evidence that NFP is mechanistically involved in motor neuron degeneration comes from transgenic mice (Côté et al., 1993; Xu et al., 1993; Lee et al., 1994) and ALS patients (Figlewicz et al., 1994) with NFP mutations. Another proposed mechanism of degeneration in ALS is increased intracellular calcium secondary to autoimmune antibodies against voltage-dependent calcium channels (Smith et al., 1992; Appel et al., 1993; Kimura et al., 1994; Smith et al., 1994) or the over-activation of glutamatergic transmission (Rothstein et al., 1990; Plaitakis, 1991; Weiss and Choi, 1991; Rothstein et al., 1993). CR and CB are two of the calcium-binding proteins that buffer intracellular calcium (Mattson et al., 1991; Lledo et al., 1992; Chard et al., 1993; Lukas and Jones, 1994), and therefore may modulate intracellular calcium levels. CR and CB are present in only a subset of neurons (Hendry et al., 1989; Antal et al., 1990; Celio, 1990; Resibois and Rogers, 1992; Andressen et al., 1993; Ren and Ruda, 1994), which, in contrast to NFP-containing neurons, are resistant to neurodegeneration (Hof et al., 1993; Alexianu et al., 1994). Evidence for the SOD-1, NFP, and calcium hypotheses of neurodegeneration have been obtained in separate model systems. In ALS patients, each of these mechanisms may exist separately in distinct populations of ALS patients, or they may interact as individual components of a general mechanism of degeneration in ALS.

The cellular pattern of degeneration in ALS exhibits a striking degree of selectivity in respect to the neuron classes affected. SOD-1 is fairly ubiquitous and unlikely to account directly for the selective vulnerability (Pardo et al., 1995), however, if the NFP

and calcium-related mechanisms of degeneration are relevant in SOD-1 transgenic mice, it would be reflected in the neuronal populations vulnerable to the SOD-1 mutation. We investigated this possibility by quantifying the cell loss of neurons immunoreactive for NFP, CR, CB, and ChAT, a selective marker in the spinal cord for motor neurons. In addition, quantitative colocalization studies were performed to determine which characteristics were dominant in conferring vulnerability or protection in neurons that were immunoreactive for more than one marker.

Materials and Methods

Animals and tissue processing. Transgenic mice with a G86R mutation of the mouse SOD-1 gene and control FVB littermates, described previously (Ripps et al., 1995), were used in this study. SOD-1 transgenic mice and age-matched controls were sacrificed when the transgenic mice displayed almost total paralysis of both forelimbs and hindlimbs, at 92 to 118 days. Mice were deeply anesthetized with an equal mixture of ketamine (100 mg/ml) and xylazine (20 mg/ml), and then perfused transcardially with cold 1% paraformaldehyde in 0.1 M phosphate buffered saline (PBS), pH 7.2, for 1 minute followed by cold 4% paraformaldehyde in PBS for 10 minutes. The spinal cords were rapidly removed, blocked coronally, and post-fixed in 4% paraformaldehyde in PBS for 6 hours. Blocks were cryoprotected in 30% sucrose for 24 hours, and sectioned on a cryostat at 40 μm.

Immunocytochemistry and histochemistry. Parallel series of sections were collected for immunocytochemistry and Nissl staining (cresyl violet). Tissue sections for single label immunocytochemistry were incubated overnight at 4°C in one of the following: 1) monoclonal antibody (mouse IgG) to nonphosphorylated epitopes on NFP-H (SMI-32, Sternberger Monoclonals, Baltimore, MD) diluted to 1:10,000 in 0.01 M PBS, pH 7.2,

containing 0.3% Triton-X 100 and 0.5 mg/ml bovine serum albumin (diluent); 2) monoclonal antibody (mouse IgG) to phosphorylated epitopes on NFP-M and NFP-H (SMI-31, Sternberger Monoclonals) diluted to 1:10,000 in diluent; 3) polyclonal antibody (goat IgG) to ChAT diluted to 1:200 in diluent (Chemicon, Temecula, CA); 4) polyclonal antibody (rabbit IgG) to CR diluted to 1:2500 in diluent (SWant, Bellinzona, Switzerland); 5) polyclonal antibody (rabbit IgG) to CB diluted to 1:3500 in diluent (SWant). The sections were then processed by the avidin-biotin-peroxidase method with Vectastain ABC kits (Vector Laboratories, Burlingame, CA) and 3,3'-diaminobenzidine.

Sections for double label immunocytochemistry were incubated overnight at 4°C in one of the following: 1) mouse monoclonal SMI-32 (1:5000) and goat polyclonal anti-ChAT (1:100); 2) mouse monoclonal SMI-32 (1:5000) and rabbit polyclonal anti-CR (1:2500); 3) mouse monoclonal SMI-32 (1:5000) and rabbit polyclonal anti-CB (1:2500); 4) goat polyclonal anti-ChAT (1:50) and rabbit polyclonal anti-CR (1:2000); 5) goat polyclonal anti-ChAT (1:50) and rabbit polyclonal anti-CB (1:2500). The sections double-labeled with SMI-32 and anti-ChAT were washed following the primary antibody incubation, incubated for 2 hours in 1:200 FITC-conjugated horse anti-mouse IgG (Vector Laboratories) and 1:200 biotinylated rabbit anti-goat IgG (Vector Laboratories), washed, and then incubated for 1 hour in 1:200 Texas Red streptavidin (Amersham, Arlington Heights, IL). The sections incubated in SMI-32 and anti-CR or anti-CB were washed after primary incubation, incubated for 2 hours in 1:200 FITC-conjugated horse anti-mouse IgG and 1:300 biotinylated goat anti-rabbit IgG (Vector Laboratories), washed, and then incubated for 1 hour in Texas Red streptavidin. The sections incubated in anti-ChAT and anti-CR or anti-CB were washed following the primary incubation, incubated for 1 hour in 1:200 biotinylated horse anti-goat IgG (Vector Laboratories), washed, incubated for 1 hour in 1:200 FITC-conjugated goat anti-rabbit IgG, washed, and then incubated for 1 hour in Texas Red streptavidin. The species specificity of the secondary antibodies was verified by omitting one or both of the primary antibodies.

Stereology. The total number of Nissl-stained, nonphosphorylated NFP-immunoreactive, ChAT-immunoreactive, CR-immunoreactive, or CB-immunoreactive neurons were counted bilaterally in the ventral horn of both the cervical (C5→C7) and lumbar (L1→L3) spinal cord enlargements from four control and four SOD-1 mutant transgenic mice using the optical fractionator (West et al., 1991). Throughout the experiment, the investigator was blinded to transgene status. The number of phosphorylated NFP-immunoreactive neurons was not determined because there was little, if any, staining of cell bodies with SMI-31. For this analysis, a Zeiss Axiophot photomicroscope with a Zeiss Plan-Neofluar 63x oil objective and a CCD camera was used to generate digitized images that were collected and analyzed on a Macintosh 840AV computer using custom-made data analysis software [NeuroZoom; developed in collaboration with the Scripps Research Institute, La Jolla, CA (Young et al., 1995; Bloom et al., 1997)]. The technique used for counting neurons in this study, the optical fractionator, provides an unbiased estimate of cell number, and it relies on random, systematic sampling from a known fraction of a structure's total volume (Bjugn, 1993; West, 1993). The mathematical formula that determines total cell number is as follows:

$$N = \sum Q^{-} \; x \; 1/ssf \; x \; 1/asf \; x \; t/h$$

where $\sum Q^{-}$ is the total number of neurons counted, *ssf* is the section sampling fraction, *asf* is the areal sampling fraction, t is the thickness, and h is the height of disector. The formula consists of three sampling fractions multiplied by the number of neurons counted in the sampled volume. The first fraction, *1/ssf*, is the total number of sections in the spinal cord enlargements divided by the number of sections analyzed, which was a 1:40 series for the Nissl-stained sections and a 1:20 series for the immunocytochemically stained sections. The extent of the spinal cord enlargements was determined visually by comparing Nissl-stained sections from each animal with the mouse atlas of Sidman et al. (1971). The second fraction, *1/asf*, is the area of the x,y step divided by the area of the counting frame,

i.e., the percentage of each section's surface area that is sampled. For this study, the percentage of the area sampled was 27.54%. On each section, the area ventral to the most dorsal extent of the central canal, including laminae VII, VIII, IX, and X, was designated ventral horn. A counting frame was positioned in a random position in the ventral horn and then moved systematically, with the aid of NeuroZoom, in the x and y directions across the ventral horn, sampling a given percentage of the area. The number of cells that were completely contained within this counting frame, or that crossed one of the two arbitrarily-defined accepted sides of the frame, were counted. The third fraction, *t/h*, is the total thickness of the section divided by the depth counted. Because the stains did not penetrate through the entire depth of the section, cells were only counted in the portion of the section where staining was visible, and this depth was divided by the total thickness of the section, measureable by visualizing staining on both surfaces.

To avoid double counting neurons with unusual shapes, Nissl-stained, ChAT-immunoreactive, and NFP-immunoreactive cells were only counted when their nuclei were visualized, which only occurred in one focal plane. The nuclei of CR- and CB-immunoreactive cells were not as easily distinguished. Fortunately, these immunoreactive cells were not densely packed in the ventral horn of the spinal cord, and therefore, careful examination of each cell prior to counting was sufficient to avoid repeatedly counting the same neuron. In addition, neurons were differentiated from non-neuronal cells, including glia, in the Nissl stain by the exclusion of cells that did not have a clearly defined nucleus, cytoplasm, and a prominent nucleolus. These criteria have been used for neuron counts in the spinal cord by other investigators (Bjugn, 1993; Bjugn and Gundersen, 1993b), and although some small neurons may be excluded, these criteria should reliably exclude all non-neuronal cells.

Quantification of double-labeling. For each double-labeling combination, a 1:40 series from both cervical and lumbar enlargements from the same animals used in the optical

fractionator technique was immunostained, as described above, and analyzed on a Zeiss Axiophot fluorescent microscope using a Zeiss Plan-Neofluar 40x objective. The percentage of double-labeling was determined by examining each immunofluorescent cell in the ventral horn with filters that allow either FITC wavelengths or Texas Red wavelengths, but not both, to pass, and counting single-labeled versus double-labeled cells. While the quantitative analysis was carried out on the Zeiss Axiophot, high resolution qualitative analysis and photomicrographs of fluorescent double-labeled sections were made on a Zeiss laser scanning confocal microscope 410 with a Zeiss Plan-Neofluar 63x oil objective. The z-axis resolution of the confocal microscope allowed for a more definitive differentiation between cytoplasmic colocalization and superimposition of independently labeled profiles. The photomicrographs were obtained by optimizing the contrast and brightness settings on the confocal microscope for each fluorescent signal, scanning the images with the two line average function, and then overlaying and pseudo-coloring the images from each double-labeling pair. The confocal images were imported into Adobe Photoshop 3.0, where they were sized and labeled.

Statistical analysis The total number of cells for each histological or immunocytochemical stain in control and SOD-1 transgenic mice were compared with a two-sided Student's *t* test. The percentage colocalization of ChAT, CR, and CB immunoreactivity with non-phosphorylated NFP and ChAT immunoreactivity in control and SOD-1 transgenic spinal cords were also compared with a two-sided Student's *t* test.

Results

Qualitative observations. As compared to controls, the ventral horn of the cervical and lumbar enlargements of SOD-1 transgenic mice exhibited an apparent decrease in the number of Nissl-stained neurons, while the dorsal horn appeared to be unaffected (Fig. 2-

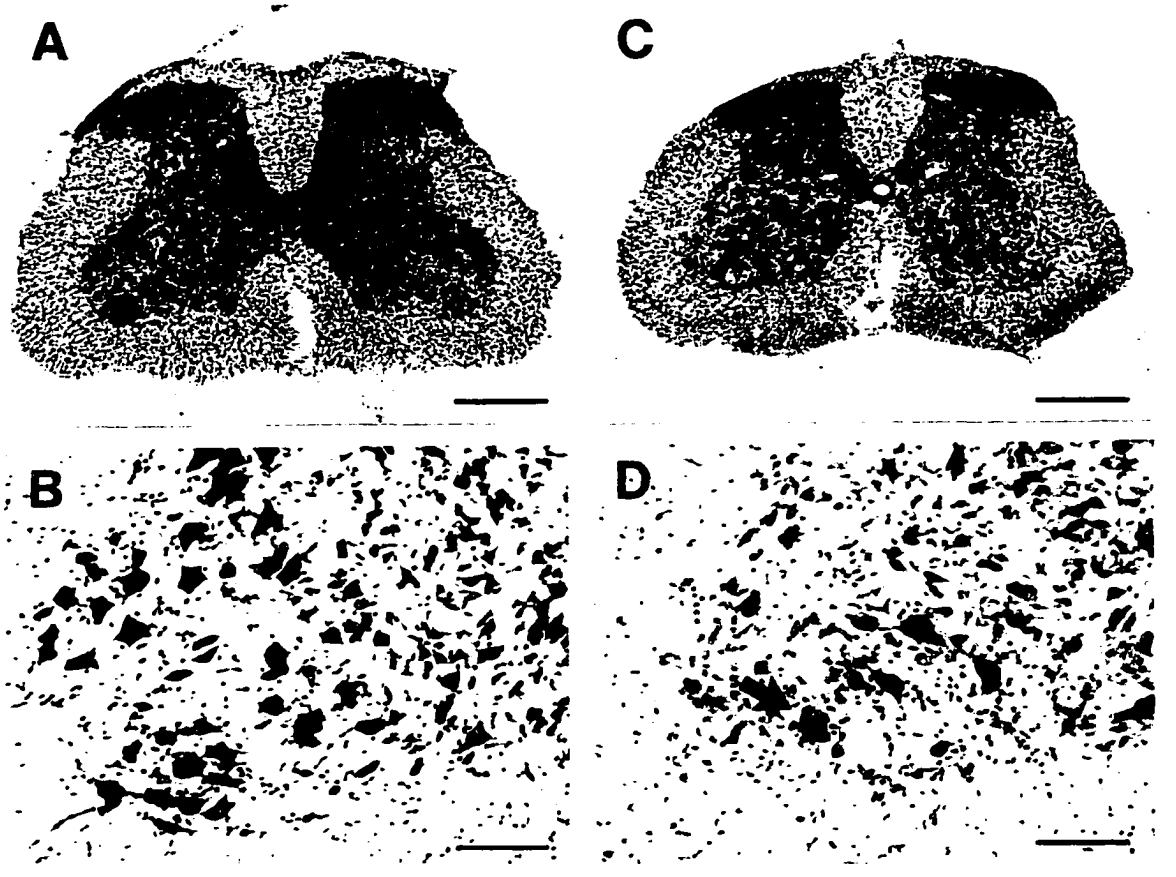

Figure 2-1. Nissl-stained sections from the lumbar spinal cord enlargement of control (A and B) and SOD-1 transgenic (C and D) mice. Neuron density in the ventral horn of the SOD-1 transgenic mouse (C) is reduced compared to the control mouse (A). In contrast, the dorsal horn of the SOD-1 transgenic mouse appears to be unaffected. B and D are higher power photomicrographs of the ventral horn in control and SOD-1 transgenic mice, respectively. The reduction in cell number in the SOD-1 transgenic mouse is clearly evident at this magnification, and a morphologically abnormal cell (*arrow*) that is likely undergoing degeneration is present as well. Scale bars: A and C, 400 μm; B and D, 100 μm.

1A-D). In addition to neuron loss, both enlargements of the SOD-1 transgenic spinal cord exhibited morphologically abnormal cells that appeared to be undergoing degeneration (Fig. 2-1D). We did not observe vacuolization in the spinal cord of endstage SOD-1 transgenic mice, or in mice at earlier time points, such as 30 and 60 day old mice (data not shown).

Immunoreactivity for nonphosphorylated NFP in cervical and lumbar spinal cord enlargements of control mice was present not only in many of the somata and processes of the large motor neurons in the ventrolateral horn (Fig. 2-2A, *arrows*), but also in the soma of neurons positioned more medially (Fig. 2-2A, *arrowheads*). There was little non-

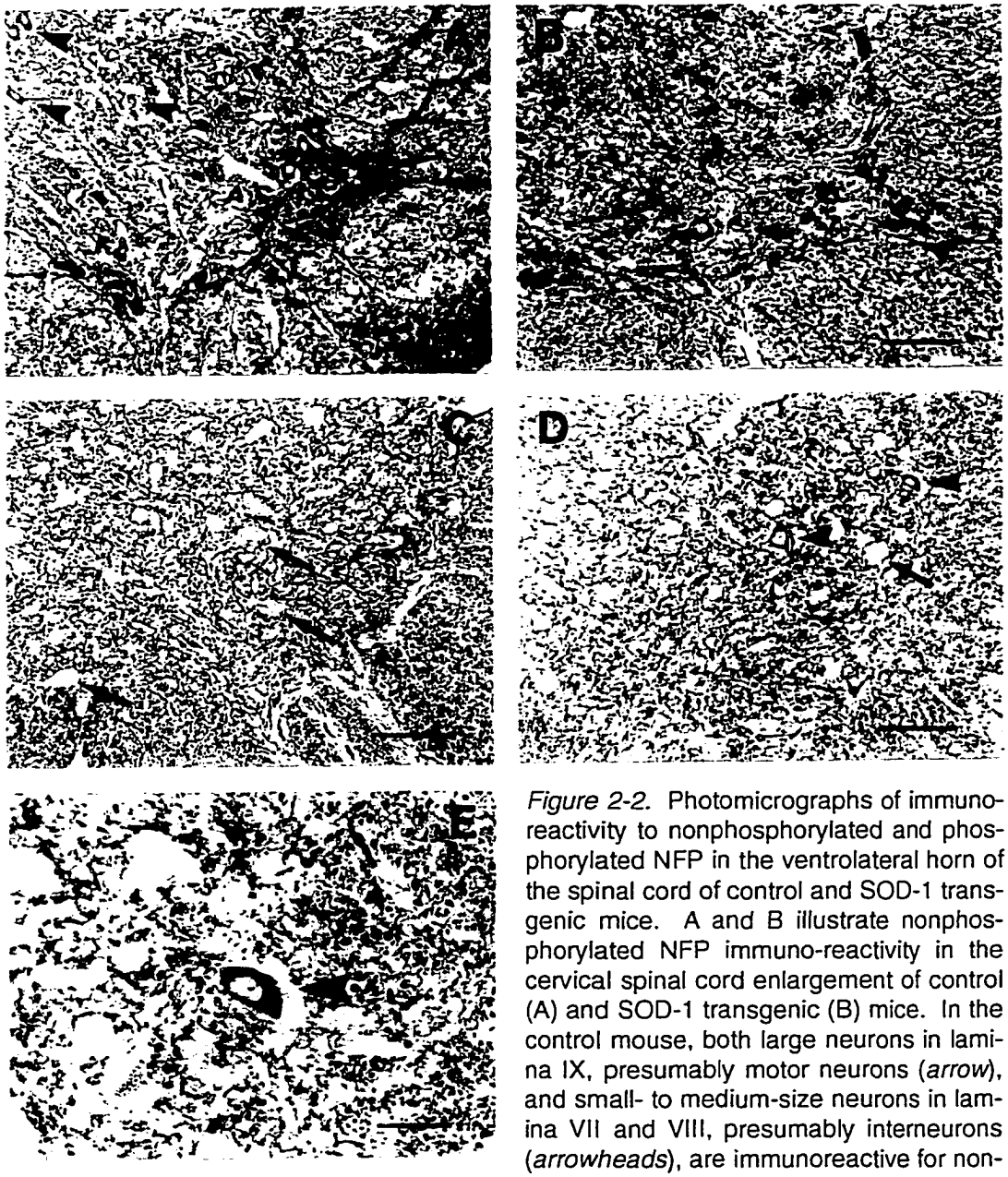

Figure 2-2. Photomicrographs of immunoreactivity to nonphosphorylated and phosphorylated NFP in the ventrolateral horn of the spinal cord of control and SOD-1 transgenic mice. A and B illustrate nonphosphorylated NFP immuno-reactivity in the cervical spinal cord enlargement of control (A) and SOD-1 transgenic (B) mice. In the control mouse, both large neurons in lamina IX, presumably motor neurons (*arrow*), and small- to medium-size neurons in lamina VII and VIII, presumably interneurons (*arrowheads*), are immunoreactive for nonphosphorylated NFP. Note the reduction in nonphosphorylated NFP-immunoreactive neurons and neuropil in the SOD-1 transgenic mouse. C - E illustrate phosphorylated NFP immunoreactivity in the lumbar spinal cord enlargement of control (C) and SOD-1 transgenic (D and E) mice. The neuropil of the control spinal cord (C) was immunoreactive without staining of the somata (*arrows*). The neuropil of the SOD-1 transgenic mouse (D) was also immunoreactive to phosphorylated NFP and many of the somata were unstained (*arrow*), however, occasional somata were heavily immunoreactive to phosphorylated NFP (D and E, *arrowheads*). Scale bars: A-D, 100 μm; E, 30 μm.

phosphorylated NFP immunoreactivity in the dorsal horn. In SOD-1 transgenic mice, there was a decrease in nonphosphorylated NFP immunoreactivity in the ventral horn grey matter, due to decreased somatic and dendritic staining (Fig. 2-2B). No nonphosphory-

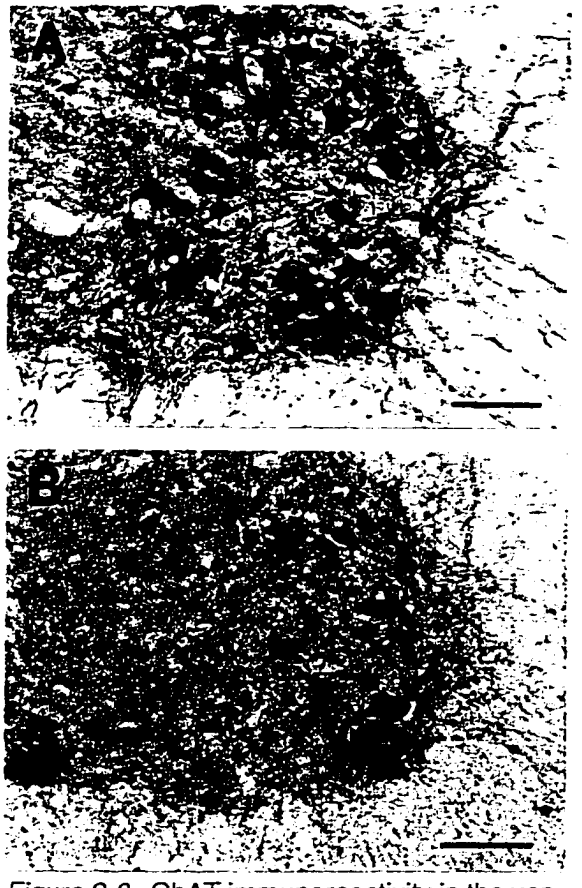

Figure 2-3. ChAT immunoreactivity in the ventrolateral horn of the lumbar spinal cord enlargement of control (A) and SOD-1 transgenic (B) mice. ChAT-immunoreactive neurons are present primarily in the ventrolateral horn of both control and SOD-1 transgenic mice. The number of ChAT-immunoreactive neurons in the SOD-1 transgenic mouse is markedly reduced, as compared to the control mouse. Scale bars: 100 μm.

lated NFP inclusion bodies were observed in either the somata or axons of SOD-1 transgenic mice.

Immunocytochemistry for phosphorylated NFP in the cervical and lumbar spinal cord enlargements revealed a very different pattern (Fig. 2-2C-E). The neuropil in the grey matter of control mice was immunoreactive for phosphorylated NFP, without labeling of the cell bodies (Fig. 2-2C). In SOD-1 transgenic mice, the neuropil in the grey matter was also immunoreactive for phosphorylated NFP (Fig. 2-2D,E). In contrast to controls, however, occasional cell bodies located in the ventral and intermediate zones of the spinal cord were intensely immunoreactive for phosphorylated NFP .

The antibody to ChAT, which labels cholinergic neurons, appeared to be specific for motor neurons in the ventral horn, and it stained both cell bodies and proximal dendrites in the spinal cord of control mice (Fig. 2-3A). The majority of the stained neurons were in the ventrolateral motor neuron groups, and the distribution pattern was similar to that revealed by retrograde labeling of spinal motor neurons (McHanwell and Biscoe, 1981; Nicolopoulos-Stournaras and Iles, 1983). In the spinal cord of SOD-1 transgenic mice, there was a marked reduction in the number of ChAT-immunoreactive neurons (Fig. 2-3B).

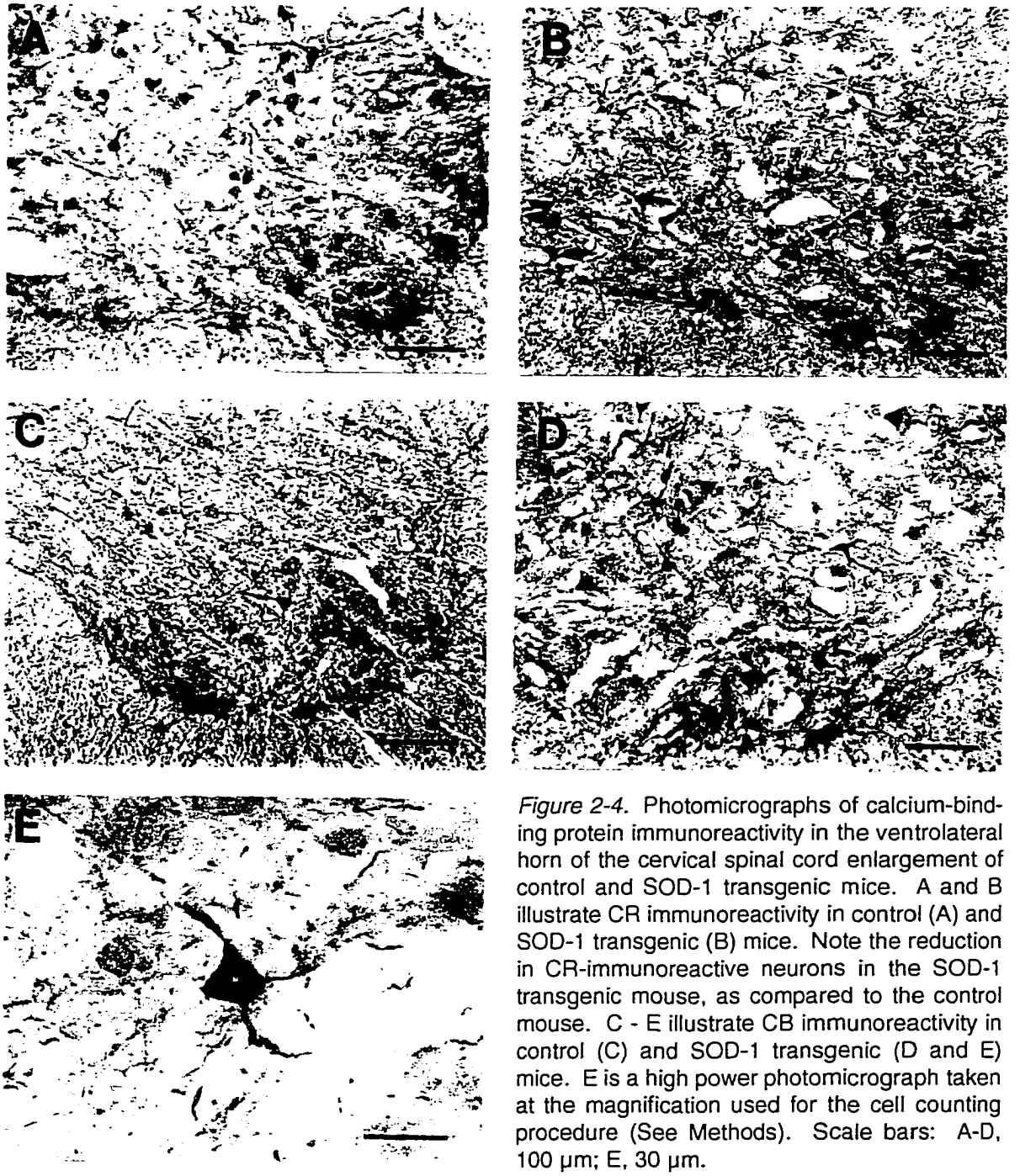

Figure 2-4. Photomicrographs of calcium-binding protein immunoreactivity in the ventrolateral horn of the cervical spinal cord enlargement of control and SOD-1 transgenic mice. A and B illustrate CR immunoreactivity in control (A) and SOD-1 transgenic (B) mice. Note the reduction in CR-immunoreactive neurons in the SOD-1 transgenic mouse, as compared to the control mouse. C - E illustrate CB immunoreactivity in control (C) and SOD-1 transgenic (D and E) mice. E is a high power photomicrograph taken at the magnification used for the cell counting procedure (See Methods). Scale bars: A-D, 100 μm; E, 30 μm.

Based on their distribution in the ventral horn of the spinal cord, the antibodies to the calcium-binding proteins, CR and CB, appeared to stain interneurons (Fig. 2-4A-E). There was little immunoreactivity for these proteins in the ventrolateral motor neuron pools, with most of the CR- or CB-immunoreactive neurons located just medial and dor-

sal to the motor neuron pools. Although it is possible that some of the CR- and CB-immunoreactive neurons are the cells of origin for the ascending spinal pathways, such as the spinothalamic tract, anatomic evidence suggests that spinothalamic neurons are not a major component of the CR- and CB-immunoreactive neurons that we counted in the ventral horn of the spinal cord because very few spinothalamic neurons are located in the ventral or intermediate zones, and the majority of spinothalamic neurons located in these zones are present in rostral cervical regions (C1→C4) (Granum, 1986; Burstein et al., 1990). Although both CR and CB immunoreactivity were present primarily in interneurons, many of the immunoreactive cells were quite large. There appeared to be a reduction in CR-immunoreactive neurons in SOD-1 transgenic mice (Fig. 2-4A,B), but qualitative assessments of changes in CB-immunoreactive neurons were difficult because these cells were less numerous and more widely dispersed than the other immunoreactive cell populations (Fig. 2-4C-E).

Cell counts. The optical fractionator provided an unbiased estimate of neuron number in the cervical and lumbar enlargements of the spinal cord. Although there was a slightly greater percentage loss of neurons in the cervical than in the lumbar enlargement, the patterns of cell loss were identical in both regions, and all statistical analyses were performed on the sum of the cell counts in the cervical and lumbar enlargements (Fig. 2-5). There was a significant reduction in Nissl-stained ($p < 0.05$), nonphosphorylated NFP-immunoreactive ($p < 0.05$), ChAT-immunoreactive ($p < 0.01$), and CR-immunoreactive ($p < 0.01$) neurons in the SOD-1 transgenics, as compared to controls . There was no significant reduction in the number of CB-immunoreactive cells ($p = 0.22$). The percent change (number of cells in SOD - number of cells in control / number of cells in control) was calculated for each population of labeled cells. There was a greater percent decline in the number of neurons immunoreactive for nonphosphorylated NFP (-50.7%), ChAT (-43.6%), and CR (-40.0%) than for Nissl-stained neurons (-35.2%), which labeled the total

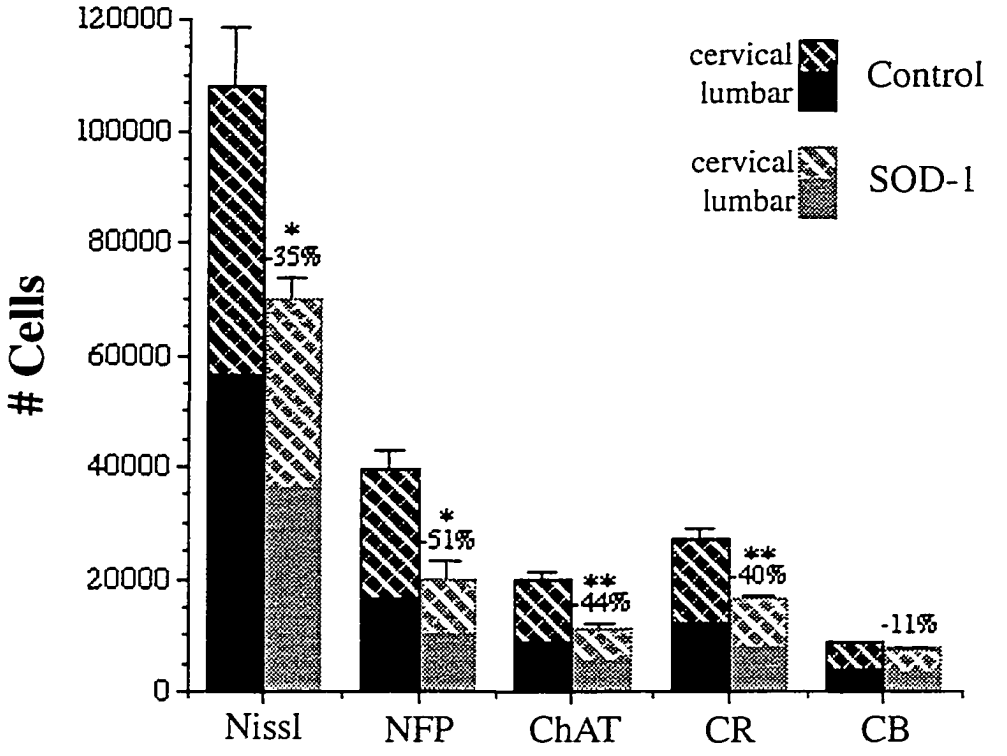

Figure 2-5. Histogram of the number of Nissl- and immunocytochemically-stained neurons in the cervical and lumbar enlargements of control and SOD-1 trangenic mice. The hatched bars represent the cervical enlargement, and the solid bars the lumbar enlargement. The number of neurons in the cervical and lumbar enlargement were summed, and the mean number of summed neurons for control (n = 4) and SOD-1 transgenic (n = 4) mice are represented in this histogram. The error bars represent the S.E.M. for the summed neuronal counts. For each stain, the percent change in the number of neurons is given for the mean of the summed neurons (See Results). In addition, a two-sided Student's *t* test was used to compare the summed values of control and SOD-1 transgenic mice (*, $p < 0.05$; **, $p < 0.01$).

neuronal population present within the ventral horn, suggesting that these immunocytochemically-defined neurons have a greater probability of degenerating, and thus are more vulnerable, than the total neuronal population.

Double-labeling. The described immunoreactive neuronal populations are not mutually exclusive, and therefore the contribution to vulnerability or resistance of a given molecule may be misinterpreted or masked by its colocalization with another relevant marker. To investigate the colocalization of immunoreactivity in these cell groups, a series of sections from control and SOD-1 transgenic mice were double-labeled for several possible combi-

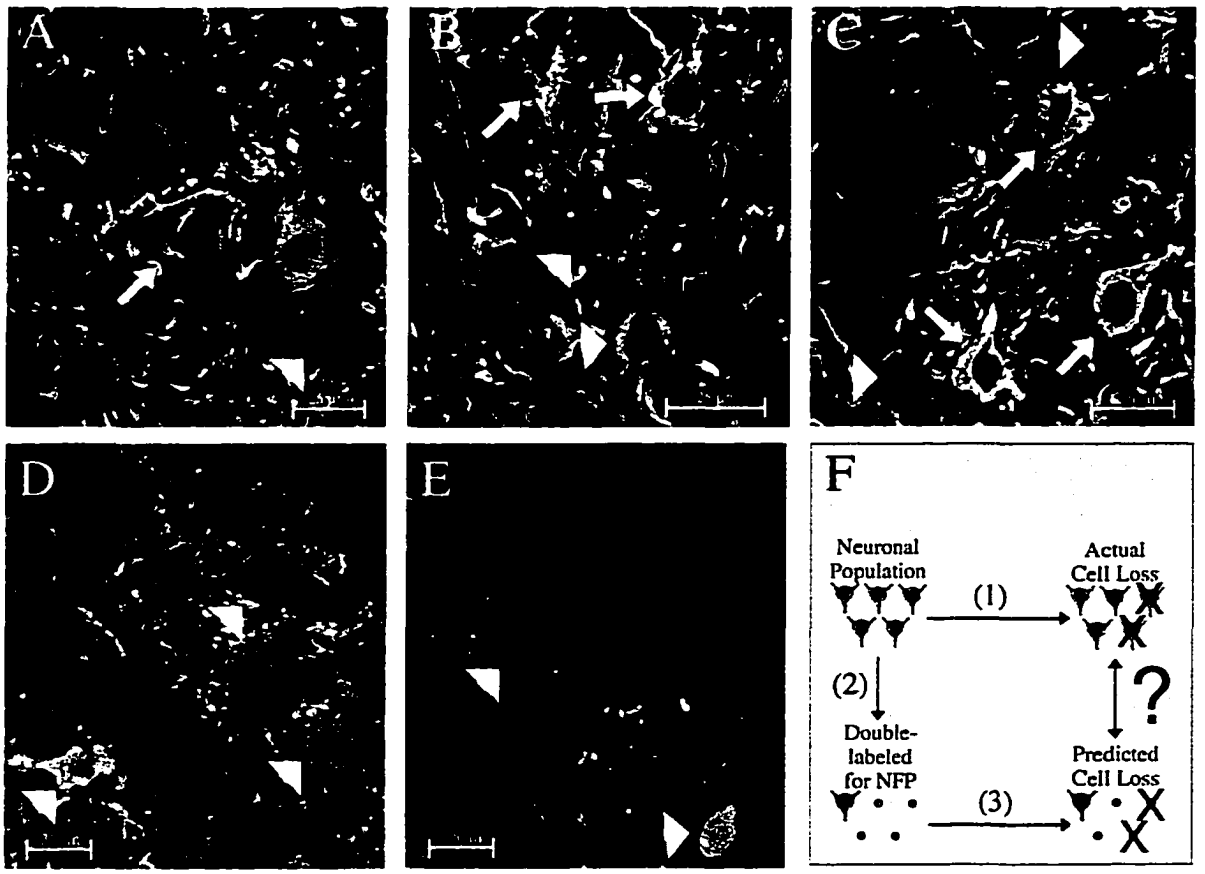

Figure 2-6. Confocal photomicrographs of immunofluorescent double-labeling in the ventral horn of the spinal cord of control mice. For all panels, the arrows refer to double-labeled neurons and the arrowheads to single-labeled neurons. A-C, Double-labeled with nonphosphorylated NFP (in green) and ChAT (A), CR (B), or CB (C), all in red. D and E, Double-labeled with ChAT (in red) and CR (D) or CB (E), both in green. The combination of red and green in double-labeled cells appears yellow. F, Schematic for prediction of cell loss and prediction table. In a given immunocytochemically-defined neuronal population, we observed a specific cell loss, using the optical fractionator, in SOD-1 transgenic mice (1). In this neuronal population, a specific number of neurons are double-labeled for NFP, determined by the total number of neurons in this population multiplied by the percentage double-labeling with NFP (2). Given that the loss of NFP-containing neurons is known, through the cell counting procedures, the number of neurons in this neuronal population that are double-labeled for NFP can be used to predict the cell loss in these neurons (3), and this predicted value compared to the actual cell loss. Scale bars: 25 μm.

nations of immunoreactivity (Fig. 2-6A-E). In control mice, ChAT-, CR-, and CB-immunoreactive cells colocalized with nonphosphorylated NFP to differing degrees (Table 2-1). ChAT-immunoreactive cells showed the greatest degree of colocalization with nonphosphorylated NFP (85.7%; 898/1048), CR-immunoreactive cells a slightly smaller degree of colocalization with NFP (73.8%; 589/798), and CB-immunoreactive

Table 2-1. Percentage colocalization with NFP and ChAT

Immuno-fluorescence	Control	SOD-1
ChAT / NFP	85.7 ± 2.5%	71.3 ± 2.9%
CR / NFP	73.8 ± 2.1%	30.2 ± 4.4%
CB / NFP	39.5 ± 7.0%	39.4 ± 2.0%
CR / ChAT	2.8 ± 0.4%	3.7 ± 1.3%
CB / ChAT	0.3 ± 0.4%	0.3 ± 0.3%

Data are mean percentage of ChAT-, CR-, and CB-immunoreactive neurons that are double-labeled with nonphosphorylated NFP, and mean percentage of CR- and CB-immunoreactive neurons double-labeled with ChAT ± S.E.M. (n = 4).

cells had the smallest degree of colocalization with NFP (39.5%; 151/382). The degree of colocalization of these three markers with nonphosphorylated NFP correlated with their cell loss. ChAT-immunoreactive cells showed the greatest percentage of double-labeling with nonphosphorylated NFP, and their mean cell number was reduced 44% in SOD-1 transgenic mice (See Fig. 2-5). CR-immunoreactive cells had the next greatest percentage of double-labeling with nonphosphorylated NFP, and they had a 40% decline in SOD-1 transgenic mice. CB-immunoreactive cells had the lowest percentage of double-labeling with nonphosphorylated NFP, and an insignificant decline in SOD-1 transgenic mice.

The percentage of ChAT- and CR-immunoreactive neurons that were double-labeled with nonphosphorylated NFP was significantly lower in the spinal cord of SOD-1 transgenics (71.3%; 476/668 and 30.2%; 208/688, respectively) than in controls (85.7% and 73.8%, respectively). If ChAT- and CR-immunoreactive neurons are degenerating independently of their colocalization with nonphosphorylated NFP, then we would expect the percentage double-labeling with nonphosphorylated NFP to be the same in SOD-1

transgenics as in controls. This was not the case, and the reduction in double-labeling with nonphosphorylated NFP in SOD-1 transgenics as compared to controls suggests that non-phosphorylated NFP is preferentially present within the ChAT- and CR-immunoreactive neurons that degenerate. In contrast, CB was colocalized with nonphosphorylated NFP (39.4%; 117/297) in SOD-1 transgenic mice to the same degree as in control animals (39.5%), suggesting that CB-immunoreactive neurons which are also immunoreactive for nonphosphorylated NFP do not preferentially degenerate.

In addition to the colocalization of CR- and CB-immunoreactive neurons with nonphosphorylated NFP, the percentage of CR- and CB-immunoreactive cells that colocalized with ChAT immunoreactivity was also determined (Table 2-1). CR- and CB-immunoreactive cells were for the most part not colocalized with ChAT immunoreactivity in control (2.8%; 22/784 and 0.3%; 1/310, respectively) or SOD-1 transgenic mice (3.7%; 25/660 and 0.3%; 1/339, respectively). The small percentage of CR- and CB-immunoreactive neurons that are double-labeled with ChAT immunoreactivity, less that 4%, is likely within the experimental error of the procedure, supporting the qualitative observation that CR and CB immunoreactivity defines interneuron, not motor neuron, populations.

Predictions of cell loss. Analysis of the cell counts and double-labeling percentages suggests that, with the exception of CB-immunoreactive neurons, immunoreactivity to nonphosphorylated NFP may be a marker for the vulnerable population of neurons. If it is true that the increased vulnerability of ChAT- and CR-immunoreactive cells is due primarily to the presence of nonphosphorylated NFP within these cells, then we should be able to predict the cell loss in these neuronal populations based upon the estimated number of these cells that contain nonphosphorylated NFP in controls and the percent decline of NFP-immunoreactive cells in SOD-1 transgenic mice as compared to controls (Fig. 2-6F). The results of this analysis are shown in Table 2-2. The actual loss of both ChAT-

Table 2-2. Prediction of neuron loss based on immunoreactivity to non-phosphorylated NFP

	Number of immuno-reactive neurons in controls	Percent of neurons double-labeled for NFP	Number of neurons double-labeled for NFP	Predicted loss (51% loss of NFP neurons)	Actual loss (control - SOD-1)
NFP	38,980	100	38,980	19,880	19,880 (0.0% difference)
ChAT	19,233	85.7	16,483	8,406	8,390 (0.2% difference)
CR	26,658	73.8	19,674	10,033	10,655 (5.8% difference)
CB	8,274	39.5	3,268	1,667	927 (44.4% difference)

Based on the number of NFP-, ChAT-, CR-, or CB-immunoreactive neurons in control mice and the percentage of these neurons that are double-labeled with nonphosphorylated NFP, the number of NFP-, ChAT-, CR-, or CB-immunoreactive neurons that are also immunoreactive for nonphosphorylated NFP was estimated (See Table 2-1). The percent change for nonphosphorylated NFP was 51% (See Figure 2-5). Therefore, if the NFP-, ChAT-, CR-, or CB-immunoreactive neurons that are double-labeled for nonphosphorylated NFP-immunoreactive degenerate at this same percentage, then we would predict the loss of the NFP-, ChAT-, CR-, or CB-immunoreactive neurons to be 51% of the number of double-labeled neurons from each immunostained group. This is the predicted loss, and it is compared to the actual loss of neurons for each immunostained group (determined by subtracting the number of neurons in the SOD-1 transgenic mice from the number of neurons in the control mice). The percent difference is calculated by dividing the difference between the predicted and actual losses by the predicted loss. The NFP-immunoreactive group is provided as an example of the extreme case where all of the neurons are immunoreactive for NFP.

and CR-immunoreactive neurons was accurately predicted by their degree of colocalization with nonphosphorylated NFP. In contrast, the actual loss of CB-immunoreactive neurons was not predicted by this group's colocalization. In fact, a greater loss of this population of cells was predicted than actually occurred, suggesting that CB immunoreactivity may define a protected neuronal population.

Discussion

The Nissl- and immunocytochemically-stained neuron counts suggest that nonphosphorylated NFP, ChAT, and CR are markers for neurons that have greater vulnerability than the total neuronal population in the ventral horn of the spinal cord, while CB-immunoreactive neurons have reduced vulnerability. The colocalization studies demon-

strated that the immunostained neuronal groups are not mutually exclusive, and that the dominant marker of neuronal vulnerability is the presence of nonphosphorylated NFP, regardless of whether the neuron is also ChAT- or CR-immunoreactive. This conclusion is supported by the prediction table, where the actual loss of both ChAT- and CR-immunoreactive neurons was accurately predicted by their percent double-labeling with nonphosphorylated NFP in controls. CB-immunoreactive neurons are the exception, appearing to be protected whether or not they also contain nonphosphorylated NFP.

In contrast to what has been reported in at least two other SOD-1 transgenic strains of mice (Dal Canto and Gurney, 1994; Wong et al., 1995), we did not observe vacuolization in SOD-1 transgenic mice of any age. There are numerous differences between our mice and the mice produced by other investigators (*e.g.*, different mutation, insertion of mouse versus human SOD-1 gene, different levels of SOD-1 enzymatic activity). Any of these factors could be responsible for the lack of vacuoles in our mice. In contrast to vacuoles, the pathology in our mice is similar to other SOD-1 transgenic mice (Dal Canto and Gurney, 1994; Wong et al., 1995) in respect to astrogliosis. We observed astrogliosis, using immunocytochemistry for glial fibrillary acidic protein, in fully symptomatic SOD-1 transgenic mice (see Chapter 3 and Morrison et al., 1998). Until the timecourse of this pathology is characterized in presymptomatic mice, it is difficult to determine whether astrogliosis is contributing to the mechanism of neurodegeneration or is involved secondarily in the phagocytosis of debris from neurons that have already degenerated.

Nonphosphorylated NFP accumulations were not observed in the cervical and lumbar spinal cord enlargements of SOD-1 transgenic mice, even though an antibody to nonphosphorylated NFP labeled a highly vulnerable population of neurons. In contrast, an antibody to phosphorylated NFP labeled pathologic accumulations in the cell body of neurons in SOD-1 transgenic mice, which may be the light microscopic equivalent of the 10 nm filament inclusions reported in EM studies of other SOD-1 transgenic mice (Dal Canto and Gurney, 1994; Wong et al., 1995). Similar accumulations of phosphorylated

NFP have been observed in autopsy material from ALS patients (Manetto et al., 1988; Munoz et al., 1988; Mizusawa et al., 1989; Troost et al., 1992). These inclusions are either abnormal accumulations of phosphorylated NFP or abnormal phosphorylation of the nonphosphorylated NFP normally present in the cell body. If the latter is true, this may account for some of the nonphosphorylated NFP-immunoreactive cell loss in SOD-1 transgenic mice. These inclusions are seen in very few cells, however, and would account for little of the nonphosphorylated NFP-immunoreactive cell loss. Phosphorylated NFP inclusions are another link between SOD-1 transgenic mice and ALS, and may provide a marker for the alterations in NFP that contribute to the vulnerability of NFP-immunoreactive neurons in SOD-1 transgenic mice.

Although not previously demonstrated in SOD-1 transgenic mice or in patients with ALS, the heightened vulnerability of nonphosphorylated NFP-immunoreactive neurons is not completely unexpected. Vulnerability of a cortical population of neurons that were immunoreactive for the same epitope of nonphosphorylated NFP was demonstrated quantitatively in Alzheimer's disease brains (Hof et al., 1990). In addition, alterations in the pattern of NFP immunoreactivity were observed in our SOD-1 transgenic mice and in autopsy material from ALS patients (Manetto et al., 1988; Munoz et al., 1988; Mizusawa et al., 1989). The strongest evidence that NFP is involved in the mechanism of motor neuron degeneration comes from genetic alterations of NFP. Transgenic mice that overexpressed NFP-L or NFP-H (Côté et al., 1993; Xu et al., 1993) or expressed mutated NFP-L (Lee et al., 1994) exhibited motor neuron pathology. In addition, mutations in the NFP-H gene have been reported in a few cases of sporadic ALS (Figlewicz et al., 1994). These data suggest that NFP may represent more than a marker for degenerating neurons in our SOD-1 transgenic mice, and may be critically involved in the mechanism of motor neuron degeneration, as seen in ALS. It is particularly interesting that we find NFP-containing neurons to be highly vulnerable in SOD-1 transgenic mice, because it suggests that disruptions of NFP may be a common feature of ALS neurodegeneration, whether initiat-

ed by mutations in SOD-1 or more directly by manipulations of the NFP genes.

Of further importance, our results suggest that CB-immunoreactive neurons are protected against neurodegeneration, even when also immunoreactive for nonphosphorylated NFP. CB-immunoreactive neurons are not double-labeled with ChAT, and therefore represent primarily a population of ventral horn interneurons. Investigators have concluded that CB and other calcium-binding proteins play a role in protecting neurons from degeneration in ALS based upon the presence of calcium-binding protein-immunoreactive neurons in brainstem and spinal motor nuclei that are less vulnerable to degeneration in ALS, such as the oculomotor, trochlear, abducens, and Onuf's nuclei (Alexianu et al., 1994). These investigators did not actually count the number of CB-immunoreactive neurons, and therefore provide only indirect evidence for the localization of CB in resistant neurons. Utilizing unbiased stereologic methods, we have counted the number of CB-immunoreactive neurons in control and SOD-1 transgenic mice and directly demonstrated that there is no significant decrease in the number of these neurons in SOD-1 transgenic mice. While our results demonstrate conclusively that CB-containing cells do not degenerate significantly, and as such, one could postulate that CB is protecting cells by binding and buffering the levels of intracellular calcium (Mattson et al., 1991; Lledo et al., 1992; Chard et al., 1993), such interpretations should be made cautiously at this point. A possible confounding factor is that CB-immunoreactive neurons may have reduced expression of the SOD-1 transgene or properties unrelated to the presence of CB, which render them resistant to the transgene product. Interestingly, CR, another calcium-binding protein, does not appear to be a marker for protected neurons. Little is known about differences in the buffering capacities of CB and CR, however, differential protective effects of members of the calcium-binding protein family have been observed in models of excitotoxic degeneration (Mockel and Fischer, 1994) and in neurodegenerative diseases (Ferrer et al., 1993). In addition, these two populations of neurons may differ in other attributes relevant to the flux of calcium, such as their respective glutamate receptor profiles. Thus,

while the reduced vulnerability of CB-immunoreactive neurons in this study suggests that increased intracellular calcium, which has been proposed as a separate mechanism of ALS neurodegeneration, may play a role in the mechanism of neurodegeneration resulting from mutations in SOD-1, the relative resistance of these neurons may also reflect additional attributes, beyond the presence of CB, that have yet to be elucidated.

Correlations between connectivity and biochemical phenotype can also be drawn from these data, and these may be crucial to the further clarification of the essential determinants of vulnerability. As previously mentioned, ChAT is a marker for cholinergic neurons, which in the ventral horn of the spinal cord are motor neurons. In contrast, double-labeling experiments demonstrate that CR- and CB-immunoreactive cells in the ventral horn do not colocalize with ChAT, and are, by exclusion, interneurons. Their immunocytochemical profile is consistent with their location in lamina VII and VIII, dorsal and medial to the ventrolateral motor neuron pools. There is some evidence that CB-immunoreactive cells in the ventral horn of primates are Renshaw cells (Arvidsson et al., 1992), which are a source of recurrent inhibition on motor neurons. Nonphosphorylated NFP is present in both motor neurons and interneurons, and highly colocalized with both ChAT and CR. Thus, the defining features in respect to connectivity of the nonphosphorylated NFP-immunoreactive neurons are still unclear, and NFP-immunoreactive neurons likely represent a heterogeneous population of neurons in the ventral horn. Further investigation aimed at anatomically subdividing this chemically-identified neuronal population is needed to extend the demonstrated linkage between biochemical phenotype and vulnerability to precise correlations with connectivity.

Another important implication of these results is that motor neurons, defined by ChAT immunoreactivity, and at least one population of interneurons, defined by CR immunoreactivity, are equally vulnerable to degeneration in this mouse model of ALS. Degeneration of interneurons has been observed in ALS, although inconsistently reported and presumed to be a late-occurring, secondary event to motor neuron degeneration

(Oyanagi et al., 1989; Hirano, 1991; Terao et al., 1994). The cell counts and quantitative double-labeling of CR-containing neurons, which defines a population of interneurons, provides an explanation for the observed loss of interneurons in the spinal cord of ALS patients. Our results suggest that interneurons are vulnerable in ALS because many of them contain NFP. Reports that motor neuron loss is more severe than interneuron loss, which were based on qualitative rather than quantitative analyses, prompted the search for motor neuron-specific characteristics leading to their selective vulnerability. Our study suggests that NFP immunoreactivity is a better predictor of vulnerability than the connectivity of a particular neuron (*e.g.*, motor neuron or interneuron), and that the driving force behind the severe loss of motor neurons in these mice, and perhaps in ALS itself, is the high percentage of motor neurons that are NFP-immunoreactive (85% in these mice).

The mechanism of neurodegeneration in these transgenic mice presumably involves biochemical disturbances resulting from the presence of the mutant SOD-1 protein. Although these transgenic mice have normal SOD-1 enzymatic activity (Ripps et al., 1995), they still develop motor dysfunction. In fact, other SOD-1 transgenic mice have motor neuron pathology and increased total SOD-1 enzymatic activity (Gurney et al., 1994; Wong et al., 1995), and SOD-1 knockout mice have no clinical or pathological signs of neurodegeneration despite the absence of SOD-1 protein (Hoffman et al., 1995). The decrease in SOD-1 enzymatic activity in familial ALS is therefore unlikely to be responsible for the neurodegeneration. Rather, the mutated protein appears to have acquired a novel function, termed a gain-of-function mutation. Although the nature of this novel function is currently unknown, investigators have proposed increased nitration of tyrosines by peroxynitrite (Ischiropoulos et al., 1992; Beckman et al., 1993; Beckman and Crow, 1993) or increased oxidative reactions of hydrogen peroxide (Wiedau-Pazos et al., 1996), either of which may alter the function or regulation of cellular proteins, as potential mechanisms. The role of intracellular calcium in this mechanism is unclear; however, increased intracellular calcium has been shown to accelerate the production of nitric

oxide and superoxide (Dawson et al., 1991; Coyle and Puttfarcken, 1993; Lafon-Cazal et al., 1993), free radicals that are precursors to both peroxynitrite (Beckman and Crow, 1993) and hydrogen peroxide (Fridovich, 1974). The role of NFP in this mechanism has also not been determined, although it may be involved either directly, through the oxidation or nitration of NFP, or indirectly, through the oxidation or nitration of proteins that normally regulate the production, phosphorylation, transport, or function of NFP subunits.

In conclusion, detailed quantitative analyses of the SOD-1 transgenic mouse model of ALS suggest the following: 1) Even though the initial genetic event is a mutation of SOD-1 rather than a direct effect on one of the NFP genes, a high somatodendritic level of nonphosphorylated NFP is a strong determinant of vulnerability; 2) CB-containing neurons in the ventral horn of SOD-1 transgenic mice are protected, whereas CR-containing neurons appear to have significant vulnerability; 3) The vulnerability of NFP-immunoreactive neurons and the resistance of CB-immunoreactive neurons to degeneration suggest that NFP and intracellular calcium, which have been linked to separate mechanisms of degeneration in ALS, may also contribute to the mechanism of degeneration initiated by SOD-1 mutations; 4) Even though lower motor neuron degeneration leads directly to the phenotypic alterations in SOD-1 transgenic mice, the neurochemical characteristics of motor neurons (*e.g.* presence of neurofilament and absence of calbindin) appear to be a more dominant determinant of vulnerability to degeneration than connectivity.

Chapter Three

Time Course of Neuropathology in the Spinal Cord of G86R Superoxide Dismutase Transgenic Mice

Reprinted with permission from John Wiley and Sons

Morrison, B.M., W.G. Janssen, J.W. Gordon, and J.H. Morrison (1998) Time course of neuropathology in the spinal cord of G86R superoxide dismutase transgenic mice. J. Comp. Neurol. *391:*64-77

Abstract

Transgenic mice with a G86R mutation in the mouse SOD-1 gene, which corresponds to a mutation observed in familial ALS, display progressive motor dysfunction leading to paralysis and premature death. In endstage SOD-1 transgenic mice, there is marked loss of spinal motor neurons and interneurons, accumulation of phosphorylated NFP inclusions, and reactive astrocytosis. The present study details the time course and ultrastructural appearance of these pathologic changes and correlates the timing of these events with the behavioral symptoms. There is no significant reduction in the number of total neurons, motor neurons, or interneurons in the ventral spinal cord of presymptomatic mice, as compared to age-matched control mice. In contrast, there is a significant reduction in the number of total neurons (-23.5%), motor neurons (-28.9%), and interneurons (-23.5%) in symptomatic SOD-1 transgenic mice. This neuron loss correlates temporally with the onset of reactive astrocytosis and the appearance of phosphorylated NFP inclusions. The identical timing of motor neuron and interneuron degeneration in this model of ALS strongly suggests that degeneration in the spinal cord of patients with ALS is not specifically directed at motor neurons, but rather more generally at several populations of neurons in the spinal cord. In addition, the late onset and rapid progression of neuron loss suggest that a toxic property is accumulating while the SOD-1 transgenic mice are presymptomatic, and that this toxic property must reach a threshold level before the onset of neuronal degeneration.

Introduction

ALS is a neurologic disease characterized by progressive muscle weakness and atrophy that leads to paralysis and eventually death (Tandan, 1994; Adams et al., 1997). Pathologically, there is extensive loss of motor neurons within the spinal cord, brainstem, and motor cortex, corticospinal tract degeneration, somatic and axonal inclusion bodies, reactive astrocytosis, and atrophy of ventral roots (Hirano et al., 1967; Hirano, 1991; Leigh and Swash, 1991). There are both sporadic and familial forms of the disease, with familial ALS accounting for approximately 5% of all ALS cases. Clinically and pathologically, the two forms of ALS are virtually identical, suggesting that there are common mechanisms of neurodegeneration (Adams et al., 1997).

The genetic linkage of mutations in the SOD-1 gene with the development of familial ALS revealed the first factor causally related to the disease (Rosen et al., 1993). Since this report, over 45 mutations of the SOD-1 gene, most of these resulting in the substitution of one amino acid, have been found in patients with familial ALS, and together these mutations account for approximately 20% of all familial ALS cases. Many of the mutant forms of SOD-1 have shorter half-lives and reduced capacity for the enzymatic clearance of superoxide radical than the wild-type enzyme (Borchelt et al., 1994; Tsuda et al., 1994; Fujii et al., 1995). This reduction in function does not, by itself, account for the motor system degeneration in patients with familial ALS, however, since transgenic mice that express mutant forms of SOD-1 develop symptoms and pathologies that mimic those found in ALS patients, without a reduction in the enzymatic clearance of superoxide radical (Gurney et al., 1994; Ripps et al., 1995; Wong et al., 1995; Bruijn et al., 1997b). In addition, SOD-1 knockout mice do not develop motor neuron degeneration and motor system dysfunction despite the complete absence of SOD-1 enzymatic activity (Reaume et al., 1996). These findings in mice strongly suggest that the mutant forms of SOD-1 are

leading to cell death not through a reduction in SOD-1 clearance of superoxide radical, but rather by acquiring a function that wild-type SOD-1 does not possess, or possesses to a small degree.

The exact nature of this gain of function is unknown; however, the locations of the point mutations in the SOD-1 protein suggest that unshielding of the Cu^{2+} may be involved (Deng et al., 1993; Wiedau-Pazos et al., 1996). Increased access of substrates to the Cu^{2+} in mutant SOD-1 would lead to catalysis of several chemical reactions, including nitration of tyrosines by peroxynitrite (Beckman et al., 1993) and oxidation of proteins by hydrogen peroxide. Mutant forms of SOD-1 have been demonstrated to catalyze the latter reaction to a greater degree than wild-type SOD-1 (Wiedau-Pazos et al., 1996; Yim et al., 1996). However, these altered properties of the mutant enzyme have not yet been causally-linked to neuronal damage in ALS.

The SOD-1 transgenic mice provide an *in vivo* system for the investigation of these putative mechanisms of neurodegeneration (Tu et al., 1997). Based on research that implicated the calcium-binding protein, CB (Alexianu et al., 1994; Ho et al., 1996), and the cytoskeletal protein, NFP (Manetto et al., 1988; Côté et al., 1993; Xu et al., 1993; Lee et al., 1994), as influences in the mechanism of ALS neurodegeneration, we investigated the vulnerability of neurons containing these proteins. Using quantitative neuroanatomic techniques, we determined that CB defined a population of neurons in the spinal cord that were protected against the mutant protein and that nonphosphorylated NFP was a marker for the vulnerable neurons in the spinal cord, suggesting that NFP and increased intracellular calcium play a role in the mechanism of neuronal degeneration in SOD-1 transgenic mice (Morrison et al., 1996).

In the present study, we investigate the time course of neurodegeneration in the G86R mutant SOD-1 transgenic mouse. The transgenic mice are behaviorally normal until approximately 100 days of age when the mice develop weakness in one or several limbs that progresses over several days to total paralysis and death (Ripps et al., 1995).

At end-stage, the transgenic mice have extensive loss of both motor neurons and interneurons in the ventral horn of the spinal cord, cytoplasmic accumulations of phosphorylated NFP, and astrocytosis (Morrison et al., 1996). These pathologies are consistent with those observed in other mutant SOD-1 transgenic mice (Dal Canto and Gurney, 1995; Wong et al., 1995; Tu et al., 1996; Bruijn et al., 1997b), as well as patients with ALS (Hirano, 1991; Leigh and Swash, 1991). In patients with ALS, it is obviously difficult to accurately determine the time course of these events. Based on autopsy specimens from patients with varying stages of disease, however, it has been suggested that motor neuron loss is the primary event and that interneuron loss and astrocytosis occur secondarily (Oyanagi et al., 1989; Terao et al., 1994). Utilizing the SOD-1 transgenic mouse model of ALS, we directly addressed these questions of chronology by quantifying the cell loss of both interneurons and motor neurons in transgenic mice at different stages of behavioral impairment. In addition, we correlated the timing of this cell loss with the appearance of cytoplasmic inclusions, astrocytosis, and behavioral deficits.

Materials and Methods

Animals and tissue processing. Transgenic mice with a G86R mutation of the mouse SOD-1 gene and control FVB littermates, described previously (Ripps et al., 1995), were used in this study. SOD-1 transgenic mice and age-matched controls were sacrificed at approximately 30 (mean = 31.5), 80 (mean = 80.6), and 100 (mean = 100.7) days of age. The final time point was determined by the onset of limb paralysis. Mice were deeply anesthetized with 0.1 ml equal mixture of ketamine (100 mg/ml) and xylazine (20 mg/ml) injected intraperitoneally, and then perfused transcardially with cold 1% paraformaldehyde in 0.1 M phosphate buffered saline (PBS), pH 7.2, for 1 minute followed by cold 4% paraformaldehyde in 0.1 M PBS for 10 minutes. The spinal cords were rapidly removed, blocked coronally, and post-fixed in 4% paraformaldehyde in 0.1 M PBS for 6 hours.

Blocks were cryoprotected in 25% sucrose in 0.01 M PBS, pH 7.2, for 24 hours, and sectioned on a cryostat at 40 μm. All protocols were conducted within NIH guidelines for animal research and were approved by the Institutional Animal Care and Use Committee (IACUC).

Immunocytochemistry and histochemistry for light microscopy. Parallel series of sections were collected for immunocytochemistry and Nissl staining (cresyl violet). Tissue sections for single label immunocytochemistry were incubated overnight at 4°C in one of the following: 1) monoclonal antibody (mouse IgG) to phosphorylated epitopes on medium and heavy chain NFP (SMI-31, Sternberger Monoclonals, Baltimore, MD) diluted to 1:10,000 in 0.01 M PBS containing 0.3% Triton-X 100 and 0.5 mg/ml bovine serum albumin (diluent); 2) polyclonal antibody (goat IgG) to ChAT diluted to 1:200 in diluent (Chemicon, Temecula, CA); 3) polyclonal antibody (rabbit IgG) to CR diluted to 1:2500 in diluent (SWant, Bellinzona, Switzerland); 4) polyclonal antibody (rabbit IgG) to glial fibrillary acidic protein (GFAP) diluted to 1:50 in diluent (Biomeda, Foster City, CA). The sections were then processed by the avidin-biotin-peroxidase method with Vectastain ABC kits (Vector Laboratories, Burlingame, CA) and 3,3'-diaminobenzidine.

Pre-embedded immuno-electron microscopy. Two symptomatic SOD-1 transgenic mice and two age-matched control littermates were deeply anesthetized with 0.1 ml equal mixture of ketamine (100 mg/ml) and xylazine (20 mg/ml) injected intraperitoneally, and then perfused transcardially with cold 1% paraformaldehyde in 0.1 M PBS for 1 minute followed by cold 4% paraformaldehyde and 0.125% glutaraldehyde in 0.1 M PBS for 10 minutes. Cervical and lumbar enlargements of the spinal cords were immediately removed and post-fixed in 4% paraformaldehyde in 0.1 M PBS for six hours. Blocks were sectioned on a vibratome series 1000 (TPI Inc., St. Louis, MO) at 50 μm. Sections were incubated overnight at 4 °C in a monoclonal antibody to phosphorylated epitopes on medi-

um and heavy chain NFP (SMI-31), which was diluted to 1:40,000 in 0.01 M PBS. The sections were then processed by the avidin-biotin method with Vectastain ABC kits (Vector Laboratories), post-fixed in 1.5% glutaraldehyde in 0.01 M PBS, and incubated in 0.05% 3,3'-diaminobenzidine containing 0.03% hydrogen peroxide in 0.01 M PBS for 2-4 minutes. The sections were *en bloc* stained with 1% uranyl acetate, fixed in 1.0% osmium tetroxide in 0.01 M PBS for 1 hour, dehydrated with graded concentrations of ethanol, dehydrated in propylene oxide, and embedded in Epon resin. Each section was wafer-embedded in resin between two strips of ACLAR plastic (Ted Pella, Redding, CA), flattened between glass microscope slides, and polymerized at 52 °C. The ventrolateral region of the spinal cord was cut from the wafers and mounted onto blank resin-embedded capsules with cyanoacrylate glue (Electron Microscopy Sciences, Fort Washington, PA). Semithin sections (2 μm) were collected onto unsubbed glass slides, coverslipped with glycerol:water (3:1) and viewed under a light microscope to identify cells with a pathologic accumulation of SMI-31 immunoreactivity within their somata. Sections containing these cells were repeatedly washed and re-embedded in Epon resin by inverting a Beem capsule over the section, filling the capsule with resin, and polymerizing overnight. Sections were removed from glass slides by immmersion in LN2. Thin sections were cut on an Ultracut E ultramicrotome (Reichert-Jung, Austria), collected on 200-mesh uncoated copper grids treated with Quick-Coat (EMS, Fort Washington, PA), and examined with a Zeiss CH-10 electron microscope at 60 kV.

Stereology. The total number of Nissl-stained, ChAT-immunoreactive, or CR-immunoreactive neurons were counted bilaterally in the ventral horn of both the cervical (C5 → C7) and lumbar (L1 → L3) spinal cord enlargements from five age-matched control and SOD-1 mutant transgenic mice in each age group using the optical fractionator (West et al., 1991). Throughout the experiment, the investigator was blinded to transgene status. For this analysis, a Zeiss Axiophot photomicroscope with a Zeiss Plan-Apochromat 63x oil

objective and a CCD camera was used to generate digitized images that were collected and analyzed on a Macintosh 840AV computer using custom-made data analysis software [NeuroZoom; developed in collaboration with the Scripps Research Institute, La Jolla, CA (Bloom et al., 1997)]. The technique used for counting neurons in this study, the optical fractionator, provides an unbiased estimate of cell number. It does not depend upon the determination of a volume of reference and a density, but rather relies on random, systematic sampling from a known fraction of a structure's total volume, and neuron number is estimated by extrapolating from this known fraction (West et al., 1991; Bjugn, 1993; West, 1993). The mathematical formula for estimating total cell number is as follows:

$$N = \sum Q^{-} \; x \; 1/ssf \; x \; 1/asf \; x \; t/h$$

where $\sum Q^{-}$ is the total number of neurons counted, *ssf* is the section sampling fraction, *asf* is the areal sampling fraction, *t* is the thickness, and *h* is the height of dissector. The formula consists of three sampling fractions multiplied by the number of neurons counted in the sampled volume. The first fraction, *1/ssf*, is the total number of sections in the spinal cord enlargements divided by the number of sections analyzed, which was a 1:40 series for the Nissl-stained sections and a 1:20 series for the immunocytochemically stained sections. The extent of the spinal cord enlargements was determined visually by comparing Nissl-stained sections from each animal with the mouse atlas of Sidman *et al.* (1971). The second fraction, *1/asf*, is the area of the x,y step divided by the area of the counting frame, *i.e.*, the percentage of each section's surface area that is sampled. The percentage sampled was 16.56% for Nissl-stained sections and 29.42% for immunocytochemically-labeled sections. On each section, the area ventral to the most dorsal extent of the central canal, including laminae VII, VIII, IX, and X, was designated ventral horn. A counting frame was positioned in a random position in the ventral horn and then moved systematically, with the aid of NeuroZoom, in the x and y directions across the ventral horn, sampling a given percentage of the area. The number of cells that were completely contained within this counting frame, or that crossed one of the two arbitrarily-defined accept-

ed sides of the frame, were counted. The third fraction, *t/h*, is the total thickness of the section divided by the depth counted. Because the stains did not penetrate through the entire depth of the section, cells were only counted in the portion of the section where staining was visible, and this depth was divided by the total thickness of the section, measurable by visualizing staining on both surfaces.

To avoid double counting neurons with unusual shapes, Nissl-stained and ChAT-immunoreactive cells were only counted when their nuclei were optimally visualized, which only occurred in one focal plane. The nuclei of CR-immunoreactive neurons were not as easily distinguished. Fortunately, these immunoreactive cells were not densely packed in the ventral horn of the spinal cord, and therefore, careful examination of each cell prior to counting was sufficient to avoid repeatedly counting the same neuron. In addition, neurons were differentiated from non-neuronal cells, including glia, in the Nissl stain by the exclusion of cells that did not have a clearly defined nucleus, cytoplasm, and a prominent nucleolus. These criteria have been used for neuron counts in the spinal cord by other investigators (Bjugn, 1993; Bjugn and Gundersen, 1993b), and although some small neurons may be excluded, these criteria should reliably exclude all non-neuronal cells.

Figure Preparation Photomicrographs were taken on a Zeiss Axiophot microscope or a Zeiss CH-10 electron microscope, developed, printed, and scanned with an AGFA Arcus II scanner. The scanned images were imported into Adobe Photoshop where they were sized, labeled, and optimized for contrast and brightness.

Statistical analysis The total number of cells for each histological or immunocytochemical stain in control and SOD-1 transgenic mice of each age group were compared with a two-sided Student's *t* test.

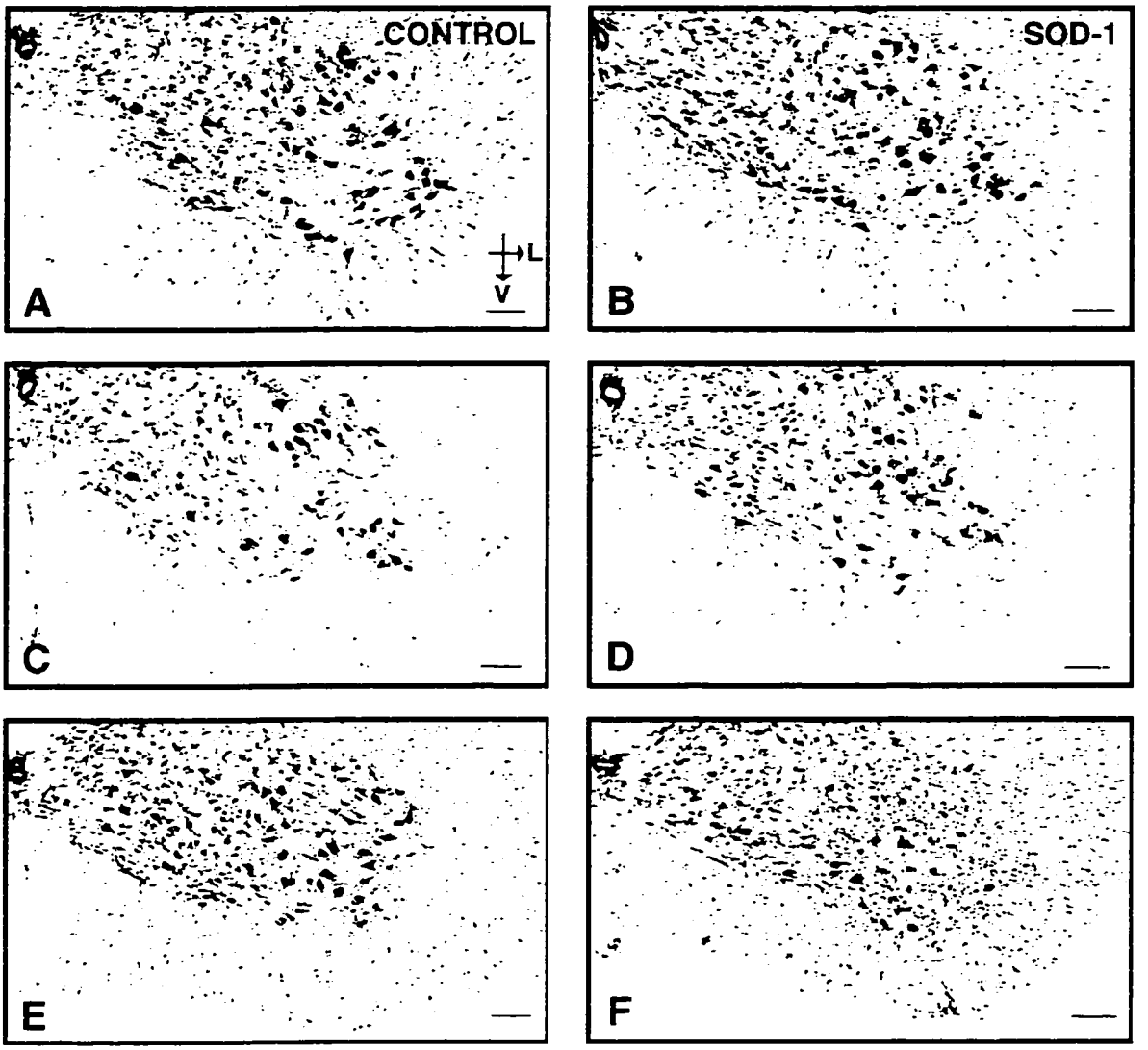

Figure 3-1. Nissl-stained sections from the cervical spinal cord enlargement of control (A, C, E) and SOD-1 transgenic (B, D, F) mice of 30 (A, B), 80 (C, D), and 100 (E, F) days of age. There is no apparent reduction in the density of Nissl-stained neurons in 30 or 80 day old SOD-1 transgenic mice (B, D), as compared to age matched control mice (A, C). In contrast, there is a reduced density of Nissl-stained neurons in 100 day old SOD-1 transgenic mice (F), as compared to 100 day old control mice (E). The directional arrows point towards the ventral (V) and lateral (L) aspects of the spinal cord. Scale bars: 100 μm.

Results

Qualitative observations of light microscopy Compared to 100 day old control mice, there was an apparent reduction in the number of Nissl-stained neurons in the ventral horn of

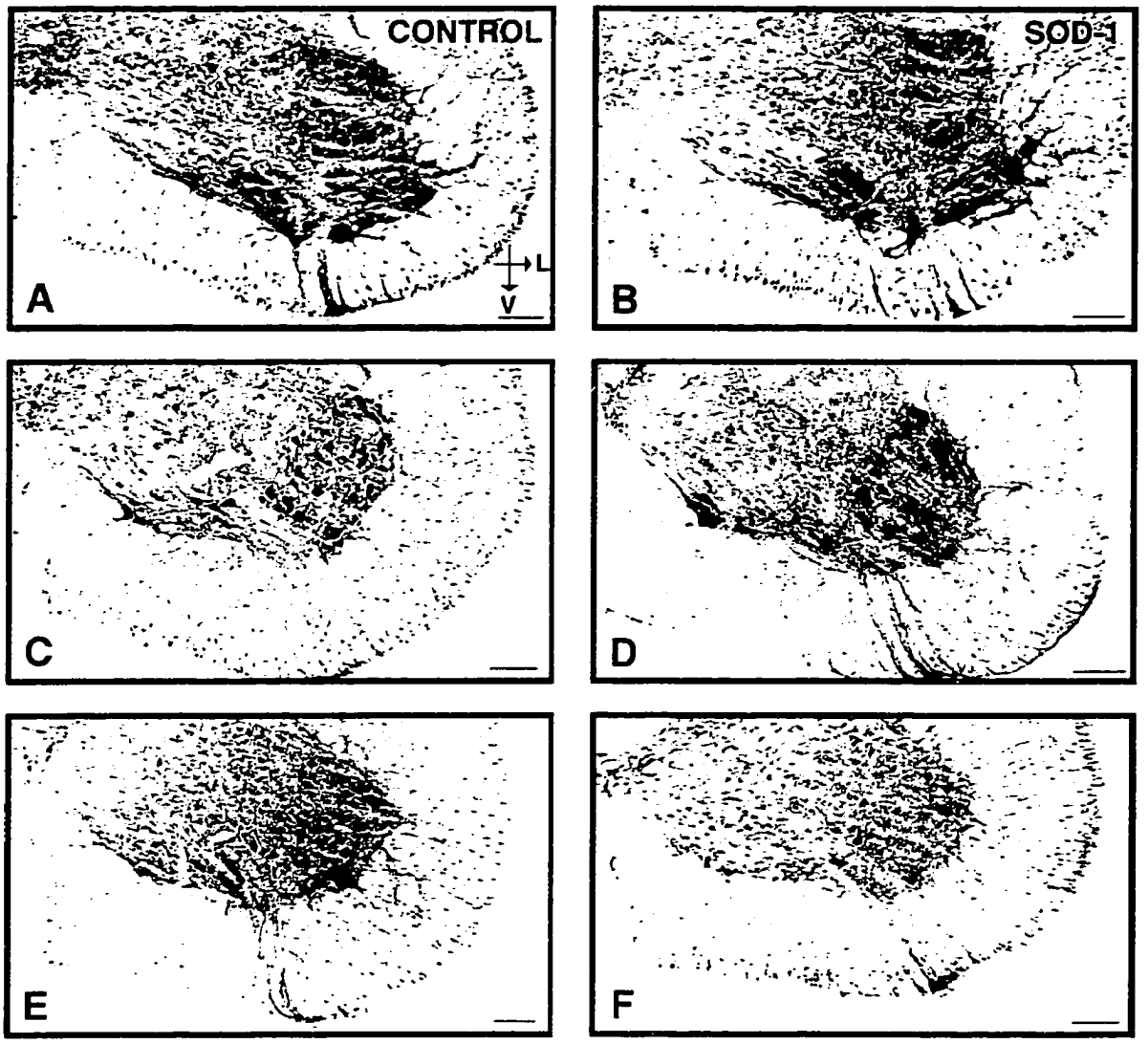

Figure 3-2. ChAT immunoreactivity in the cervical spinal cord enlargement of control (A, C, E) and SOD-1 transgenic (B, D, F) mice of 30 (A, B), 80 (C, D), and 100 (E, F) days of age. ChAT immunoreactivity defines motor neurons in the ventrolateral horn of the spinal cord. There is no difference in the density of ChAT-immunoreactive neurons in 30 or 80 day old SOD-1 transgenic mice (B, D), as compared to age matched control mice (A, C). In contrast, there is a reduced density of ChAT-immunoreactive neurons in 100 day old SOD-1 transgenic mice (F), as compared to 100 day old control mice (E). The directional arrows point towards the ventral (V) and lateral (L) aspects of the spinal cord. Scale bars: 100 μm.

the cervical and lumbar spinal cord enlargements from 100 day old SOD-1 transgenic mice (Fig. 3-1E,F). In contrast, there was no apparent reduction in the number of Nissl-stained neurons for either the 30 or 80 day old SOD-1 transgenic mice as compared to age-matched control mice (Fig. 3-1A-D). In contrast to several other SOD-1 transgenic mice (Dal Canto and Gurney, 1995; Wong et al., 1995), large vacuoles were not observed in

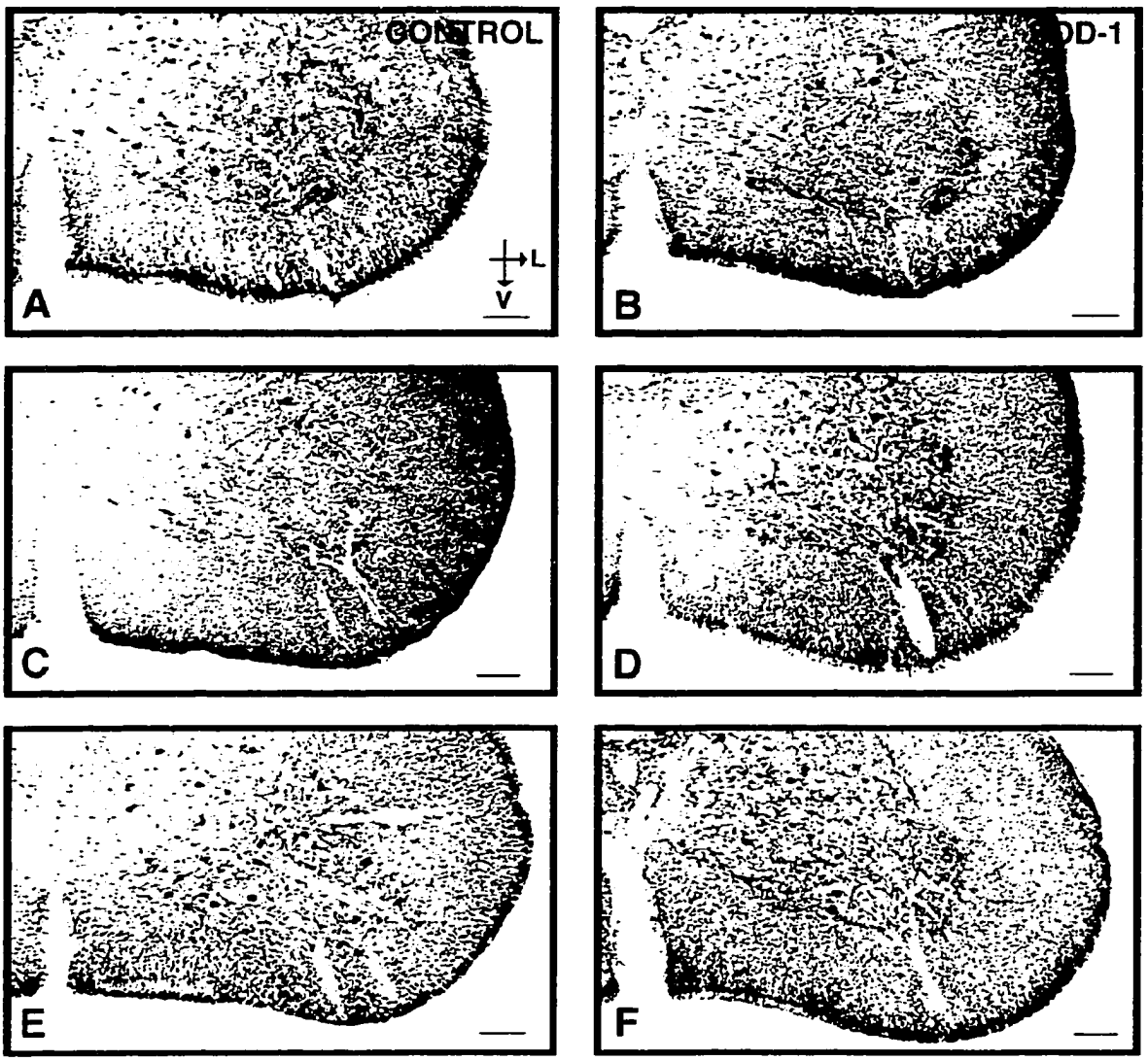

Figure 3-3. CR immunoreactivity in the cervical spinal cord enlargement of control (A, C, E) and SOD-1 transgenic (B, D, F) mice of 30 (A, B), 80 (C, D), and 100 (E, F) days of age. CR-immunoreactive neurons are located just dorsal and medial to the position of the spinal motor neurons, consistent with a role as spinal interneurons. The low density of CR-immunoreactive neurons in the ventral spinal cord make qualitative determinations of cell loss difficult. There is some indication, however, that CR-immunoreactive neurons are reduced in the 100 day old SOD-1 transgenic mice (F), as compared to all control mice and 30 or 80 day old SOD-1 transgenic mice (A-E). The directional arrows point towards the ventral (V) and lateral (L) aspects of the spinal cord. Scale bars: 100 μm.

spinal cord neurons of G86R SOD-1 transgenic mice at any age.

In order to label the motor neurons in the spinal cord specifically, sections were immunostained for ChAT (Fig. 3-2). Labeling was restricted to large neurons present in lamina IX of the spinal cord, and the pattern of ChAT immunoreactivity was similar to that observed by retrograde labeling of motor neurons through peripheral nerves. In the spinal

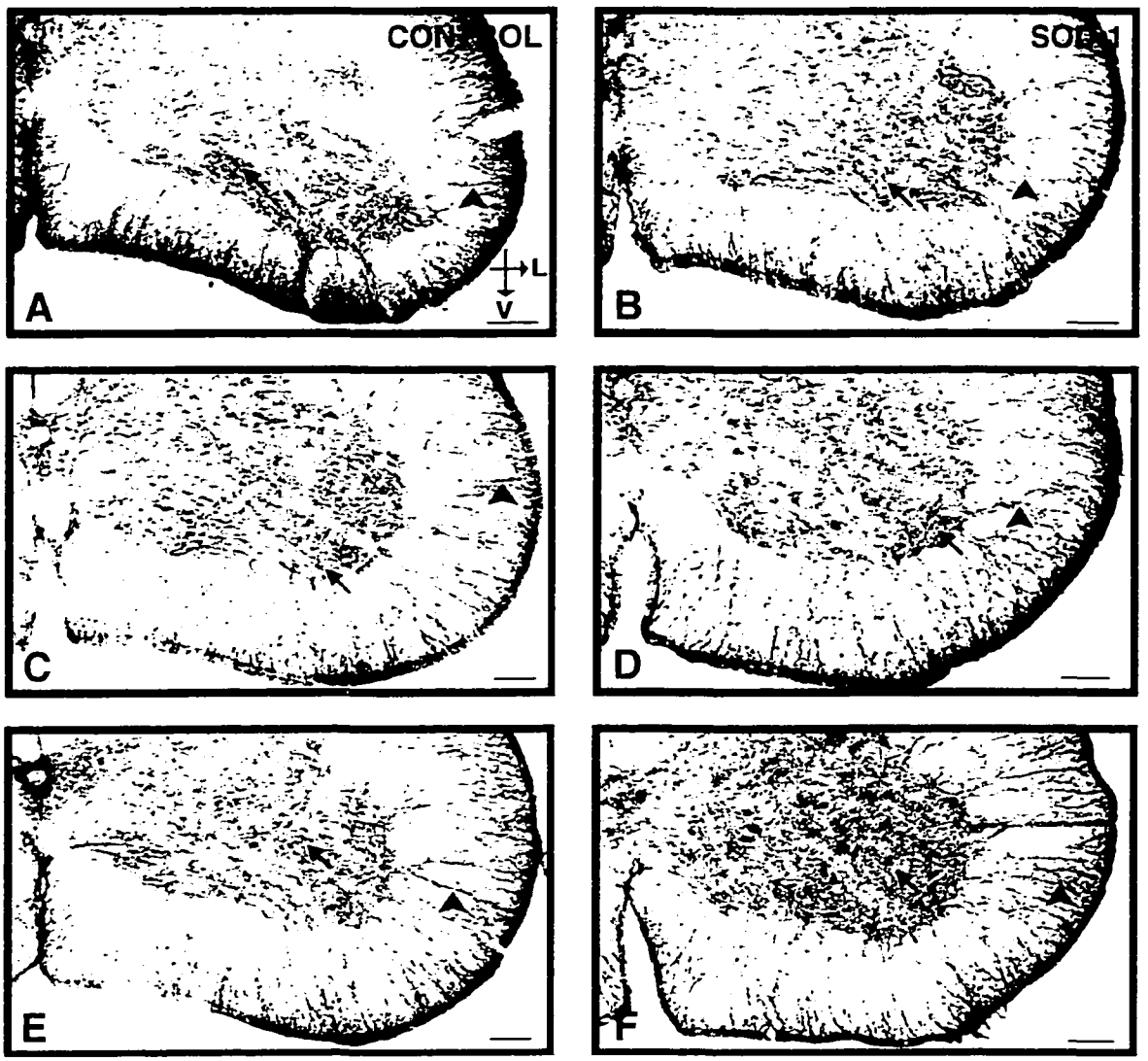

Figure 3-4. GFAP immunoreactivity in the cervical spinal cord enlargement of control (A, C, E) and SOD-1 transgenic (B, D, F) mice of 30 (A, B), 80 (C, D), and 100 (E, F) days of age. In control and 30 or 80 day old SOD-1 transgenic mice, fibrous astrocytes in the white matter are most strongly immunoreactive for GFAP (*arrowheads*), with only a few lightly immunoreactive protoplasmic astrocytes in the gray matter (*arrows*). In contrast to the pattern in these mice, GFAP immunoreactivity in 100 day old SOD-1 transgenic mice strongly labels protoplasmic astrocytes (F, *arrows*), and there is an apparent increase in the intensity of GFAP-immunoreactivity in the fibrous astrocytes, as well (F, *arrowhead*). This is the pattern of reactive astrocytosis. The directional arrows point towards the ventral (V) and lateral (L) aspects of the spinal cord. Scale bars: 100 μm.

cord of 100 day old SOD-1 transgenic mice, there was an apparent reduction in the number of ChAT-immunoreactive neurons as compared to the spinal cord of 100 day old control mice (Fig. 3-2E,F), while 30 or 80 day old SOD-1 transgenic mice showed no apparent reduction in the number of ChAT-immunoreactive neurons compared to age-matched

control mice (Fig. 3-2A-D).

The cellular vulnerability of interneurons in the spinal cord was investigated by immunostaining sections for CR. Double-labeling experiments have demonstrated that CR does not colocalize with ChAT-immunoreactivity in the spinal cord (Morrison et al., 1996). In addition, CR-immunoreactive neurons in the ventral portion of the spinal cord were present primarily in lamina VII and VIII (Fig. 3-3). Based on their location dorsal and medial to the motor neuron cell groups and their lack of immunoreactivity for ChAT, these neurons appear to be a population of spinal interneurons. Qualitative assessments of CR-immunoreactive neuron loss in the SOD-1 transgenic mice were difficult to make based on the low density of these neurons in the ventral horn of the spinal cord. Therefore, although there was some indication that the number of CR-immunoreactive neurons in the ventral horn of spinal cords from 100 day old SOD-1 transgenic mice was reduced as compared to age-matched controls (Fig. 3-3E,F), a definitive answer to this question required quantitative techniques.

In addition to investigating neuron loss, we were also interested in the age of onset of astrocytosis and phosphorylated NFP inclusions in the spinal cord. These pathologic alterations had been observed in endstage SOD-1 transgenic mice (Morrison et al., 1996). In control mice of all ages and 30 or 80 day old SOD-1 transgenic mice, GFAP-immunoreactivity was primarily present within fibrous astrocytes in the white matter of the spinal cord (Fig. 3-4A-E, *arrowheads*), with only a few GFAP-immunoreactive protoplasmic astrocytes in the gray matter (Figs. 3-4A-E, *arrows*, and 3-6A). In contrast to the pattern of immunoreactivity in these mice, there were numerous darkly stained GFAP-immunoreactive protoplasmic astrocytes in the spinal cord of 100 day old SOD-1 transgenic mice (Figs. 3-4F, *arrow*, and 3-6B). This astrocytic response was present in the ventral and intermediate zones of the spinal cord, but was absent from the dorsal horn. In addition, there was an increase in GFAP-immunoreactivity within fibrous astrocytes in the white matter of the spinal cord (Fig. 3-4F, *arrowhead*).

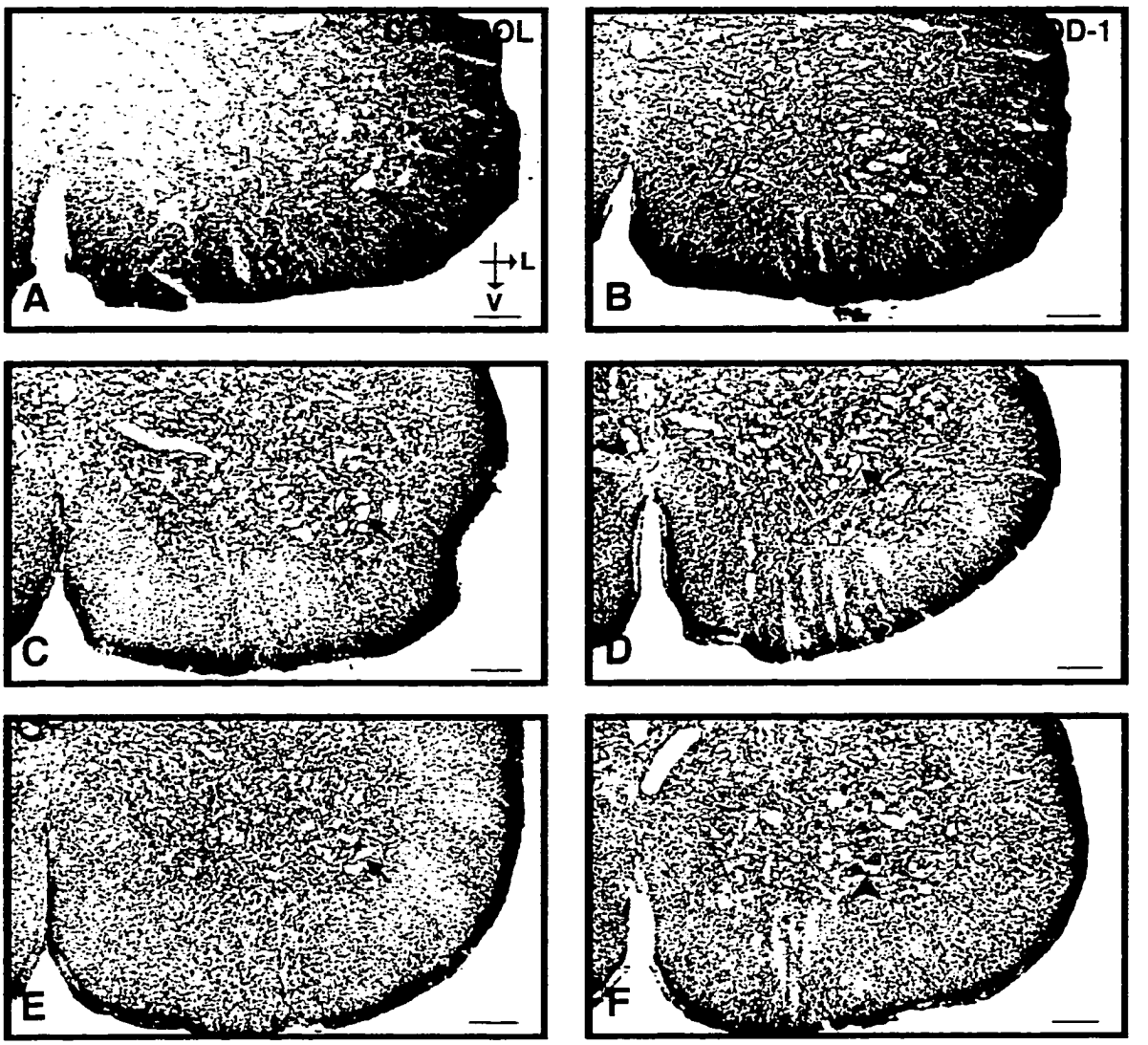

Figure 3-5. Phosphorylated NFP immunoreactivity in the lumbar spinal cord enlargement of control (A, C, E) and SOD-1 transgenic (B, D, F) mice of 30 (A, B), 80 (C, D), and 100 (E, F) days of age. In control and 30 or 80 day old SOD-1 transgenic mice, immunoreactivity for phosphorylated NFP is present within the neuropil of the spinal cord without labeling somata (*arrows*). In 100 day old SOD-1 transgenic mice, somata intensely labeled with phosphorylated NFP immunoreactivity are found quite frequently in the ventrolateral horn of the spinal cord (F, *arrowhead*). The directional arrows point towards the ventral (V) and lateral (L) aspects of the spinal cord. Scale bars: 100 µm.

The age of onset of phosphorylated NFP inclusions was identical to reactive astrocytosis. Phosphorylated NFP in control mice of all ages and 30 or 80 day old SOD-1 transgenic mice was present within the neuropil of the spinal cord, but was absent from somata (Figs. 3-5A-E and 3-6C, *arrows*). In contrast, numerous somata in the spinal cord of 100 day old SOD-1 transgenic mice were strongly immunoreactive for phosphorylated

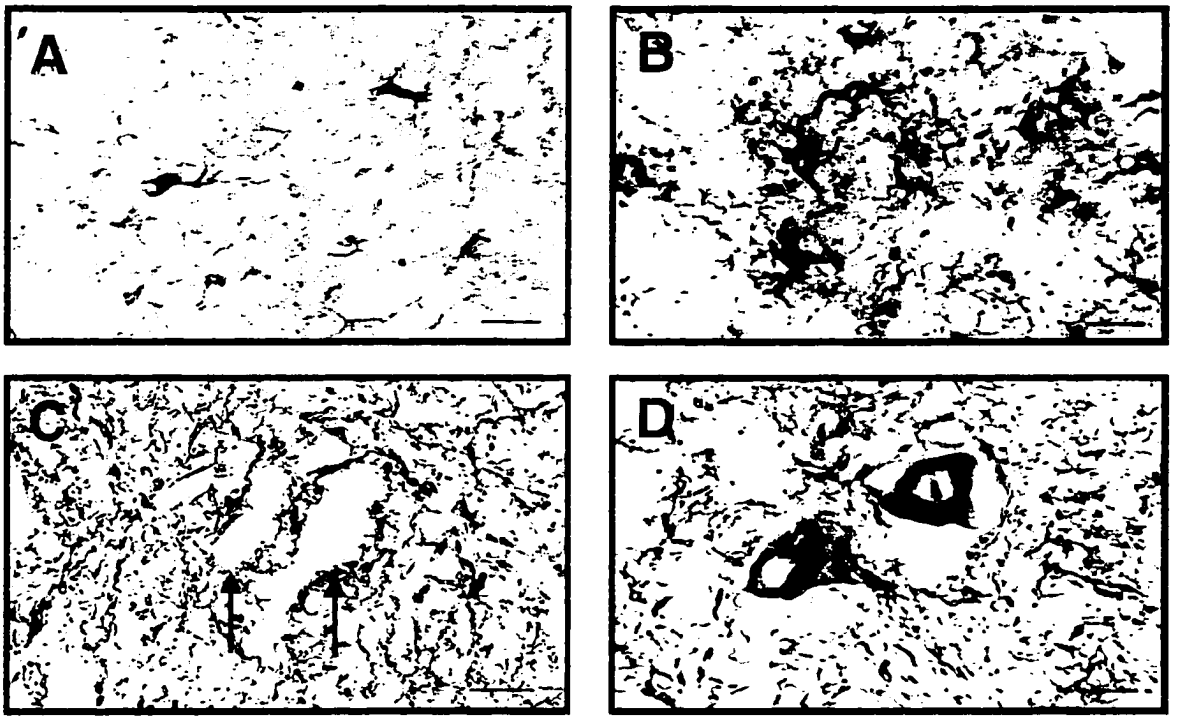

Figure 3-6. High power photomicrographs of GFAP (A, B) and phosphorylated NFP (C, D) immunoreactivity in the ventral horn of the spinal cord from 100 day old control (A, C) and SOD-1 transgenic (B, D) mice. At this magnification, the increased number of GFAP-immunoreactive protoplasmic astrocytes in the 100 day old SOD-1 transgenic mice (B), as compared to control mice (A), is clearly evident. In addition, the lack of immunoreactivity for phosphorylated NFP in the neuronal somata of control mice (C; *arrows*) and the striking appearance of the phosphorylated NFP inclusions in 100 day old SOD-1 transgenic mice (D) is also quite apparent. Scale bars: 20 μm.

NFP (Figs. 3-5F, *arrowhead*, and 3-6D).

Pre-embedded immuno-electron microscopy. In order to investigate the ultrastructural appearance of the accumulations of phosphorylated NFP in ventral horn neurons observed by light microscopy (Figs. 3-5F and 3-6D), spinal cord sections stained for phosphorylated NFP were processed for electron microscopy. As was observed in light microscopic analysis of these immunocytochemically-stained sections, occasional somata in the ventral horn of symptomatic SOD-1 transgenic mice were immunoreactive for phosphorylated NFP (Fig. 3-7A-E), while most somata in symptomatic SOD-1 transgenic mice and all somata in presymptomatic or control mice were non-immunoreactive. The pathologically immunoreactive somata were densely packed with both heavily immunoreactive fila-

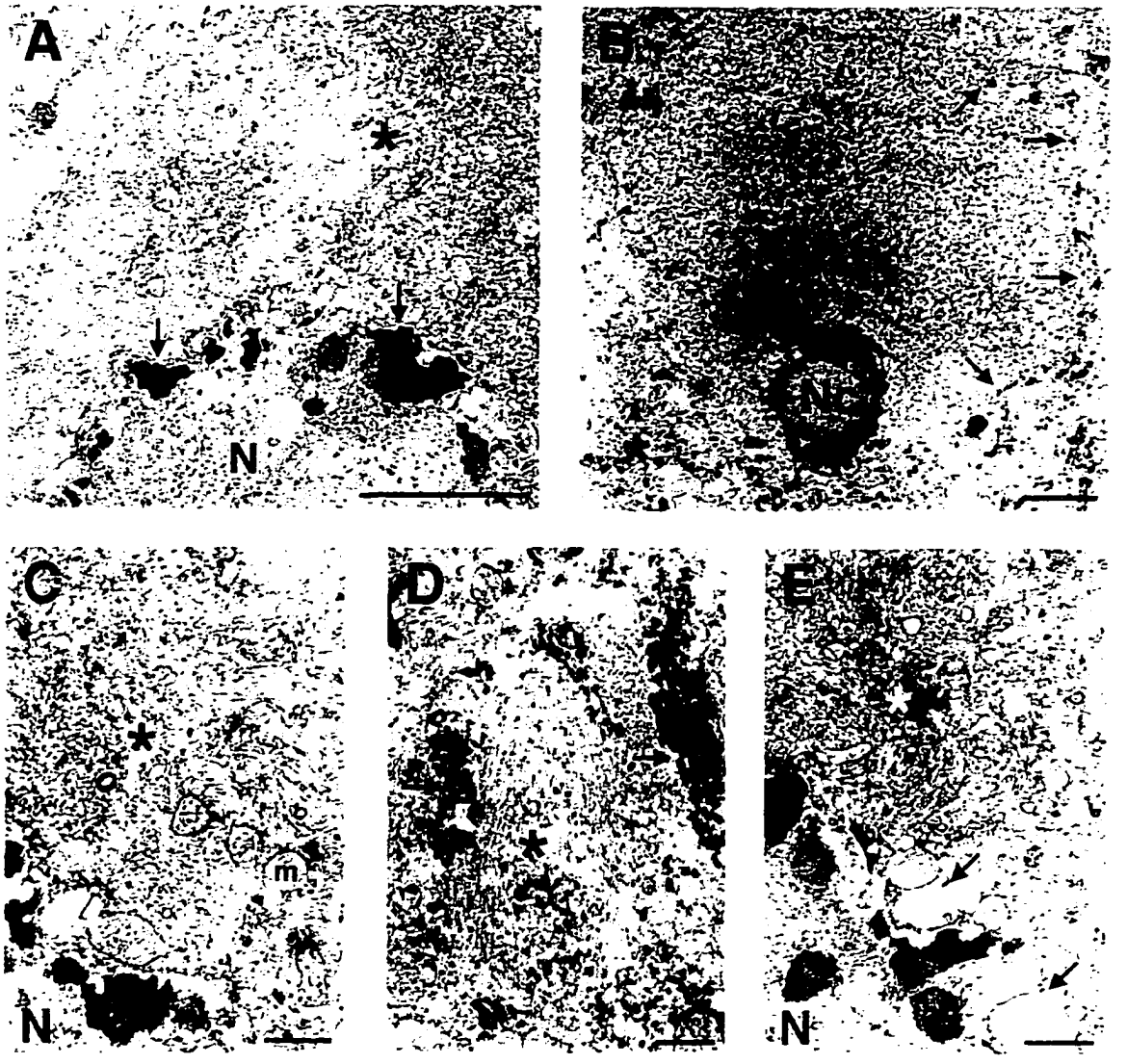

Figure 3-7. Pre-embedded immuno-electron microscopy of phosphorylated neurofilament (NFP)-immunoreactive somata in the spinal cord of SOD-1 transgenic mice (A-E). (A) Lower magnification of neuron whose cytoplasm (*indicated by* *) is filled with filaments that are strongly immunoreactive for phosphorylated NFP, as well as some intermediate filaments that are less immunoreactive. Interestingly, there are large aggregates of chromatin (*arrows*) along the periphery of the nucleus (*N*). (B) Lower magnification of neuron whose cytoplasm also contains filaments immunoreactive for phosphorylated NFP (*indicated by* *). The nucleus of this neuron has an irregular shape, and yet does not exhibit dramatic chromatin clumping at its periphery, and appears to have an intact nuclear membrane (*arrows*) and nucleolus (*Nc*). (C) Higher magnification of neuron with accumulations of cytoplasmic filaments. Phosphorylated NFP-immunoreactive filaments are densely packed in the cytoplasm of this neuron (*indicated by* *), and oriented both longitudinally and cross-sectionally. The chromatin is clumped at the periphery of the nucleus (*N*). In addition, mitochondria (*m*), some exhibiting abnormal morphology, are embedded in the NFP-rich cytoplasm. (D) Higher magnification of NFP array in the soma of a neuron. Bundles of lightly- or non-immunoreactive filaments (*indicated by* *) are interwoven with phosphorylated NFP-immunoreactive filaments (*arrows*). (E) In addition to containing pathologic accumulations of phosphorylated NFP bundles in the cytoplasm (*indicated by* *), this neuron has microvacuoles (*arrows*) at the border of its nucleus (*N*). In addition, the nucleus also has chromatin aggregates at its periphery. Scale bars: A,B, 3.5 μm; C-E, 0.7 μm.

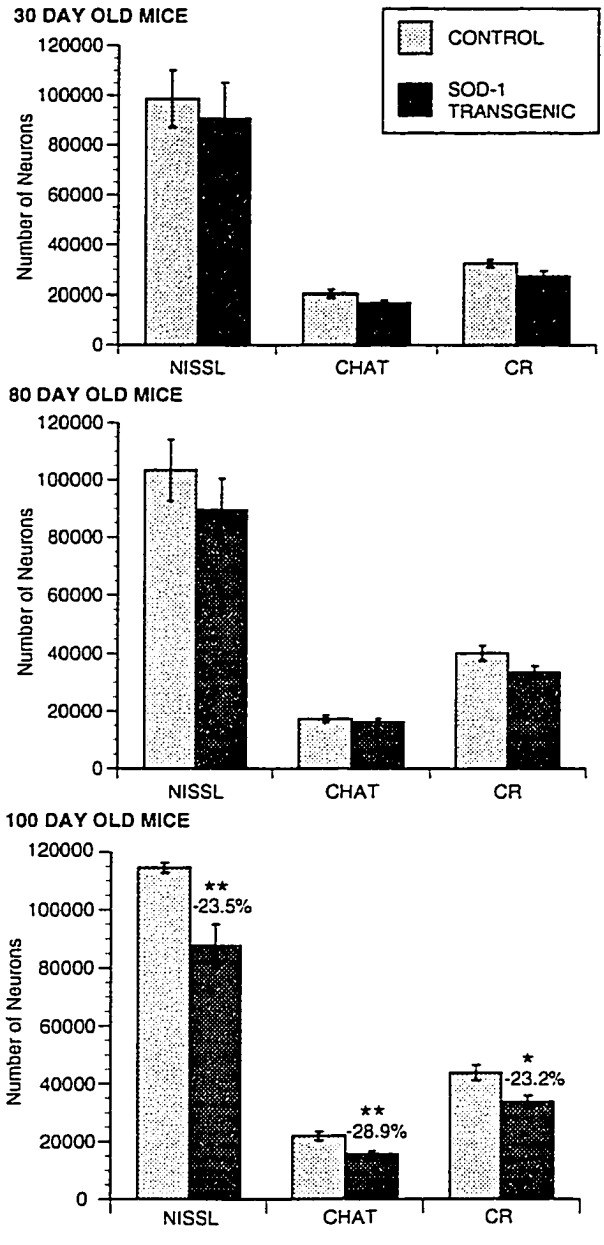

Figure 3-8. Histograms of the mean number of Nissl-stained, ChAT-immunoreactive, and CR-immunoreactive neurons in the cervical and lumbar enlargements of control and SOD-1 transgenic mice at 30, 80, and 100 days of age. For each significant change in neuron number, the percentage change (number of cells in SOD-1 transgenic mice - number of cells in control mice / number of cells in control) is given. The error bars represent the S.E.M. (n = 5). *, $P < 0.05$; **, $P < 0.01$.

ments (Fig. 3-7D, *arrows*) and lightly immunoreactive or non-immunoreactive filaments (Fig. 3-7D, *asterisk*). The bundles of filaments were oriented both longitudinally and cross-sectionally. In addition to the abnormal phosphorylation and density of NFP in these neurons, the nuclei frequently were misshapen (Fig. 3-7B) and had chromatin aggregates at their periphery (Fig. 3-7A,C,E). The mitochondria had a swollen appearance (Fig. 3-7C,E), and several microvacuoles were found bordering the nucleus (Fig. 3-7E). These characteristics were not observed in neighboring neurons whose cytoplasm was not filled with aberrantly phosphorylated NFP.

Cell counts The number of Nissl-stained, ChAT-immunoreactive, and CR-immunoreactive neurons in the ventral portion of the cervical and lumbar spinal cord enlargements from both control and SOD-1 transgenic mice at 30, 80, and 100 days of age were counted using the optical fractionator (Fig. 3-7).

There was a significant reduction in the number of Nissl-stained ($P < 0.01$), ChAT-immunoreactive ($P < 0.01$), and CR-immunoreactive ($P < 0.05$) neurons in the 100 day old SOD-1 transgenic mice, as compared to 100 day old control mice. In contrast, there was no significant reduction of any of these populations of neurons in SOD-1 transgenic mice at earlier time points.

Discussion

The first significant loss of both motor neurons and interneurons occurred in early symptomatic (*i.e.*, 100 day old) SOD-1 transgenic mice. The neuron loss correlated temporally with astrocytosis and the appearance of phosphorylated NFP inclusions within the ventral horn of the spinal cord. The early symptomatic mice had motor deficits in one limb. Over the next ten days, the motor dysfunction progressed to total paralysis and death. Over this same time period, the percentage cell loss of Nissl-stained neurons increased from 23.5% to 35%, the percentage cell loss of motor neurons increased from 28.9% to 44%, and the loss of CR-immunoreactive interneurons increased from 23.2% to 40% (Morrison et al., 1996). Over a ten day period, this represents a very rapid loss of neurons in the spinal cord, following several months during which there was no significant cell loss.

Methodologic considerations

The cell counts in this paper are presented as comparisons between control and SOD-1 transgenic mice at each time point (30, 80, and 100 days of age). Comparisons were made only within age groups, because of an apparent increase in the number of neurons in both control and SOD-1 transgenic mice as they age. We believe that this increase reflects an inaccuracy in defining the cervical and lumbar enlargements in juvenile mice by internal morphologic landmarks, rather than hyperplasia of spinal cord neurons. The

landmarks that we employed were initially established for adult mice by comparing Nissl-stained sections to the mouse atlas of Sidman et al. (1971) and proved to be reliable for this age. When applied to younger mice, however, these landmarks appear to have defined a smaller segment of spinal cord. For example, the cervical enlargement was defined by the photographs of C5 → C7 in the mouse atlas. In juvenile mice, these same morphologic characteristics do not occur as definitively at the rostral and caudal ends of C5 and C7, respectively, but rather across a transition region at the rostral and caudal portions of the enlargement, probably because of postnatal changes in the shape of the enlargement (Sakla, 1969). As the neurons hypertrophy, with increases in the size of their somata and their dendritic arbor, the enlargements increase in both cross-sectional area and length, likely altering the internal morphologic landmarks that we used to define the beginning and end of the spinal cord enlargements. Due to our conservative delineation of the rostral and caudal endpoints, these changes led to a consistent 5 - 10% underestimation of the enlargement length in young mice as compared to adults. We are therefore confident that the increase in neuron number as the mice age is a result of a systematic difficulty in defining the boundaries of the spinal cord enlargements in young mice with the same precision as in adult mice. Since the present experimental design did not take into account such age-related changes in cytoarchitectonic characteristics, comparisons across time are not as valuable as direct comparisons between the two groups at the same age. Based on these direct comparisons, we have concluded that no significant reduction of neurons occurs in SOD-1 transgenic mice prior to the onset of symptoms. Because the increase in neuron number in control mice is mirrored by an equivalent increase in SOD-1 transgenic mice, these same-age comparisons appear to be valid and our conclusions justified.

Ultrastructure of aberrant neurofilament accumulations

Electron microscopy has demonstrated that the somatic inclusions are composed of dense NFP bundles, some immunoreactive for phosphorylated NFP and some not, that

course throughout the cytoplasm. Interestingly, the ultrastructural appearance of the accumulations in these SOD-1 transgenic mice is more similar to the interwoven pattern of NFP bundles in axonal spheroids, than the dispersed NFP in the somata of motor neurons of ALS patients (Hirano et al., 1984), despite the fact that we observe these NFP accumulations within neuronal somata in our SOD-1 transgenic mice. The neurofilamentous accumulations are also similar to the ultrastructural appearance of intermediate filaments within motor neurons of transgenic mice overexpressing (Côté et al., 1993; Xu et al., 1993), or expressing altered (Lee et al., 1994), NFP. Cytoplasmic NFP inclusions have only been reported in one other line of SOD-1 transgenic mice, the low expressor of the G93A SOD-1 mutant (Dal Canto and Gurney, 1997). In these mice, dense bundles of intermediate filaments were also observed in the somata of motor neurons. Neurons with pathologic alterations in NFP also manifest both nuclear changes (*i.e.*, irregular shape and chromatin clumping), as well as cytoplasmic alterations (abnormal mitochondria and microvacuoles), suggesting that these neurons are undergoing degeneration. Adjacent neurons whose cytoplasm did not contain these bundles of NFP did not show these signs of degeneration. The observation of microvacuoles is extremely interesting, as light microscopic analysis of spinal cord sections from G86R SOD-1 transgenic mice failed to detect these pathologic structures. Perhaps the SOD-1 transgenic mice in this study are developing vacuoles, but the progression of this pathology is retarded compared to the G37R and G93A mice, which both have numerous large vacuoles in presymptomatic mice. The similarity of pathologic specimens from ALS patients and NFP transgenic mice with the SOD-1 transgenic mice further supports the hypothesis that there are common components to their mechanisms of degeneration.

Comparison to other SOD-1 transgenic mice

In addition to the G86R SOD-1 transgenic mice, the time course of neuronal degeneration and other reflections of neuropathology have also been investigated in SOD-

1 transgenic mice with different point mutations in the SOD-1 gene, specifically G93A (Chiu et al., 1995; Tu et al., 1996), G37R (Wong et al., 1995), and G85R, which is the human counterpart to our mouse SOD-1 mutation (Bruijn et al., 1997b). All of these transgenic mice have a mutated form of the human SOD-1 gene, as opposed to the mice used in this study which have a mutation in the mouse SOD-1 gene. Despite the differences in the genetics of the mice, the pathology and time course of pathology is remarkably similar. First, all SOD-1 transgenic mice fail to show motor neuron loss prior to onset of symptoms, and the motor neuron loss at endstage for all mice is approximately 50%. Quantification of motor neuron loss in the other transgenic mice was not made using unbiased counting techniques, and most of the studies looked at ventral root axons as a reflection of motor neuron cell loss, and yet, the results of these studies are highly consistent with our own. Second, in the transgenic lines that show NFP pathology (*i.e.*, G93A, G37R, and G86R), this pathology does not occur until the onset of symptoms. In contrast to neuron loss and NFP pathology, the timing of astrocytosis appears to be less consistent. The G37R and G85R transgenic mice display reactive astrocytosis in presymptomatic mice, while G93A and G86R mice do not display astrocytosis prior to the onset of symptoms. Finally, the presence of vacuoles within neuropil and neuronal somata is also quite dissimilar, with the G37R and G93A mice showing vacuolation presymptomatically, the G86R mice showing microvacuoles that are only observed in electron microscopic photographs from symptomatic mice, and the G85R mice not displaying vacuoles at any time point. At this point, we do not understand why the different SOD-1 mutations give slightly different pathologic presentations in transgenic mice. The insertion of mutant genes from different species (*e.g.*, mouse and human) should not be overlooked as one possible reason, however, since transgenic mice overexpressing wild-type human SOD-1 exhibit vacuolation of motor neurons (Dal Canto and Gurney, 1995) and abnormalities in the neuromuscular junction of the hypoglossus muscle (Avraham et al., 1988). Interestingly, despite the many differences, the mice have in common that they do

not have any motor neuron loss or NFP pathology prior to the onset of symptoms.

Selective vulnerability of both motor neurons and interneurons

A particularly interesting finding from this study is the identical age of onset for loss of interneurons as for motor neurons. Published autopsy results from humans with ALS have suggested that although spinal interneurons degenerate, this degeneration likely occurs secondary to the loss of spinal motor neurons (Hirano, 1991). This conclusion has been based on qualitative estimations of cell loss and morphometric analyses of cell size in patients with severe versus moderate ALS symptoms (Oyanagi et al., 1989; Terao et al., 1994). The heterogeneity of ALS patients, in regards to progression of symptoms and neuropathology, makes these studies, which were based on only a few cases, very difficult to interpret. In addition, qualitative studies comparing motor neuron and interneuron loss with standard histologic preparations are problematic because we have found that significant degeneration of interneurons is more difficult to detect than similar reductions in motor neurons. This is due to the small size of spinal interneurons, as compared to motor neurons, and the lack of clustering into groups, as occurs with the pools of motor neurons. The morphometric studies appear more reliable, but it is difficult to separate motor neuron and interneuron populations based on size characteristics in a neurodegenerative disorder. Using morphometric analyses, investigators have observed that there is a reduction in both large- and medium-sized spinal cord neurons in severely affected patients, while more moderately affected patients show only a loss of large spinal cord neurons (Oyanagi et al., 1989; Terao et al., 1994). If the degenerating motor neurons were shrinking prior to dying, than this would elevate the number of medium-sized neurons and mask a potential reduction in these neurons, which are presumed to be spinal interneurons. The lack of any study in human ALS that accurately quantified both the loss of interneurons and the motor neurons, makes our study of the SOD-1 transgenic model of ALS particularly interesting. We had previously observed that a population of interneurons in the

spinal cord of endstage SOD-1 transgenic mice have approximately the same percentage loss as spinal motor neurons (Morrison et al., 1996). We now expand this result to show that temporally the onset of degeneration for these two populations of neurons is the same. These results in the SOD-1 transgenic mouse strongly suggest that the degeneration in the spinal cord of ALS patients is not specifically directed towards motor neurons and involves other neurons as well. Therefore, the search for motor neuron-specific characteristics that lead to the selective vulnerability in ALS may be misguided and a search for broader characteristics of vulnerable neurons in the spinal cord (*i.e.*, their biochemical phenotype) would be more appropriate.

Implications of late degeneration

Why is the degeneration so late and the cell loss so catastrophic? The mutant SOD-1 protein is present since birth, and yet, we find no sign of neuronal damage until the onset of symptoms at 100 days of age. What could account for this delay in neuronal damage? Two general theories could explain the delay and the rapid cell loss. First, perhaps there is an accumulation of toxicity that must reach a threshold level before the neurons are destroyed. One potential toxic process could be the accumulation of proteins damaged by free radicals or oxidants. Mutant SOD-1 is better able to oxidize proteins in the presence of hydrogen peroxide than is wild type SOD-1 (Wiedau-Pazos et al., 1996; Yim et al., 1996). In addition, it has been proposed that mutant SOD-1 will better catalyze the nitration of tyrosines in the presence of peroxynitrite than the wild type enzyme (Beckman et al., 1993). Supporting this hypothesis, increased levels of free 3-nitrotyrosine have been reported in G37R SOD-1 transgenic mice, as compared to control mice (Bruijn et al., 1997a). Either of these reactions, or another reaction catalyzed by the unshielded Cu^{2+} within the mutant SOD-1, would damage cellular components and this damage could accumulate over time until a level is reached at which the neuron is no longer able to function. Another possible toxic process may be the accumulation of an

excitotoxic environment around the neurons. In ALS patients (Rothstein et al., 1995) and the G85R SOD-1 transgenic mice (Bruijn et al., 1997b), investigators have observed a decrease in the glial glutamate transporter, GLT-1. Glutamate transporters are the primary mechanism by which glutamate is removed from the synapse and reducing these transporters would lead to an increase in synaptic glutamate, greater stimulation of glutamate receptors, and excitotoxicity in the postsynaptic neuron (Rothstein, 1995). Perhaps damage to the glutamate transporter is accumulating over the first 100 days and the subsequent elevation in extracellular glutamate levels overwhelms the compensatory mechanisms of the neurons, which leads to degeneration.

In addition to the accumulation of toxicity, a second explanation for the delay in neuronal pathology is that there is a change in the protective mechanisms within neurons with age. Perhaps the neurons in the SOD-1 transgenic mice are constantly stressed compared to neurons in control mice, but they are able to compensate for this stress while the animal is young, but less efficiently as the animal ages. To this point, there is no evidence that this is the case in the SOD-1 transgenic mice. In fact, the different ages of onset and duration of symptoms for the different SOD-1 transgenic mice, and even for high and low expressors with the same mutation, suggest that the increased vulnerability is unlikely due to neuronal aging.

Clearly, the final goal of our research into the pathogenesis of neuronal death in the SOD-1 transgenic mice is the discovery of an effective treatment for the disease. Although no treatment was developed or tested in this study, the results suggest that an effective therapy might be possible, if sensitive enough functional assays were used to reveal the earliest signs of pathology. The neuron loss is both late and precipitous in the SOD-1 transgenic mice. If the time course of neuron loss in ALS is the same as in SOD-1 transgenic mice, then the onset of early clinical symptoms likely occurs with very little neuron loss. Therefore, if a therapy can be devised to protect the remaining neurons in patients with ALS, and the disease can be diagnosed early enough, then the patient will

survive with sufficient neurons intact and a full recovery can reasonably be expected.

Chapter Four

Light and Electron Microscopic Distribution of the AMPA Receptor Subunit, GluR2, in the Spinal Cord of Control and G86R Mutant Superoxide Dismutase Transgenic Mice

Morrison, B.M., W.G.M. Janssen, J.W. Gordon, and J.H. Morrison (1998) Light and electron microscopic distribution of the AMPA receptor subunit, GluR2, in the spinal cord of control and G86R superoxide dismutase transgenic mice. J. Comp. Neurol. *395:*523-534

Abstract

Excitotoxicity has been hypothesized to contribute to the neurodegeneration in ALS. The pattern of selective vulnerability in the spinal cord of ALS patients, mutant SOD-1 transgenic mice, and mice treated with excitotoxins is similar, supporting a role for excitotoxicity in the mechanism of ALS degeneration. The distribution of AMPA receptors with different calcium permeabilities has been proposed as an explanation for this differential vulnerability. GluR2 appears to be dominant for determining the calcium permeability of AMPA receptors, and thus their potential for contributing to excitotoxicity. In the present study, we investigate the cellular and ultrastructural distribution of GluR2-immunoreactivity in the spinal cord of control and G86R SOD-1 transgenic mice. GluR2 immunoreactivity is equally present within vulnerable neurons (*i.e.*, motor neurons and CR-immunoreactive neurons) as well as non-vulnerable neurons (*i.e.*, CB-immunoreactive neurons and dorsal horn neurons). In addition, post-embedding immuno-electron microscopy reveals that GluR2 is present in synapses of dorsal and ventral horn neurons, and that the percentage of labeled synapses and number of immunogold particles per synapse does not vary between these spinal cord regions. Comparing control mice to SOD-1 transgenic mice, the distribution and intensity of GluR2-immunoreactivity, both at the light and electron microscopic levels, does not appear to be altered. The results of this study suggest that the cellular and synaptic distribution of GluR2 is not a determinant of the selective vulnerability observed in SOD-1 transgenic mice or ALS patients.

Introduction

ALS is a neurologic disease characterized by progressive muscle weakness that results from degeneration of both upper and lower motor neurons (Hirano et al., 1967; Hirano, 1991; Tandan, 1994; Adams et al., 1997). There are both sporadic and familial forms of the disease, with familial ALS accounting for approximately 5% of all ALS cases. Clinically and pathologically, the two forms of ALS are virtually identical suggesting common mechanisms of neurodegeneration (Adams et al., 1997). The genetic linkage of mutations in the SOD-1 gene with the development of familial ALS revealed the first factor causally related to the disease (Rosen et al., 1993), and the development of transgenic mice expressing these mutant forms of SOD-1 have provided a valuable animal model of the disease (Gurney et al., 1994; Ripps et al., 1995; Wong et al., 1995; Bruijn et al., 1997b). Interestingly, these mice develop symptoms and pathology that mimic those found in ALS patient without a reduction in the enzymatic clearance of superoxide radical. In addition, SOD-1 knockout mice do not develop motor system degeneration despite a complete absence of SOD-1 enzymatic activity (Reaume et al., 1996). These findings strongly suggest that the mutant forms of SOD-1 are not leading to cell death through a reduction in the SOD-1 clearance of superoxide radical, but rather by acquiring a function which wild-type SOD-1 either does not possess or possesses to a small degree. Although there is some evidence that mutant SOD-1 may catalyze the nitration of tyrosines by peroxynitrite (Beckman et al., 1993; Beal et al., 1997; Bruijn et al., 1997a; Crow et al., 1997a; Ferrante et al., 1997) and the oxidation of proteins by hydrogen peroxide (Wiedau-Pazos et al., 1996; Yim et al., 1996), the critical gain-of-function of the mutant SOD-1, and therefore the mechanism of neurodegeneration in SOD-1 transgenic mice and ALS patients, is currently unknown.

One mechanism that has been proposed to account for ALS neurodegeneration is

excitotoxicity. Excitotoxicity, which results from the overactivation of glutamate receptors, could theoretically be caused by several events: elevated synaptic glutamate, increased number of glutamate receptors, heightened sensitivity of glutamate receptors to agonists, greater activation of intracellular signaling pathway following receptor activation, reduced inhibitory drive on neurons, or diminished effectiveness of an inhibitory mediator of glutamate receptor function. Regardless of the initiating event, a key mediator of excitotoxicity appears to be the concentration of free intracellular Ca^{2+} (Choi, 1987; Meldrum and Garthwaite, 1990; Tymianski et al., 1993). Increased intracellular Ca^{2+} can activate a number of phospholipases, proteases, and endonucleases that could be responsible for the cellular toxicity and death (Orrenius et al., 1992).

In the pathogenesis of ALS, excitotoxicity appears to be secondary to increased synaptic glutamate. ALS patients have elevated levels of plasma and cerebrospinal fluid glutamate and reduced parenchymal glutamate, suggesting an alteration in the metabolism and processing of glutamate (Perry et al., 1987b; Plaitakis and Caroscio, 1987; Plaitakis et al., 1988; Rothstein et al., 1990). In addition, ALS patients have a decrease in both glutamate transporter activity and the amount of a specific glial glutamate transporter, GLT-1, in affected areas of the nervous system such as motor cortex and the spinal cord, but not in unaffected areas such as the hippocampus and caudate (Rothstein et al., 1992; Rothstein et al., 1995). Two other glutamate transporters, EAAC1 and GLAST, were moderately reduced and unaffected, respectively. In contrast to the reduction of GLT-1 protein in the nervous system, there is no reduction in the level of mRNA for any of the glutamate transporters, suggesting that the alteration is post-transcriptional (Bristol and Rothstein, 1996). In addition, reducing glutamate transporter activity, either by pharmacological antagonists (Rothstein et al., 1993) or antisense oligonucleotides (Rothstein et al., 1996), in a spinal cord slice preparation or *in vivo* leads to elevated extracellular glutamate and selective degeneration of spinal motor neurons. This modification of glutamate transporters could account for the observed alterations in glutamate metabolism.

The mechanism leading to altered glutamate transporter activity in ALS is currently unknown. However, free radicals, which may be increased in familial ALS patients with mutations in the SOD-1 gene, alter glutamate transporter activity (Pogun et al., 1994; Volterra et al., 1994), and may be one mechanism by which transporter activity is reduced in ALS patients.

Whether or not a particular neuron degenerates following increased synaptic glutamate may depend upon several factors including the potential for binding or sequestering free intracellular calcium, and also the specific glutamate receptors present in excitatory synapses. Calcium-binding proteins provide one mechanism by which free intracellular calcium is reduced within neurons (Mattson et al., 1991; Lledo et al., 1992; Chard et al., 1993; Lukas and Jones, 1994). Spinal motor neurons are remarkable for their lack of CB, CR, and PV (Garcia-Segura et al., 1984; Antal et al., 1990; Ince et al., 1993; Alexianu et al., 1994; Ren and Ruda, 1994; Morrison et al., 1996), and thus may have a reduced capacity for buffering calcium loads and an increased vulnerability to excitotoxicity. In contrast to calcium-binding proteins, the distribution of glutamate receptor subunits in the spinal cord and their potential link to patterns of selective vulnerability have not been adequately studied.

Glutamate receptors fall into two general categories, ionotropic and metabotropic [for reviews see (Nakanishi, 1992; Seeburg, 1993; Hollmann and Heinemann, 1994)]. The ionotropic receptors, which flux Na^+ and sometimes Ca^{2+} following ligand-binding, are divided into three groups: NMDA, AMPA, and kainate. Excitotoxicity was originally attributed primarily to NMDA receptors (Choi, 1987), as these receptors are permeable to Ca^{2+} when ligand-binding and depolarization are coupled (Hollmann and Heinemann, 1994), but recent studies have implicated AMPA and/or kainate receptors in excitotoxicity, particularly with respect to potential excitotoxic mechanisms in ALS. First, neurodegeneration following inhibition of glutamate transporters is attenuated by antagonists to non-NMDA glutamate receptors, but not by antagonists to NMDA receptors (Rothstein et

al., 1993). Second, NMDA infused into the spinal cord leads primarily to degeneration in the dorsal horns of the spinal cord, while infusion of kainate, which would activate AMPA and kainate receptors, leads to selective degeneration in the ventral horns (Ikonomidou et al., 1996). Third, motor neurons are selectively vulnerable to kainate exposure in mixed spinal cord cultures (Carriedo et al., 1996). Non-NMDA glutamate receptors appear to be pentamers, composed of some combination of GluR1-4 for AMPA receptors and GluR5-7 and KA-1 and -2 for kainate receptors (Hollmann et al., 1989; Boulter et al., 1990; Keinanen et al., 1990; Brose et al., 1994). Certain subunit transcripts are subject to RNA editing, a mechanism which strongly influences properties such as Ca^{2+} permeability and rectification characteristics, with GluR2 almost completely edited to the arginine codon at the Q/R site (Sommer et al., 1991; Puchalski et al., 1994). When present in the AMPA receptor, edited GluR2 dominates the Ca^{2+} permeability and current-voltage characteristics, and as such, AMPA receptors that contain GluR2 are not permeable to Ca^{2+} (Geiger et al., 1995).

Given the importance of Ca^{2+} flux in the excitotoxic mechanism of neurodegeneration, it is critical to determine the specific populations of neurons that contain GluR2. All neurons in the spinal cord and motor cortex, areas that have reduced glutamate transporter activity, do not degenerate in ALS (Hirano, 1991; Leigh and Ray-Chaudhuri, 1994). In the G86R SOD-1 transgenic mouse, several populations of neurons in the ventral horn of the spinal cord degenerate [*i.e.*, ChAT-immunoreactive motor neurons and CR-immunoreactive interneurons], while adjacent neurons (*i.e.*, CB-immunoreactive interneurons) do not (Morrison et al., 1996; Morrison et al., 1998). One possible cause of differential vulnerability in this and other animal models of ALS, as well as in human ALS, is the selective distribution of GluR2. If the Ca^{2+} permeability of AMPA receptors is a determinant of selective vulnerability in ALS, then neurons that contain GluR2 should be less vulnerable than neurons that do not contain GluR2.

GluR2 mRNA is found in both dorsal and ventral horn neurons in the rat spinal

cord (Sato et al., 1993; Tolle et al., 1993; Jakowec et al., 1995b; Tolle et al., 1995). In the human spinal cord, both dorsal and ventral horn neurons, including motor neurons, also appear to contain GluR2 mRNA (Tomiyama et al., 1996; Virgo et al., 1996), with the exception of one study that reported motor neurons to be lacking GluR2 mRNA (Williams et al., 1997). The one published study that looked at the distribution of GluR2 protein in the spinal cord, using a polyclonal antibody, found that motor neurons in the rat were lightly immunoreactive for GluR2 when examined by light microscopy, but lacked immunoreactivity in pre-embedded immuno-electron microscopy (Petralia et al., 1997). This inconsistency prevents any definitive conclusions about the localization of GluR2 protein in the spinal cord. In the present study, we investigated the distribution of GluR2 in the spinal cord of mice, using a previously characterized monoclonal antibody (Vissavajjhala et al., 1996), by both confocal microscopy and post-embedding immuno-electron microscopy. In addition to the cellular and synaptic distribution of this protein in control mice, we investigated whether the specific populations of neurons immunoreactive for GluR2 correlated with the neurons that were demonstrated previously to be resistant to degeneration in G86R SOD-1 transgenic mice (Ripps et al., 1995; Morrison et al., 1996; Morrison et al., 1998), and whether the pattern of GluR2 immunoreactivity was altered in G86R SOD-1 transgenic mice.

Materials and Methods

Animals and tissue processing. Transgenic mice with a G86R mutation of the mouse SOD-1 gene and control FVB litter mates, described previously (Ripps et al., 1995), were used in this study. SOD-1 transgenic mice and age-matched controls intended for light microscopic analyses were sacrificed at presymptomatic [means = 72.7 (n=3) and 71.0 (n=3) days old, respectively] and symptomatic [means = 114.0 (n=4) and 113.8 (n=4) days old, respectively] ages. These mice were deeply anesthetized with 0.1 ml of an equal mix-

ture of ketamine (100 mg/ml) and xylazine (20 mg/ml) injected intraperitoneally, and then perfused transcardially with cold 1% paraformaldehyde in 0.1 M phosphate buffered saline (PBS), pH 7.2, for 1 minute followed by cold 4% paraformaldehyde/ 0.025% glutaraldehyde in 0.1 M PBS for 10 minutes. In addition to control and SOD-1 transgenic mice, one rat was perfused transcardially, after being given a lethal dose of chloral hydrate, with cold 1% paraformaldehyde in 0.1 M phosphate buffered saline (PBS), pH 7.2, for 1 minute followed by cold 4% paraformaldehyde in 0.1 M PBS for 10 minutes. The spinal cords of all animals were rapidly removed, blocked coronally, post-fixed in 4% paraformaldehyde in 0.1 M PBS for 6 hours, and cut on a vibratome at a thickness of 50 µm. Mice intended for electron microscopy were perfused transcardially with cold 1% paraformaldehyde in 0.1 M PBS for 1 minute followed by cold 1% paraformaldehyde/ 2.5% glutaraldehyde/ 0.1% picric acid in 0.1 M PBS for 10 minutes. The spinal cords were removed, blocked, post-fixed for 2 hours in a 1% paraformaldehyde/ 2.5% glutaraldehyde/ 0.1% picric acid solution, and cut on a vibratome at a thickness of 50 µm. All protocols were conducted within NIH guidelines for animal research and were approved by the Institutional Animal Care and Use Committee (IACUC).

Immunofluorescence for light microscopy. Sections for single-label immunofluorescence were incubated at 4 °C overnight in a monoclonal antibody to GluR2 [Chemicon, Temecula, CA; for antibody characterization see (Vissavajjhala et al., 1996)] diluted to 3.36 µg/ml in 0.01 M PBS, pH 7.2, containing 0.5% BSA and 2% normal horse serum (diluent). The sections were then washed in 0.01 M PBS, incubated in diluent containing 1:400 biotinylated horse anti-mouse IgG (Vector laboratories, Burlingame, CA) for 1 hour, washed, and incubated for 1 hour in diluent containing 1:200 FITC Avidin D (Vector laboratories). In a series of control spinal cord sections, GluR2 immunoreactivity was blocked by pre-incubation of the primary antibody with a 100 fold molar excess of GluR2 fusion protein prior to the overnight incubation in primary antibody. The primary anti-

body and fusion protein were incubated on a nutator overnight at 4 °C, centrifuged for 10 minutes, and then incubated with spinal cord sections.

Sections for double-label immunofluorescence were incubated at 4 °C overnight in diluent that contained the monoclonal antibody to GluR2 (3.36 μg/ml) as well as a polyclonal antibody to ChAT (Chemicon; 1:50), CR (SWant, Bellinzona, Switzerland; 1:2000), or CB (SWant; 1:2000). The sections were washed in 0.01 M PBS, incubated in diluent containing 1:400 biotinylated horse anti-mouse IgG and either 1:200 texas red rabbit anti-goat IgG (for ChAT antibody) or 1:200 texas red horse anti-rabbit IgG (for CR or CB antibodies) for 2 hours, washed, and incubated for 1 hour in diluent containing 1:200 FITC Avidin D. The species specificity of the secondary antibodies was verified by omitting one or both of the primary antibodies.

Quantification of double-labeled immunofluorescence. For each double-labeling combination, a 1:40 series from the cervical enlargement was immunostained, as described above, and analyzed on a Zeiss Axiophot fluorescent microscope using a Plan-Neofluar 40x objective. The percentage of double-labeling was determined by examining each immunofluorescent cell in the ventral portion of the spinal cord with filters that allowed either FITC wavelengths or Texas Red wavelengths, but not both, to pass and then counting single-labeled vs. double-labeled cells. While the quantitative analysis was carried out on the Zeiss Axiophot, high resolution qualitative analysis and photomicrographs of fluorescent double-labeled sections were made on a Zeiss laser scanning confocal microscope 410. The z-axis resolution of the confocal microscope allowed for a more definitive differentiation between cytoplasmic colocalization and superimposition of independently labeled profiles.

Post-embedding immuno-electron microscopy. Sections were processed by a technique modified from Phend et al. (1992, 1995). Briefly, the sections were treated sequentially

with 1% tannic acid/maleate buffer (MB), 0.1% $CaCl_2$/MB, 1% uranyl acetate (UA)/MB, and 0.5% platinum chloride/MB. Sections were then dehydrated through a graded ethanol series up to 70% ethanol, treated with 1% *para*-phenylenediamine, 1% UA/70% ethanol, dehydrated to 100% ethanol, treated with propylene oxide and infiltrated with Epon-Spurr (4:6) resin. Sections were placed between strips of ACLAR plastic film and polymerized at 50 °C for 36 hours. Regions from the dorsal and ventral horns were cut out and glued onto plastic blocks. Thin sections were collected on 300 mesh uncoated nickle grids. Grids were treated with 10% sodium *meta*-periodate/TBS, pH 7.6, followed by treatment with 1% sodium borohydride/dH_2O. Grids were preincubated in TBS, pH 7.6, containing 10% normal goat serum (NGS), 0.5% BSA, 0.1% gelatin and 0.01% NP-10, and then incubated at 40 °C overnight in primary antibody (monoclonal GluR2 antibody at 2.25 ug/ml) in TBS, pH 7.6, containing 1% NGS, 0.5% BSA, 0.1% gelatin and 0.01% NP-10. The grids were washed in TBS, pH 8.2, and then incubated for 1 hour in secondary antibody [1:40 goat anti-mouse IgG (H&L) conjugated to 10 nm gold particles] in TBS, pH 8.2, containing 0.1% NGS, 0.5% BSA, and 0.1% gelatin. The grids were then washed, stained with lead citrate and UA, and examined at 60 kV on a Zeiss CH-10 electron microscope.

Quantification of electron microscopy. Grids from dorsal and ventral horns of the spinal cord of control and SOD-1 transgenic mice, which had been processed for GluR2 post-embedding immunoelectron microscopy, were analyzed on a Zeiss CH-10 electron microscope at 60 kV. For each area (*i.e.*, dorsal or ventral horn), GluR2 immunoreactivity on one randomly chosen mesh from each of three grids was quantified. For each morphologically-recognized synapse in this mesh, the presence or absence of immunogold particles was determined; and if present, the number of gold particles was recorded. From these data, the percentage of GluR2 immunoreactive synapses and the average number of gold particles per labeled synapse was determined for the dorsal and ventral horns of con-

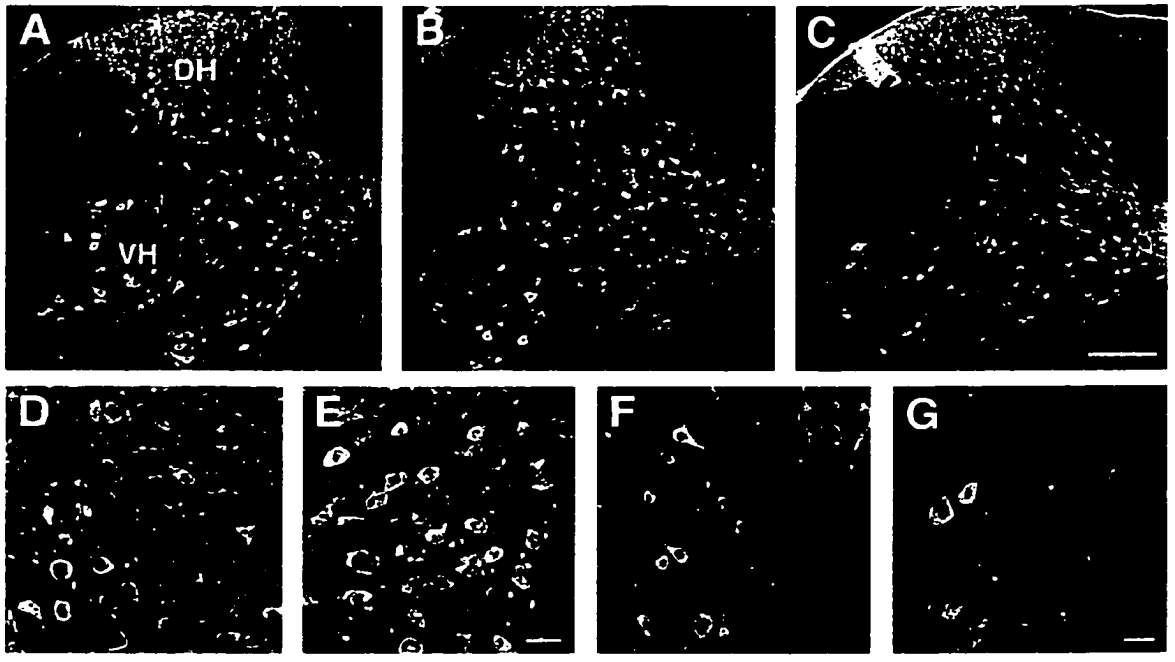

Figure 4-1. GluR2 immunofluorescence in the cervical spinal cord enlargement of control (A), presymptomatic (B), and symptomatic (C) SOD-1 transgenic mice. Neurons in both the dorsal horn (*DH*) and ventral horn (*VH*) appear to be immunoreactive for GluR2. In the ventral horn, several large motor neurons are strongly immunoreactive for GluR2 in all three groups of mice. Notice that there is little immunoreactivity in the white matter of the spinal cord. In D - G, GluR2 immunoreactive neurons from the dorsal (D,E) and ventral (F,G) horns of control (D,F) and symptomatic SOD-1 transgenic (E,G) mice are photographed at a higher magnification. Scale bar: A-C, 200 μm; D and E, 10 μm; F and G , 40 μm.

trol and SOD-1 transgenic mice.

Figure Preparation. Photomicrographs taken on the Zeiss CH-10 electron microscope were developed, scanned with an AGFA Arcus II scanner, and then imported into Adobe Photoshop. Photomicrographs taken on the Zeiss laser scanning confocal microscope 410 were directly imported into Adobe Photoshop. In Adobe Photoshop, the images were sized, labeled, and optimized for contrast and brightness.

Results

Single-label immunofluorescence. GluR2 immunoreactivity was present within all laminae of the mouse spinal cord (Fig. 4-1A). In dorsal (Fig. 4-1D) and ventral horns (Fig. 4-1F), both somata and neuropil were immunoreactive, although somata appeared to be

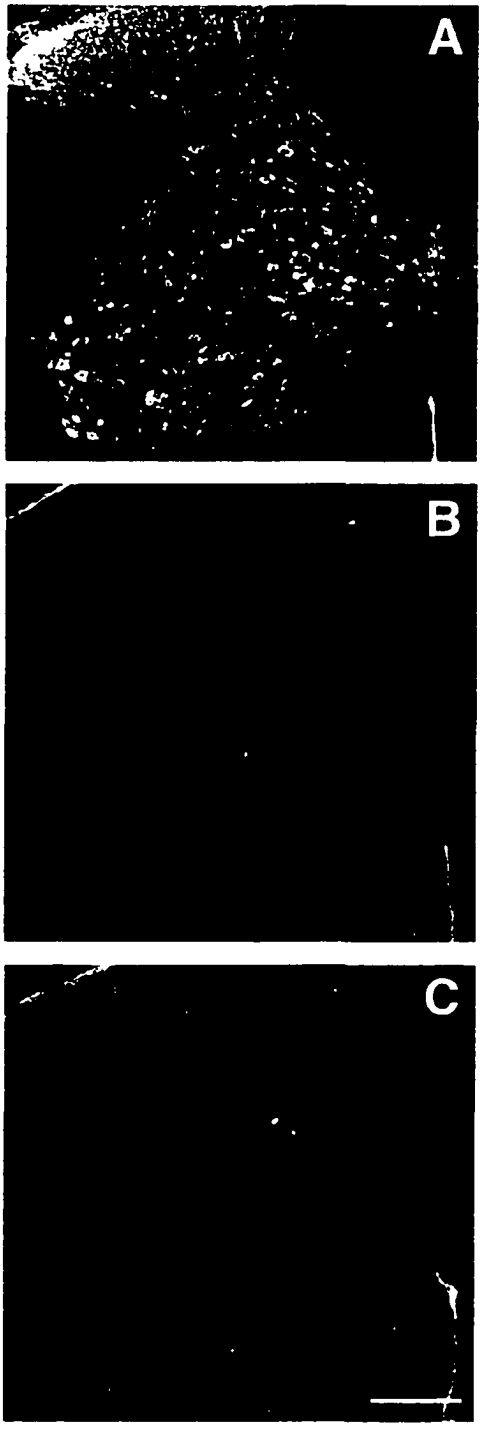

Figure 4-2. Blocking of GluR2 immunofluorescence. As compared to a spinal cord section immunostained by the normal procedure (A), pre-incubating the GluR2 antibody with GluR2 fusion protein (B) or omitting the GluR2 antibody (C) completely attenuate GluR2 immunofluorescence. Scale bar: 200 μm.

more intensely labeled. Within the ventral horn, large neurons that were likely to be motor neurons, as well as smaller neurons, were clearly immunoreactive for GluR2 (Fig. 4-1A,F). In contrast to the numerous immunoreactive structures in the gray matter, there appeared to be an almost complete absence of immunoreactivity in the white matter of the spinal cord.

In addition to the distribution of GluR2 immunoreactivity in control mice, we were interested in whether this distribution was altered in SOD-1 transgenic mice. To this end, spinal cord sections from presymptomatic and symptomatic SOD-1 transgenic mice were processed for GluR2 immunofluorescence. GluR2 immunoreactivity in presymptomatic SOD-1 transgenic mice did not appear to be different, in either distribution or intensity, than GluR2 immunoreactivity in control mice (Fig. 4-1B). In the spinal cord of symptomatic SOD-1 transgenic mice, as compared to control mice, there was an apparent reduction in the density of GluR2-immunoreactive neurons and neuropil within the ventral horn (Fig. 4-1C,G), but not the dorsal horn (Fig. 4-1C,E) that corresponded to the previously described neuron loss in the spinal cord of these mice (Morrison et al., 1996; Morrison et al.,

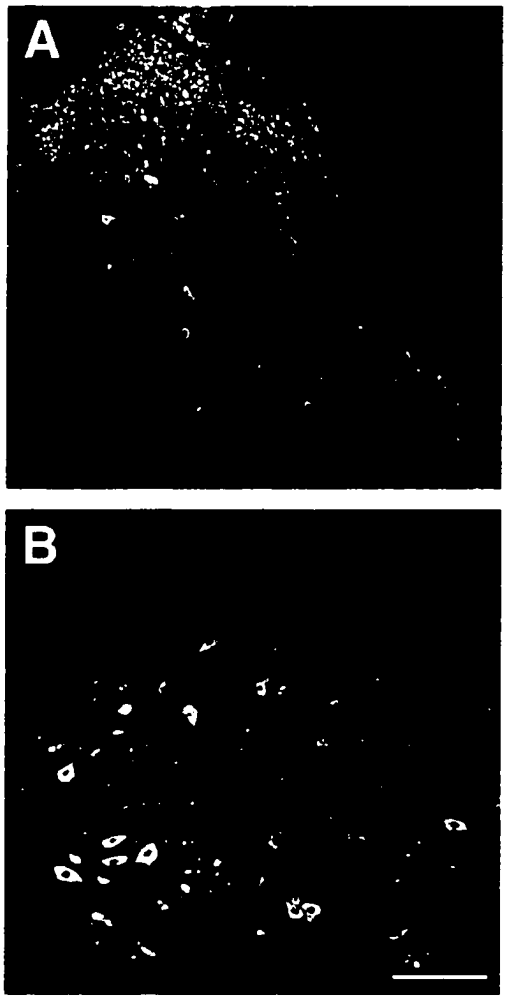

Figure 4-3. GluR2 immunofluorescence in the cervical spinal cord enlargement of a rat. Immunoreactivity for GluR2 is clearly evident in both the dorsal (A) and ventral (B) horns of the spinal cord. The pattern of immunoreactivity is very similar to the mouse spinal cord, and the motor neurons are strongly immunoreactive for GluR2. Scale bar: 200 μm.

1998). Within the surviving neurons, there was no apparent alteration in the intensity of GluR2 immunoreactivity.

Evaluation of antibody specificity. The GluR2-specific antibody utilized in these experiments was characterized previously (Vissavajjhala et al., 1996). The GluR2 antibody was shown to be specific for GluR2 in radioimmunoassays, Western blots of transfected cells and hippocampal homogenates, and immunocytochemistry of transfected cells, rat hippocampus, and rat neocortex. Because the present experiment was done in mouse spinal cord, we completed two additional controls for the specificity of the antibody binding. First, pre-incubation of the antibody with GluR2 fusion protein completely blocked the immunofluorescence for GluR2 in the mouse spinal cord (Fig. 4-2B), as compared to a section that was incubated in non-blocked GluR2 antibody (Fig. 4-2A). Sections immunostained with the blocked GluR2 antibody (Fig. 4-2B) were identical to sections that were not incubated with any GluR2 antibody (Fig. 4-2C). Second, to investigate whether the antibody has differential specificity in the mouse as compared to the rat, which was the species in which the antibody specificity was originally tested (Vissavajjhala et al., 1996), the distribution of GluR2 immunoreactivity in the spinal cord of a rat was investigated. The pattern of immunoreactivity was identical to

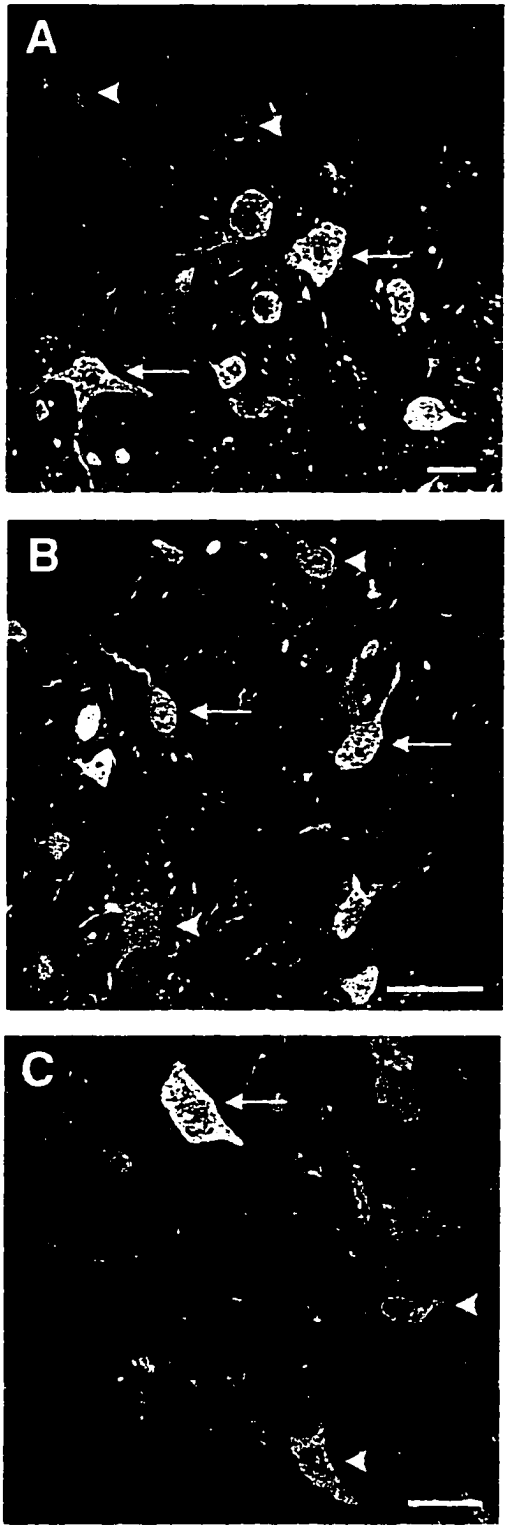

Figure 4-4. Double-labeling of GluR2 with ChAT (A), CR (B), and CB (C). In all three panels, GluR2 immunofluorescence is in green, while ChAT, CR, and CB are in red. Neurons immunoreactive only for GluR2 (*arrowheads*), as well as double-labeled neurons (*arrows*), are evident in each photomicrograph. It is apparent in these photomicrographs that there are no single-labeled ChAT-, CR-, or CB-immunoreactive neurons, but rather these neuronal populations are all double labeled with GluR2. Scale bars: A, 40 μm; B and C, 20 μm.

that observed in the mouse. Neurons and neuropil in both the dorsal (Fig. 4-3A) and ventral horns (Fig. 4-3B) were immunoreactive for GluR2. Taken together, these experiments indicate that the GluR2 immunoreactivity in mouse spinal cord is as specific as the GluR2 immunoreactivity previously described in rat hippocampus and neocortex.

Double-labeling immunofluorescence. In order to investigate the specific populations of spinal cord neurons that are immunoreactive for GluR2, we double-labeled sections for GluR2 and either ChAT, CR, or CB (Fig. 4-4). ChAT-immunoreactive neurons in the ventral portion of the spinal cord are motor neurons, while both CR-immunoreactive and CB-immunoreactive neurons are spinal interneurons (Morrison et al., 1996). These neuronal populations are differentially vulnerable in G86R SOD-1 transgenic mice. ChAT- and CR-immunoreactive neurons degenerate, while CB-immunoreac-

Table 4-1. Percentage colocalization of GluR2-immunoreactivity within neurons immunoreactive for ChAT, CR, and CB in the ventral spinal cord of control and SOD-1 transgenic mice

	Control	SOD-1 transgenic
ChAT	100 % (401/401)	100 % (432/432)
CR	97.7 % (861/881)	99.4% (927/933)
CB	99.3 % (282/284)	97.2 % (280/288)

tive neurons are not vulnerable and do not degenerate (Morrison et al., 1996; Morrison et al., 1998). Qualitatively, it appeared that almost 100% of these neuronal populations were immunoreactive for GluR2 (Fig. 4-4). The percentage co-localization of GluR2 with these markers for distinct neuronal populations in the spinal cord was quantified (Table 4-1), and the results from both control and SOD-1 transgenic mice support our qualitative observation. In respect to these three neuronal populations in the ventral portion of the mouse spinal cord, GluR2 appears to be ubiquitously expressed.

Post-embedding immunoelectron microscopy. GluR2 fluorescence is present within virtually all neurons of the mouse spinal cord. Most of this immunoreactivity appears to be a cytoplasmic or synthetic pool of GluR2, not the pool of GluR2 localized to the synapse. Since the function of GluR2 as a component of the AMPA receptor occurs at the synapse, and synapses can only be resolved by electron microscopy, mouse spinal cord sections were processed for post-embedding GluR2 immunoelectron microscopy. GluR2 immunoreactivity, as labeled by 10 nm gold particles, was clearly present in numerous synapses within both the dorsal and ventral horns of the spinal cord (Fig. 4-5). In addition to being present in control mice (Fig. 4-5A,B), GluR2 was also clearly localized to synapses of the dorsal and ventral horn in presymptomatic (Fig. 4-5C,D) and symptomatic (Fig. 4-5E,F) SOD-1 transgenic mice. Within the ventral horn of the spinal cord in both control and SOD-1 transgenic mice, many GluR2-immunoreactive synapses had the mor-

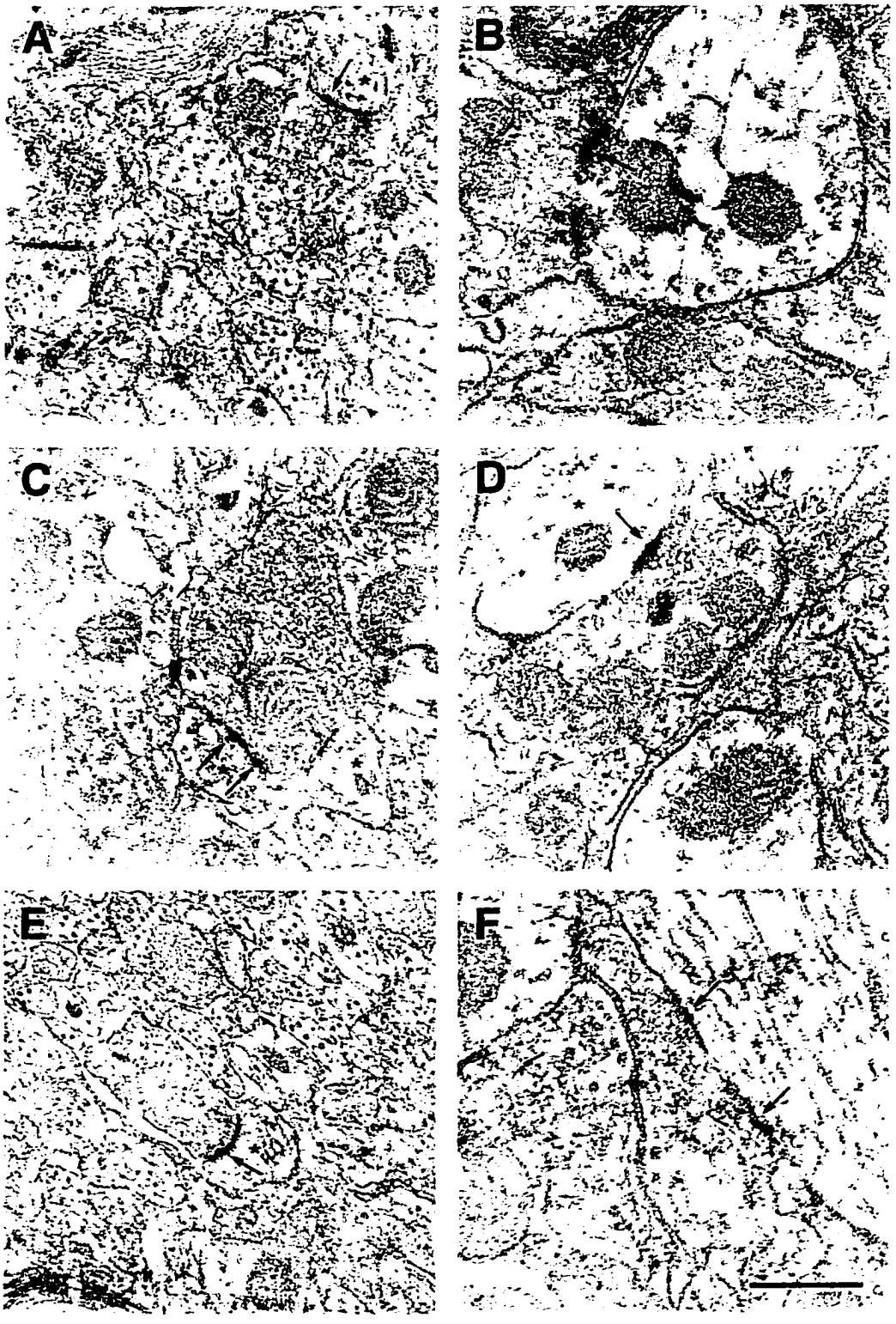

Figure 4-5. Post-embedding immunoelectron microscopy for GluR2. GluR2-immunoreactive synapses (*indicated by arrows*) are evident in both the dorsal (A,C,E) and ventral (B,D,F) horns of control (A,B), pre-symptomatic SOD-1 transgenic (C,D), and symptomatic SOD-1 transgenic (E,F) mice. The immunogold particles clearly cluster within synapses in these photomicrographs. Post-synaptic elements are indicated by *asterisks*, and the post-synaptic elements of unlabeled synapses are indicated by *asterisks* without *arrows* in A and C. Scale bar: 0.4 μm.

Table 4-2. Quantification of post-embedding electron microscopy for GluR2

Animal	Region of spinal cord	Percentage of synapses labeled	Number of gold particles per labeled synapse (mean ± S.E.M.)
Control 1	dorsal horn	38.6 % (157 / 407)	2.05 ± 0.10
	ventral horn	35.6 % (160 / 450)	2.39 ± 0.13
Control 2	dorsal horn	29.3 % (132 / 450)	2.30 ± 0.12
	ventral horn	24.9 % (112 / 450)	2.58 ± 0.19
SOD-1	dorsal horn	27.1 % (122 / 450)	2.41 ± 0.15
pre-symptoms	ventral horn	35.1 % (123 / 350)	2.85 ± 0.14
SOD-1	dorsal horn	29.7 % (104 / 350)	2.21 ± 0.16
symptomatic	ventral horn	33.5 % (134 / 400)	2.58 ± 0.15

phologic characteristics of a symmetric synapse (*i.e.*, lack of a clearly defined post-synaptic density). Contrary to what has been described in the cerebral cortex (Hendrickson et al., 1981; Hendry et al., 1983; DeFelipe et al., 1988; Peters and Harriman, 1992), this suggests that a subset of excitatory synapses in the ventral horn of the spinal cord are symmetric. This alteration in morphology from the conventional asymmetric excitatory synapse is intriguing, and suggests that the post-synaptic receptor complex of these synapses may differ biochemically and functionally from the asymmetric AMPA-mediated synapses in the dorsal horn of the spinal cord or other regions of the central nervous system.

In addition to our qualitative observations, we quantified the percentage of GluR2-labeled synapses and the number of gold particles in dorsal and ventral horns of control and SOD-1 transgenic mice. The percentage of labeled synapses was not different between the dorsal and ventral horns, nor was it altered in SOD-1 transgenic mice (Table 4-2). In addition, the mean number of gold particles per labeled synapse was similar for

all spinal cord regions in control and SOD-1 transgenic mice. Therefore, there is no quantitative difference in the synaptic localization of GluR2 between dorsal and ventral horns of control mice, or between these regions in control and SOD-1 transgenic mice.

Discussion

In the present study, we have investigated the distribution of the AMPA receptor subunit, GluR2, in the spinal cord. GluR2 is present within both dorsal and ventral horn neurons. Within the ventral horn, almost 100% of ChAT-immunoreactive motor neurons, CR-immunoreactive interneurons, and CB-immunoreactive interneurons were immunolabeled for GluR2. Because light microscopy of GluR2 primarily labeled the presumed synthetic pool of this protein, post-embedding immunoelectron microscopy for GluR2 was utilized to localize this AMPA receptor subunit to the synapse. GluR2 was present in numerous synapses in both the dorsal and ventral horns. Quantifying the percentage of labeled synapses and the number of immunogold particles per labeled synapse demonstrated that there was no apparent difference between the density and distribution of GluR2 within the synapses of the ventral horn versus the dorsal horn. These normative data in the spinal cord strongly suggest that the presence or absence of GluR2 is not a determinant of the selective vulnerability of specific spinal cord neurons, since vulnerable neurons (*i.e.*, motor neurons and CR-immunoreactive neurons) as well as non-vulnerable neurons (*i.e.*, CB-immunoreactive neurons and dorsal horn neurons) in SOD-1 transgenic mice (Morrison et al., 1996; Morrison et al., 1998) are strongly immunoreactive for GluR2 and have numerous GluR2-immunoreactive synapses. These results obviously do not rule out the possibility that AMPA receptors which do not contain GluR2, and thus flux Ca^{2+}, may coexist with GluR2-containing receptors in the synapses of vulnerable neurons. However, the hypothesis that vulnerable neurons in the spinal cord lack GluR2 and GluR2-containing synapses, whereas resistant neurons contain GluR2, does not appear to

be validated by our findings. In addition to being relevant to SOD-1 transgenic mice, these data are relevant to any model of motor neuron degeneration where AMPA receptor-mediated excitotoxicity is a potential mechanism of neuronal degeneration.

In addition to investigating the distribution of GluR2 in the spinal cord of control mice, we evaluated whether there was any alteration in the distribution or expression of GluR2 in the spinal cord of G86R SOD-1 transgenic mice, as has been reported in models of transient forebrain ischemia (Pellegrini-Giampietro et al., 1992; Gorter et al., 1997) and cerebellar degeneration (Margulies et al., 1993). With the exception of the reduced density of neurons in the ventral horn of symptomatic SOD-1 transgenic mice, GluR2 immunoreactivity was unaltered in SOD-1 transgenic mice. Both dorsal and ventral horn neurons in transgenic mice were immunoreactive for GluR2, and the intensity of this immunoreactivity was not markedly different from control mice. The percentage double-labeling of ChAT-, CR-, and CB-immunoreactive neurons with GluR2 in SOD-1 transgenic mice was unaltered from control mice. In addition, GluR2 was present in approximately the same percentage of synapses, and with the same mean number of immunogold particles, in the dorsal and ventral horns of SOD-1 transgenic mice as in control mice. These results demonstrate that the distribution of GluR2, even at the synaptic level, is unaltered in G86R SOD-1 transgenic mice.

Motor neurons and glutamate receptors

Our immunocytochemical results expand the available information on the glutamate receptor profile of motor neurons. Previous studies have demonstrated that motor neurons in rodent spinal cord contain GluR2 mRNA (Sato et al., 1993; Tolle et al., 1993; Jakowec et al., 1995b; Tolle et al., 1995; Temkin et al., 1997), and our study extends these findings to GluR2 protein. In addition to GluR2, *in situ* hybridization studies have demonstrated the presence of mRNA for AMPA receptor subunits GluR1, GluR3 and GluR4 in motor neurons (Sato et al., 1993; Tolle et al., 1993; Jakowec et al., 1995b; Tolle

et al., 1995; Tomiyama et al., 1996; Virgo et al., 1996), and immunocytochemistry has demonstrated immunoreactivity for GluR1, GluR2/3, and GluR4 in motor neurons (Martin et al., 1993; Tachibana et al., 1994; Bonnot et al., 1996; Williams et al., 1996). In addition to these AMPA receptor subunits, motor neurons also contain NMDA and kainate receptor subunits, as demonstrated by *in situ* hybridization (Furuyama et al., 1993; Luque et al., 1994) and immunocytochemistry (Petralia et al., 1994a; Petralia et al., 1994b; Bonnot et al., 1996). Therefore, motor neurons *in situ* appear to have NMDA, kainate and AMPA receptors, with multiple subunits represented in each class of glutamate receptor. For the most part, the glutamate receptor subunits expressed by motor neurons do not appear to differ from other spinal cord neurons. The one consistent difference between motor neurons and other spinal cord neurons appears to be a relative lack of GluR1. This deficit, which is apparent in adult mice, appears to develop postnatally in rodents (Jakowec et al., 1995a; Jakowec et al., 1995b), and has been described by both *in situ* hybridization (Furuyama et al., 1993; Sato et al., 1993; Tolle et al., 1993) and immunocytochemistry (Tachibana et al., 1994; Williams et al., 1996). It is unclear whether a glutamate receptor which lacks GluR1 would be functionally distinct from one that contained this subunit, however this property of glutamate receptors should be investigated because it is the only reported difference between the glutamate receptor subunits expressed in motor neurons versus those expressed in other spinal cord neurons, and therefore, may contribute to the selective vulnerability of motor neurons.

Motor neurons and calcium permeability

Motor neurons, which are preferentially vulnerable to kainate-induced toxicity *in vivo* (Ikonomidou et al., 1996 and *in vitro* (Carriedo et al., 1995), selectively take up cobalt in the presence of kainate, suggesting the presence of Ca^{2+}-permeable AMPA/kainate receptors (Carriedo et al., 1996). If GluR2 is present within spinal motor neurons than how do we explain the observed Ca^{2+}-permeability? The most obvious

explanation is that the cobalt uptake study was conducted in spinal cord cultures, while our study and others that have investigated the distribution of glutamate receptor subunits have been conducted *in situ*. Perhaps embryonic-derived motor neuron cultures do not develop glutamate receptors in an identical manner to motor neurons that develop to maturity *in situ*. This has been demonstrated in primary cultures obtained from neocortex, hippocampus, and cerebellum (Schmitt et al., 1996; Paschen et al., 1997). In these studies, the percentage of Q/R edited GluR5 and GluR6 mRNA, as well as the amount of total GluR5 mRNA, is altered in embryonic and cultured neurons as compared to adult neurons.

In addition to this putative difference between cultured and *in situ* neurons, our results cannot exclude the possibility that a population of GluR2-negative AMPA receptors may exist on motor neurons and be responsible for the kainate-induced neurotoxicity and cobalt permeability. This could be achieved by an increase in a non-GluR2 AMPA receptor subunit relative to GluR2, for the stoichiometry between AMPA receptor subunits, rather than the total amount of GluR2, is likely the dominant determinant of Ca^{2+} permeability for a population of AMPA receptors. A few neurons and glia have been shown to totally lack GluR2, however most neurons, including motor neurons, contain some level of GluR2. The relative amount of GluR2 versus other AMPA receptor subunits appears to be critical for determining the Ca^{2+} permeability of AMPA receptors within a given neuron (Geiger et al., 1995). Although a large differential between GluR2 and other AMPA subunits cannot be excluded, the relative amount of GluR2 mRNA in motor neurons does not appear to be markedly less than non-GluR2 AMPA subunits (Furuyama et al., 1993; Sato et al., 1993; Tolle et al., 1993). As such, GluR2-lacking AMPA receptors in motor neurons appear to be unlikely as a driving force for their vulnerability.

A second putative mechanism for Ca^{2+}-permeable AMPA receptors in motor neurons is that while GluR2 is present, it may not be edited at the Q/R site. The incorporation of unedited GluR2 into an AMPA receptor results in a receptor that is permeable to

Ca^{2+} (Burnashev et al., 1992; Burnashev et al., 1995), and therefore could provide an explanation for Ca^{2+}-permeable AMPA receptors that appear to contain GluR2. Neither the GluR2-specific antibody used in this study nor the riboprobes used in the *in situ* hybridization studies are capable of discriminating between edited and non-edited forms. Utilizing RT-PCR, only the edited form of GluR2 mRNA has been detected in the rodent brain as a whole (Sommer et al., 1991) or in specific neurons (Jonas et al., 1994; Geiger et al., 1995), but until recently, the spinal cord and motor neurons had not been directly investigated. However, a recently published study found that all of the GluR2 mRNA in avian motor neuron cultures was RNA edited at the Q/R site (Temkin et al., 1997). Although it is possible that rodent and primate motor neurons differ from chick motor neurons, and the RNA editing of GluR2 in mammalian motor neurons should be investigated, it is unlikely that motor neurons contain unedited GluR2.

If the Ca^{2+}-permeability is not due to the AMPA receptor subunits present within motor neurons, then the most obvious explanation for the cobalt flux observed by Carriedo et al. (1996) is that the pertinent receptors are kainate receptors. This possiblity cannot be excluded by these investigators, and as such, they refer to Ca^{2+}-permeable AMPA/kainate receptors. RT-PCR studies have determined that mRNA for the kainate receptor subunits GluR5-7 and KA-1 and -2 are present within cultured motor neurons from the rat spinal cord (Temkin et al., 1997). Similar to the role of GluR2 in AMPA receptors, GluR6 can be RNA edited from Q to R, producing a subunit that inhibits Ca^{2+} influx when present in the kainate receptor (Burnashev et al., 1995). Unlike the almost complete editing of GluR2, only 75% of GluR6 was edited in the rat brain (Sommer et al., 1991). At this point, the degree to which GluR6 is edited in motor neurons has not been determined, and therefore, unedited GluR6 may exist in kainate receptors of motor neurons and provide a mechanism for the observed cobalt flux. The selective loss of motor neurons following intrathecal kainate, but not intrathecal AMPA, also suggests that kainate receptors may be the true mediators of selective vulnerability to kainate toxicity.

Kainate activates both AMPA and kainate receptors, while AMPA preferentially activates AMPA receptors (Hollmann and Heinemann, 1994). Therefore, if AMPA receptors on motor neurons mediate the selective vulnerability of these neurons, then one would expect AMPA to induce a similar pattern of cell death as kainate. Instead, AMPA induces marked loss of dorsal horn neurons, likely mediated through Ca^{2+}-permeable AMPA receptors on a subset of these neurons (Kyrozis et al., 1995; Gu et al., 1996), with little or no degeneration of motor neurons (Kwak and Nakamura, 1995). The selectivity of motor neuron degeneration following kainate, but not AMPA, suggests that motor neurons have Ca^{2+}-permeable kainate receptors, not AMPA, and that these receptors mediate the selective vulnerability.

Regardless of whether the critical receptor is kainate or AMPA or whether the GluR2 is RNA edited at the Q/R site, the inclusion or exclusion of specific subunits may not be the only determinant of Ca^{2+} permeability. Other components of receptor complexes, like the associated post-synaptic density proteins or intracellular signaling mechanisms, may also modulate the ionic properties of non-NMDA glutamate receptors. An appreciation for the critical role played by these glutamate receptor-associated or -binding proteins is just now beginning to emerge (Maas et al., 1997).

Putative roles for GluR2 in ALS neurodegeneration

Our finding that GluR2 immunoreactivity is unaltered in G86R SOD-1 transgenic mice does not rule out a potential role for GluR2 in the pathogenesis of ALS. Although GluR2 is present in the neurons and synapses of vulnerable neurons, our anatomical study does not give a reflection of GluR2 function. For example, GluR2 may be post-translationally modified in ALS patients, or even in the SOD-1 transgenic mice that we analyzed. If this modification does not effect the antigenicity or distribution of GluR2 then we would be unable to detect this alteration. AMPA receptor subunits can be post-translationally modified by normal or abnormal cellular enzymes. These modifications include

phosphorylation, glycosylation, nitration or oxidation, and can drastically alter receptor function (Hollmann and Heinemann, 1994; Levitan, 1994). An intriguing hypothesis is that mutations in SOD-1 cause degeneration by post-translationally modifying specific proteins important in glutamate transmission, including glutamate transporters, glutamate receptors, or intracellular components of glutamate signaling. The results of this study can neither confirm or exclude this hypothesis, however it is of interest as a mechanism for integrating the SOD-1 and glutamate hypotheses of ALS neurodegeneration.

Chapter Five

Summary and Conclusions

In the previous four chapters, we have provided the background and rationale for the experiments conducted, the methodology and results for these experiments, and any relevant conclusions indicated by these results. All of the experiments in this thesis were conducted in G86R SOD-1 transgenic mice and littermate controls. These mice have been a valuable resource, providing insights into the pathogenesis of ALS degeneration and bringing us closer to developing a rational and effective therapy for the disease. In this final chapter, we will summarize the important points from the earlier chapters, compare our results with those of others who are investigating SOD-1 transgenic mice, attempt to integrate the numerous studies of the mechanism of degeneration into a logical framework, and provide a possible mechanism to explain these studies.

Summary of Results

As we began the study of the G86R SOD-1 transgenic mouse, the only previous study of these mice had demonstrated the following: the mutant SOD-1 gene was expressed in these transgenic mice, the mice had normal levels of SOD-1 enzymatic activity, the mice developed a gait disturbance that progressed to total paralysis and death at approximately 100 days of age, and there was some loss of Nissl-stained cells and the appearance of argyrophilic degeneration in the spinal cord and brainstem (Ripps et al., 1995). With this background, we began to investigate the mechanism of degeneration in these mice.

Chapter two

In this study, we investigated the selective vulnerability of specific neurochemically-defined neuronal populations in the spinal cord of SOD-1 transgenic mice. Based on the symptomatology of the mice, we presumed that motor neurons would degenerate,

but we were interested in how the loss of motor neurons compared to cell loss of other neuronal populations in the spinal cord. In addition, all motor neurons and other neuron populations in the spinal cord did not completely degenerate, and we were interested in whether specific proteins correlated with either the neurons that were vulnerable or resistant to degeneration. Using unbiased stereologic counts of immunocytochemically-labeled neurons, we determined that both motor neurons and CR-immunoreactive spinal interneurons showed significant cell loss in endstage SOD-1 transgenic mice. This was extremely important, because our study is the only one to conclusively demonstrate the loss of spinal interneurons in SOD-1 transgenic mice or in ALS itself, and this finding has important ramifications for putative mechanisms of ALS degeneration. In contrast to CR-immunoreactive interneurons, CB immunoreactivity defined a population of interneurons that were not vulnerable to degeneration, suggesting that CB may protect neurons from degeneration by interacting with some component of the degeneration mechanism. Of the neuronal populations that degenerated (*i.e.*, motor neurons and CR-immunoreactive interneurons), there was less than 50% loss of neurons. Therefore, is there some protein that confers vulnerability or protectiveness to neurons in these populations? CB would obviously be a candidate for reducing the vulnerability of a given neuron, but the lack of double-labeling of CB with either CR-immunoreactive interneurons or motor neurons rules out an involvement in these neuronal populations. We chose to investigate whether NFP played a role in the degeneration of neurons in these populations.

NFP has been causally linked to motor neuron degeneration by transgenic mice that overexpress or express mutant forms of NFP genes (Côté et al., 1993; Xu et al., 1993; Lee et al., 1994). In addition, pathologic accumulation of NFP in the somata and proximal dendrites of spinal cord neurons is a predominant pathology in both ALS patients (Manetto et al., 1988; Munoz et al., 1988; Mizusawa et al., 1989; Troost et al., 1992) and SOD-1 transgenic mice (Wong et al., 1995; Morrison et al., 1996; Tu et al., 1996; Morrison et al., 1998). The percentage loss of NFP-immunoreactive neurons in the spinal

cord of SOD-1 transgenic mice was 51%. The higher percentage loss of this neuronal population than motor neurons or CR-immunoreactive neurons suggests that an individual neuron in this population has a greater probability for degeneration. Of the neuronal populations in the spinal cord that we investigated, the NFP-immunoreactive neurons were the most vulnerable. NFP-immunoreactive neurons are not a separate population of neurons from motor neurons, CR-, and CB-immunoreactive interneurons, however, but rather a percentage of each of these neuronal populations are composed of NFP-immunoreactive neurons. We hypothesized that the neurons that contain NFP in these neuronal populations will preferentially degenerate over those that do not. In order to investigate this, we first quantified the exact percentage of motor neurons and CR- and CB-immunoreactive interneurons that were also immunoreactive for NFP. By multiplying this percentage by the total number of neurons in each population, we were able to estimate the number of motor neurons and CB- and CR-immunoreactive interneurons that are also immunoreactive for NFP. The same percentage of these NFP-containing neurons should degenerate as for the population of NFP-containing neurons as a whole. Therefore, we predicted the loss of motor neurons and CB- and CR-immunoreactive neurons based on their immunoreactivity for NFP. The predicted loss was very close to the actual loss for motor neurons and CR-immunoreactive neurons, suggesting that NFP is a key mediator of neuronal vulnerability and likely plays a role in the mechanism of degeneration. In contrast, NFP immunoreactivity vastly over-predicted the loss of CB-immunoreactive neurons, suggesting that CB confers a resistance to vulnerability regardless of NFP content and that CB interacts with a component of the mechanism of ALS degeneration that precedes the contribution of NFP.

Chapter three

In chapter two, we found that both motor neurons and interneurons have degenerated in endstage SOD-1 transgenic mice, and that various proteins appear to play a role in

the selective vulnerability of these neurons. In this chapter, we investigated the time course of this neuron loss, and correlated the timing of neuron loss with the onset of motor symptoms and the development of pathologic alterations in NFP and GFAP. G86R SOD-1 transgenic mice display a disturbance of gait at approximately 100 days old as the first sign of motor dysfunction. This minor dysfunction progresses rapidly over the next ten days to total paralysis and death at approximately 110 days old, which is the endstage time point investigated in chapter two. In this experiment, we investigated the pathology in 30, 80, and 100 day old mice. The 30 and 80 day old mice are presymptomatic, while the 100 day old mice were defined not by their age, but by the first recognition of motor impairment. There was no significant loss of motor neurons or CR-immunoreactive interneurons in 30 or 80 day old mice, while both of these neuronal populations showed significant cell loss at the onset of symptoms (*i.e.*, 100 day old). These results further the conclusion of chapter two that a subset of interneurons is as vulnerable as motor neurons to degeneration in the spinal cord of SOD-1 transgenic mice. Not only do both of these populations degenerate, but we did not observe any difference in the time of degeneration onset. In addition to cell loss, we investigated the pathologic somatic accumulation of phosphorylated NFP and the marked increase in GFAP-immunoreactive astrocytes in SOD-1 transgenic mice at different time points. Neither of these pathologies were observed in presymptomatic SOD-1 transgenic mice, while both were prevalent at the onset of symptoms. These pathologies, therefore, occur simultaneous with both neuronal cell loss and symptom onset.

Our results from chapter two and three portray an extremely rapid and devastating neurodegeneration (see Figure 5-1). After laying dormant for over three months, the onset of neurological symptoms in the mice at approximately 100 days occurs coincident with a 28.9% loss of motor neurons, a 23.2% loss of CR-immunoreactive interneurons, and the pathologic alteration of NFP and GFAP. Over the following 10 days, the symptoms of the mice progress from a gait disturbance to total paralysis, and the neuron loss increases to

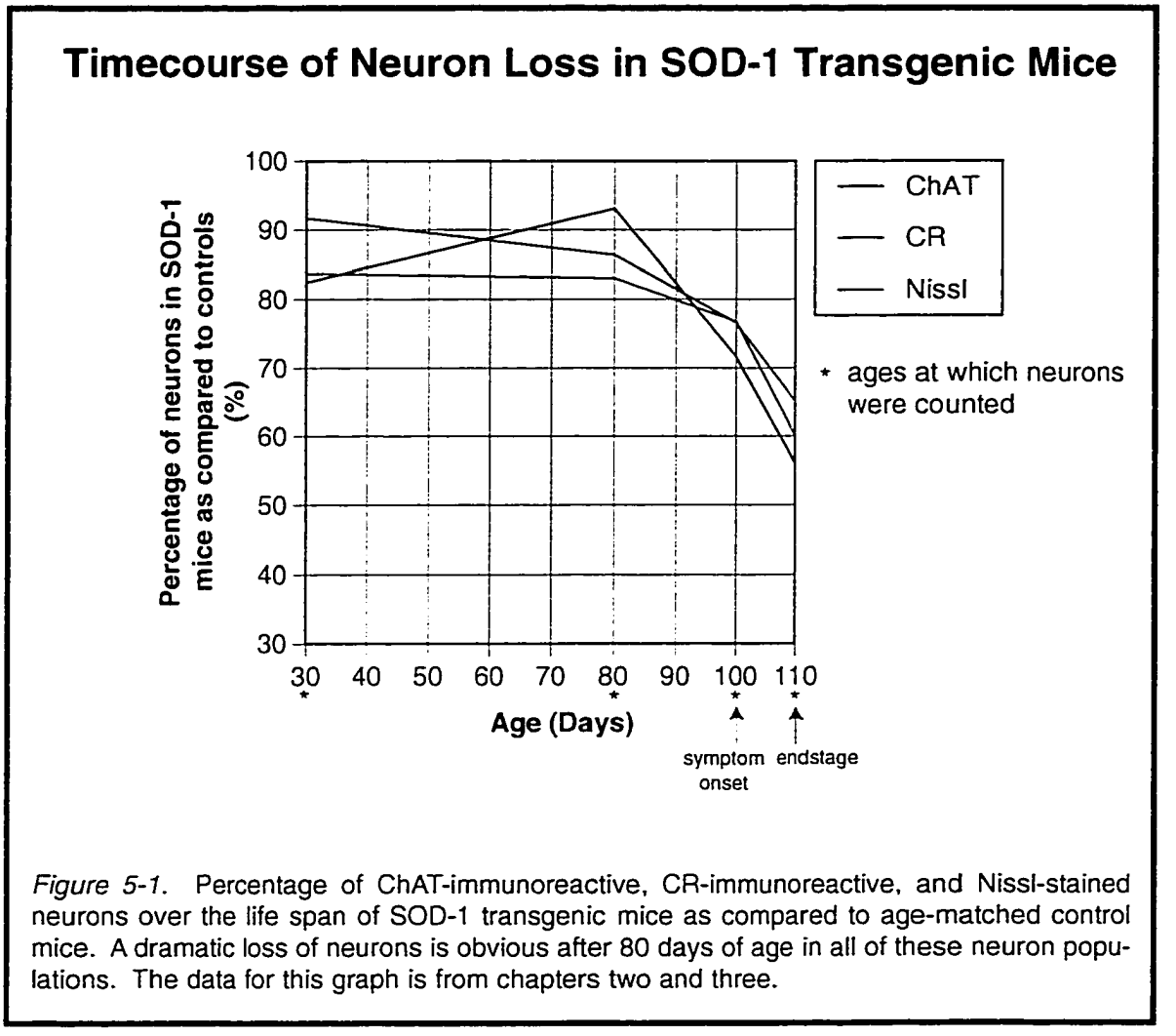

Figure 5-1. Percentage of ChAT-immunoreactive, CR-immunoreactive, and Nissl-stained neurons over the life span of SOD-1 transgenic mice as compared to age-matched control mice. A dramatic loss of neurons is obvious after 80 days of age in all of these neuron populations. The data for this graph is from chapters two and three.

44% in motor neurons and 40% in CR-immunoreactive interneurons. Any putative mechanism of degeneration should explain both the delay in onset and the rapid progression of degeneration in SOD-1 transgenic mice.

Chapter four

The selective vulnerability of NFP-containing neurons described in chapter two may be a reflection of NFP being directly altered by mutations in SOD-1. Alternatively, NFP may not be directly affected by mutant SOD-1, but rather, make a subset of neurons more vulnerable to degeneration by a mechanism that does not involve NFP. One such mechanism for degeneration in SOD-1 transgenic mice is excitotoxicity. NFP-containing

neurons have been shown to be selectively vulnerable to kainate toxicity in a cell culture model, and these vulnerable NFP-containing neurons appear to contain calcium-permeable AMPA/kainate receptors (Carriedo et al., 1996). Therefore, a possible explanation for the selective vulnerability of NFP-immunoreactive neurons in SOD-1 transgenic mice is that an excitotoxic environment is produced in the spinal cord of these mice and that the calcium-permeable AMPA/kainate receptors on NFP-containing neurons result in elevated levels of intracellular calcium and neurodegeneration. One possible cause of calcium-permeable AMPA/kainate receptors is an AMPA receptor that lacks the GluR2 subunit. GluR2 dominates the functional characteristics of AMPA receptors, and the absence of GluR2 produces an AMPA receptor that is permeable to calcium (Geiger et al., 1995). Therefore, utilizing the GluR2-specific antibody developed in our laboratory (Vissavajjhala et al., 1996), we investigated the cellular and synaptic distribution of GluR2 in the spinal cord of control and SOD-1 transgenic mice.

In control mice, GluR2 immunoreactivity appeared to be present in virtually every neuron in the spinal cord. Immunoreactivity for GluR2 was present in motor neurons in the ventral horn of the spinal cord, interneurons in the intermediate zone, and neurons in the dorsal horn. Quantitative double-labeling of GluR2 with ChAT to label motor neurons and CB and CR to label interneurons demonstrated that almost 100% of these neuronal populations, which were the same ones investigated in the experiments of chapters two and three, were immunoreactive for GluR2. The presence of GluR2 in almost all neurons in the spinal cord precludes a role of this protein in selective vulnerability. In addition, the localization of GluR2 to motor neurons and CR-immunoreactive interneurons, neuronal populations that clearly degenerate in our SOD-1 transgenic mice, strongly suggest that the absence of GluR2 from a particular neuron is not necessary for neuronal vulnerability. Though the cellular localization of GluR2 was not a determinant of vulnerability, perhaps the synaptic localization of GluR2 would provide an explanation for the increased vulnerability of ventral horn neurons in SOD-1 transgenic mice and models of kainate tox-

icity. Therefore, we utilized a post-embedding immunogold technique to localize GluR2 to the synapse. GluR2 was synaptically localized in both the vulnerable ventral horn and the resistant dorsal horn, and the percentage of labeled synapses and number of immunogold particles per labeled synapse did not differ between these regions. These results demonstrate that neuronal vulnerability is not determined by the presence or absence of GluR2, but alterations of GluR2 may still be a component of the mechanism of degeneration in SOD-1 transgenic mice.

Alterations in the expression, synaptic localization, or integration into AMPA receptors of GluR2 would produce an excitotoxic environment by increasing the percentage of AMPA receptors that flux calcium. To investigate this hypothesis, we compared the immunoreactivity for GluR2 in SOD-1 transgenic mice to control mice. Using the same techniques as above, we determined that there was no alteration in the cellular or synaptic distribution of GluR2 in SOD-1 transgenic mice. The percentage double-labeling of GluR2 with ChAT, CR, and CB was unaltered, there was no apparent difference in immunoreactive intensity, the percentage of GluR2-labeled synapses was identical with control, and the number of immunogold particles per labeled synapse was unchanged. These studies obviously cannot rule out that GluR2 may be functionally altered by mutant SOD-1, but the anatomic distribution of GluR2, even to the resolution of a single synapse, is clearly unaltered in SOD-1 transgenic mice.

Comparison of SOD-1 Transgenic Mouse Models

Behavioral Deficits

Transgenic mice with four different mutations of SOD-1 have been produced to date. Three have mutations in the human SOD-1 gene that lead to G37R (Wong et al., 1995), G93A (Gurney et al., 1994), and G85R (Bruijn et al., 1997b) substitutions in the SOD-1 protein, while one, which was utilized in this thesis, has a G86R mutation in the

Table 5-1. Comparison of SOD-1 transgenic mice

	Symptom Onset (days)	Mortality Age (days)	Motoneuron Loss	Interneuron Loss	NFP Pathology	Reactive Astrocytosis	Vacuoles	SOD-1 Inclusions
G86R Mouse (Ripps)	100	110	@ symptom onset	@ symptom onset	@ symptom onset	@ symptom onset	none	not evaluated
G93A Human (Gurney)	91 (tremor) 125 (weak) *G1 line*	136 *G1 line*	@ symptom onset	not evaluated	@ symptom onset	@ symptom onset	prior to symptoms	not evaluated
G37R Human (Wong)	105 150 165 180	not evaluated	@ symptom onset	not evaluated	@ symptom onset	prior to symptoms	prior to symptoms	not evaluated
G85R Human (Bruijn)	225	240	@ symptom onset	not evaluated	none	prior to symptoms	none	prior to symptoms

mouse gene that corresponds to a mutation observed in humans at residue 85 (Ripps et al., 1995). Although these transgenic mice have different mutations in SOD-1, the behavioral deficits are remarkably similar. All of the SOD-1 transgenic mice are normal at birth, but begin to show motor dysfunction at 3 to 9 months of age. In the G93A and G37R SOD-1 transgenic mice, this motor dysfunction begins as a limb tremor which progresses to limb weakness. The G85R and G86R transgenic mice do not display limb tremor, but only limb weakness, as their initial symptom. In all mutant SOD-1 mice, the symptoms progress from limb weakness to total paralysis and premature death. The age of onset of these symptoms is dependent upon the specific mutation, and appears to correlate with the level of mutant SOD-1 expressed. High expressors have an earlier onset than low expressors (Wong et al., 1995; Bruijn et al., 1997b; Dal Canto and Gurney, 1997). Although SOD-1 transgenic mice can have very dissimilar ages of onset, which range from 100 to 225 days, the duration from onset of muscle weakness to total paralysis is rapid in all cases (*i.e.*, 10 - 15 days; see Table 5-1).

Pathology

The pathology in SOD-1 transgenic mice strongly resembles the pathology in ALS patients. Investigators have reported loss of motor neurons and interneurons, neurofilament inclusions, astrocytosis, and muscle atrophy in SOD-1 transgenic mice, all of which have been observed in patients with ALS (Hirano et al., 1967; Hirano, 1991; Leigh and Swash, 1991). One advantage of an animal model of ALS is that early symptomatic and presymptomatic mice can be sacrificed and examined to determine the onset of pathology. A consistent pathology in all SOD-1 transgenic mice, and the one that leads to the behavioral deficits, is the loss of motor neurons. In all studies of SOD-1 transgenic mice, the onset of motor neuron loss was found to be coincident with the onset of motor weakness, with the magnitude of the motor neuron loss at endstage being approximately 50% in the studies that quantified neuron number (Chiu et al., 1995; Wong et al., 1995; Morrison et al., 1996; Bruijn et al., 1997b). In most SOD-1 transgenic mice (*i.e.*, G86R, G93A, and G37R), the normal organization of the cytoskeletal protein NFP is disrupted by abnormally phosphorylated or aberrantly organized NFP that form focal or diffuse inclusions in the soma or axon (Wong et al., 1995; Morrison et al., 1996; Tu et al., 1996; Morrison et al., 1998). In all of these transgenic mice, the NFP inclusions are not observed presymptomatically, but rather appear at the onset of symptoms. Another pathology that is observed in all SOD-1 transgenic mice and ALS patients is reactive astrocytosis. In response to neuronal damage, astrocytes replicate, hypertrophy, and express increased amounts of GFAP (Eddleston and Mücke, 1993; Montgomery, 1994). In G86R and G93A SOD-1 transgenic mice, the astrocytosis is coincident with symptom onset and neuron loss, while in the G37R and G85R mice the astrocytosis occurs prior to the onset of symptoms. Although the SOD-1 transgenic mice have many characteristics in common, there are still many differences between these models, and these differences may illuminate dissimilarities in the mechanisms of degeneration.

The most obvious difference between the pathologies in the different transgenic mice is the occurrence of vacuoles in the G93A and G37R SOD-1 transgenic mice (Dal Canto and Gurney, 1994; Wong et al., 1995; Mourelatos et al., 1996), and their absence from the G86R and G85R transgenic mice [(Morrison et al., 1996; Bruijn et al., 1997b; Morrison et al., 1998); see Table 5-1]. Given that the alteration of the SOD-1 protein in the G86R mouse and the G85R human mutations of SOD-1 are identical, the lack of vacuoles may be mutation specific. Although this explanation cannot be ruled out, it is more likely that the vacuoles are due to the large amount of mutant protein present in the G93A and G37R transgenic mice. The G85R transgenic mice express low amounts of mutant protein and do not have vacuoles. In addition, a low expressing line of mice with the G93A mutation has recently been characterized, and these transgenic mice have fewer vacuoles than the high expressing lines (Dal Canto and Gurney, 1997). If the appearance of vacuoles is dependent on the level of expression, then this would explain why vacuoles are not observed in familial ALS patients with mutations in the SOD-1 gene. ALS patients have only one copy of the mutant gene, and therefore have much lower expression levels of mutant SOD-1 than do transgenic mice that have multiple copies.

A second dissimilarity between the SOD-1 transgenic mice with different mutations is the timing of astrocytosis. The G86R and G93A transgenic mice display reactive astrocytosis coincident with the onset of symptoms (Tu et al., 1996; Morrison et al., 1998), while the G37R and G85R transgenic mice show this pathology presymptomatically [(Wong et al., 1995; Bruijn et al., 1997b); see Table 5-1]. The difference in onset between the G85R mice and the G86R mice suggests that this difference is not dependent on the specific mutation, as these mutations are identical. Interestingly, the G86R and G93A mice, the two transgenic mice that do not display astrocytosis presymptomatically, develop symptoms more rapidly than the other two mutant mice. Perhaps astrocytosis is not observed presymptomatically in these mice due to a difficulty observing presymptomatic changes in mice with such rapid onset of symptoms.

Investigations into the Mechanism of Degeneration

Since the original description of SOD-1 mutations in familial ALS patients (Rosen et al., 1993), researchers have committed considerable time and resources to determining the mechanism of degeneration that results from SOD-1 mutations. This flurry of activity has produced numerous articles and several important findings, but as yet, there is no consensus as to the mechanism of degeneration. This is partly due to the complexity of the mechanism of degeneration, but also perhaps to individual researchers investigating only one aspect of the degenerative mechanism without attempting to integrate their work with that of other researchers. In the following section, we will attempt to organize the completed experiments by placing them into the following framework: gains-of-function, impairments in cellular function, selective vulnerability, and manipulations that reduce toxicity. Every study completed to date fits into one of these categories, and the interactions between the results in these categories may provide insight into the mechanism of degeneration.

Gains-of-function

Investigators have hypothesized that the mutations in SOD-1 produce disease by a gain, not a loss, of function. In respect to loss of function, researchers are referring to the classic enzymatic clearance of superoxide radical by SOD-1. The evidence for a gain-of-function is three-fold. First, mutant forms of SOD-1 exist that do not have a reduced capacity for the clearance of superoxide radical, and yet produce disease in patients (Borchelt et al., 1994; Nishida et al., 1994; Tsuda et al., 1994; Fujii et al., 1995). Second, all SOD-1 transgenic mice have normal to elevated levels of this classic enzymatic reaction, due to wild-type murine SOD-1, and yet develop symptoms and pathology that strongly resemble ALS (Gurney et al., 1994; Ripps et al., 1995; Wong et al., 1995; Bruijn

et al., 1997b). Third, SOD-1 knockout mice, in which there is no contribution of SOD-1 to the clearance of superoxide radical, do not develop motor neuron degeneration or symptoms of motor system dysfunction (Reaume et al., 1996). Thus, it is clear that mutant SOD-1 has gained some property that wild-type SOD-1 either does not possess, or possesses to a much smaller degree, and this is termed a gain-of-function. Although ruling out a loss of function was quite easy, determining the critical gain-of-function for causing disease has proven quite difficult. The reason for this is that the only limits on potential gains-of-function is the imagination of the investigators. At this point, researchers have demonstrated three different gains-of-function for mutant SOD-1, but none of these three have yet been shown to be necessary for neurodegeneration. The three demonstrated gains-of-function are peroxynitrite-mediated tyrosine nitration, peroxidase reaction, and abnormal binding to cellular proteins. With the exception of the abnormal binding, these are enzymatic activities that wild-type SOD-1 possesses to a small degree, which is probably the reason that they were investigated, and the mutant forms of SOD-1 appear to have an increased capacity for catalyzing these reactions.

Peroxynitrite ($ONOO^-$) is a potent oxidant produced from superoxide radical and nitric oxide. The breakdown of peroxynitrite into several reactive intermediates is catalyzed by SOD-1 (Beckman et al., 1992; Ischiropoulos et al., 1992; van der Vliet et al., 1995). Although there are several products of this breakdown, the nitration of tyrosines appears to be relatively specific for this reaction. Therefore, using nitrotyrosines as a marker of this reaction, several investigators have investigated whether the mutant forms of SOD-1 favor the breakdown of peroxynitrite and whether there is an increase in the amount of nitrotyrosines in SOD-1 transgenic mice and ALS patients. Utilizing mass spectroscopy, increased free nitrotyrosines (*i.e.*, nitrotyrosines that are not incorporated into peptides or proteins) have been reported in the spinal cord of ALS patients (Beal et al., 1997), G93A SOD-1 transgenic mice (Ferrante et al., 1997), and G37R SOD-1 transgenic mice (Bruijn et al., 1997a). In addition, ALS patients and G93A SOD-1 transgenic

mice have increased immunoreactivity for nitrotyrosine in the spinal cord (Abe et al., 1995; Beal et al., 1997; Ferrante et al., 1997). Although these studies suggest that mutant SOD-1 may catalyze the breakdown of peroxynitrite and the nitration of tyrosines, only *in vitro* biochemical studies can demonstrate this conclusively. Unfortunately, the biochemical evidence is indirect. Mutant SOD-1 has a reduced affinity for zinc, and therefore is more likely than wild-type SOD-1 to exist in a zinc-lacking state (Crow et al., 1997a). Removing the zinc from SOD-1 results in an enzyme that catalyzes the peroxynitrite-mediated tyrosine nitration to a greater extent than SOD-1 that contains zinc, suggesting, although indirectly, that mutant forms of SOD-1 may nitrate tyrosines to a greater extent than wild-type SOD-1. If mutant SOD-1 favors the nitration of tyrosines, it is important to determine the specific proteins that are susceptible, as nitration of key tyrosines in proteins could dramatically alter their function. This is obviously the case for tyrosines involved in phosphorylation, as nitration inhibits the capacity for phosphorylation (Kong et al., 1996), but a charged nitronium ion will affect the function of most proteins by altering their tertiary structure and disrupting interactions with other subunits or proteins.

As we discovered first hand, determining the specific proteins that have abnormal nitration of tyrosines is not an easy task. We investigated the light, medium, and heavy chains of NFP, GFAP, and GluR2 to determine whether there was increased nitrotyrosines in SOD-1 transgenic mice. Given the importance of NFP in the pathology and selective neuronal vulnerability in SOD-1 transgenic mice, NFP subunits were obvious choices for investigation. In addition, tyrosines on the light chain of NFP can be nitrated in the presence of SOD-1 and peroxynitrite *in vitro*, and this disrupts assembly into NFP fibrils (Crow et al., 1997b). In addition to NFP subunits, we also investigated whether there are nitrotyrosines in GFAP and GluR2. GFAP is an astrocytic cytoskeletal protein that has an analogous role in astrocytes to that of NFP in neurons (Rutka et al., 1997). It is also a long-lived protein, and alterations in GFAP, both proliferation of GFAP-immunoreactive astrocytes and GFAP inclusions within astrocytes, have been reported in SOD-1 trans-

genic mice (Wong et al., 1995; Tu et al., 1996; Bruijn et al., 1997b; Morrison et al., 1998). The final protein investigated was the AMPA subunit, GluR2, which as discussed above plays an important role in regulating the calcium-permeability of AMPA receptors. If GluR2 is altered by nitration of key tyrosines, it may alter its function or integration into the pentameric structure of the AMPA receptor, resulting in an AMPA receptor that has increased permeability to calcium and perhaps a greater propensity for contributing to excitotoxicity.

Each of these proteins were immunoprecipitated, and then split into two equal volumes that were run in separate lanes, with one lane being immunoblotted with an antibody specific for the immunoprecipitated proteins and the second lane immunoblotted with a nitrotyrosine antibody. This provided an indication of whether the immunoprecipitated protein was immunoreactive for nitrotyrosine, and if immunoreactive, provided a means for quantification by forming a ratio of the nitrotyrosine immunoreactivity over the immunoprecipitated protein immunoreactivity. Through this technique, we were able to investigate whether there is immunoreactivity for nitrotyrosines in these immunoprecipitated proteins in control mice and whether this immunoreactivity is increased in SOD-1 transgenic mice. In all five of the immunoprecipitated proteins, we were unable to detect immunoreactivity for nitrotyrosines in the control mice or the SOD-1 transgenic mice. In fact, even after chemically nitrating tyrosines in these proteins with tetranitromethane (Riordan et al., 1966; Sokolovsky et al., 1966; Inano and Tamaoki, 1986; Shimokawa et al., 1990; Takeda et al., 1990), only the nitrotyrosines in GluR2 were immunoreactive with the available antibodies. Thus, it appears that the available antibodies are unable to recognize nitrotyrosines in most proteins, severely limiting both their usefulness and the conclusions that we could draw from this study. At this point, however, we have no evidence that tyrosines in NFP, GFAP, or GluR2 are aberrantly nitrated in SOD-1 transgenic mice.

The second gain-of-function proposed for mutant SOD-1 is an increase in the peroxidase reaction. Two groups of investigators have demonstrated that in the presence of

hydrogen peroxide, mutant SOD-1 oxidizes a spin trap to a greater extent than wild-type SOD-1 (Wiedau-Pazos et al., 1996; Yim et al., 1996). This increased oxidation, but not the normal baseline activity, is attenuated by chelating the copper in the mutant SOD-1. This suggests that greater exposure of the copper ion, perhaps secondary to a conformational change in mutant SOD-1, may contribute to the increase in peroxidase activity. Similar to nitration of tyrosines, the exact proteins affected by this altered activity are unknown. However, glutamate has been shown to be altered by this reaction *in vitro* (Yim et al., 1996), and provides a putative mechanism by which mutations in SOD-1 may induce an excitotoxic degeneration.

The final gain-of-function that has been demonstrated for mutations in SOD-1 is altered binding to lysyl-tRNA synthetase (KARS) and translocon-associated protein delta (TRAP) (Kunst et al., 1997). Using yeast two-hybridization, and then confirmed by immunoprecipitation, the G85R mutant SOD-1 bound to these two proteins, while wild-type SOD-1 did not bind to any proteins. KARS is the enzyme that catalyzes the activation of the amino acid lysine and the formation of lysyl-tRNA (Freist and Gauss, 1995). If the abnormal binding of mutant SOD-1 with this enzyme disrupts its function, then one would expect a disruption in protein synthesis that would be devastating to cellular survival. The second protein, TRAP, is a protein that participates in the translocation of newly synthesized proteins into the endoplasmic reticulum (ER) (Hartmann et al., 1993). The translocation of proteins is obviously important for their accurate localization to the cell surface, lysosomes, ER or Golgi apparatus, and blocking the sites of transport with mutant SOD-1 could also be devastating to cellular function. Besides the two proteins reported to interact with mutant SOD-1, other proteins may bind to mutant SOD-1 *in vivo* and lead to aggregation of the SOD-1. These aggregates of SOD-1 have been reported in both SOD-1 transgenic mice (Bruijn et al., 1997b) and a cell culture model of ALS in which mutated SOD-1 was transfected (Durham et al., 1997; Roy et al., 1997). These SOD-1 aggregates should be investigated in greater detail to determine the proteins asso-

ciated with them, as this may provide insight into the mechanism by which these aggregates occur.

Impairments in cellular function

The second level at which the mechanism of degeneration resulting from mutations in SOD-1 have been investigated is the specific impairments in cellular function. For the most part, these disruptions in cellular function have not been proven, but merely suggested, by pathologic alterations in SOD-1 transgenic mice or cell lines transfected with mutant SOD-1. These pathologies include disruptions in the morphology of mitochondria, Golgi apparatus, and smooth endoplasmic reticulum (Dal Canto and Gurney, 1994; Dal Canto and Gurney, 1995; Wong et al., 1995; Mourelatos et al., 1996). In addition, abnormal accumulations of NFP have been reported in ventral horn neuron cell bodies of SOD-1 transgenic mice (Wong et al., 1995; Morrison et al., 1996; Tu et al., 1996; Morrison et al., 1998) and ALS patients (Hirano et al., 1967; Hirano, 1991; Leigh and Swash, 1991), and this accumulation is mirrored by an equivalent decrease of NFP in ventral root axons (Zhang et al., 1997). Finally, the glutamate transporter, GLT-1, is reduced in the spinal cord of SOD-1 transgenic mice (Bruijn et al., 1997b). Most, if not all, of these pathologies have been reported previously in ALS patients, and although not conclusive proof of a disruption in cellular function, in conjunction with direct studies of functional deficits, they provide strong supporting evidence.

Studies of functional deficits are much more difficult to complete than studies of pathologies. Perhaps for this reason, only one study directly investigating a functional deficit in SOD-1 transgenic mice has been published. Zhang et al. (1997) has reported that SOD-1 transgenic mice have an impairment in both fast and slow axonal transport. In addition, the transport of NFP was specifically investigated, and all NFP subunits show reduced transport into ventral root axons in SOD-1 transgenic mice. Although all NFP subunits are eventually involved, the disruption in NFP-L transport appears to precede the

deficits in other NFP subunits. In fact, reduced NFP-L transport appears to occur before the onset of symptoms in these transgenic mice. This study provides an explanation for the accumulation and inclusions of NFP that have been reported in SOD-1 transgenic mice and ALS patients (Hirano et al., 1967; Hirano, 1991; Leigh and Swash, 1991; Wong et al., 1995; Morrison et al., 1996; Tu et al., 1996; Morrison et al., 1998). In addition, the initial disruption of NFP-L is particularly interesting. This subunit is critical for the formation of NFP fibrils (Hirokawa et al., 1984; Lee et al., 1993; Lee and Cleveland, 1996), and transgenic mice with mutations in the rod domain of NFP-L demonstrate severe motor neuron pathology and more closely mimic the phenotype and pathology of ALS than transgenic mice with other alterations in NFP subunits (Côté et al., 1993; Xu et al., 1993; Lee et al., 1994).

The other direct evidence of a functional deficit caused by the SOD-1 mutation is in a neuroblastoma cell line that has been transfected with mutant forms of SOD-1 (Carri et al., 1997). Although these studies are conducted in neuroblastoma cells, which may not respond the same as spinal cord neurons *in vivo*, the use of a cell culture system allows a more detailed observation of cellular function. In this study, the investigators report that the cell lines transfected with mutant SOD-1 show mitochondrial depolarization and increased intracellular calcium. Mitochondrial depolarization is an indication of a dysfunctional mitochondria, as depolarized mitochondria do not have the proton motive force necessary to generate ATP. Reduced production of ATP from mitochondrial oxidative phosphorylation would have dramatic effects on cellular energy, and could lead to disruptions in many cellular functions. In addition, these results suggest that the disruptions in mitochondrial morphology reported in SOD-1 transgenic mice may be a marker of mitochondrial dysfunction. The increase in intracellular calcium reported in these cell lines may be secondary to reduced calcium sequestration in depolarized mitochondria or to reduced activity of ATP-dependent calcium pumps in cellular membranes. Regardless of the exact mechanism responsible for the mitochondrial depolarization and increased intra-

cellular calcium, this study demonstrates that these alterations occur in response to mutations in SOD-1 and must be considered in the mechanism of degeneration.

Selective vulnerability

Through some mechanism, the above gains-of-function and functional deficits interact to produce a specific pattern of neuronal vulnerability. In order to fully explain the neurodegeneration, a putative mechanism must account for the specificity of the neuron loss. This is particularly true in the case of ALS caused by mutations in SOD-1, since mutant SOD-1 is expressed in virtually every cell of the body and yet only causes degeneration in the spinal cord, a few motor nuclei in the brainstem, and the motor cortex. In addition to examining the mechanism of degeneration from the beginning (*i.e.*, the mutants in SOD-1), another approach is to begin at the end, with the determination of the specific neurons vulnerable to degeneration in SOD-1 transgenic mice. This was the main focus of my thesis.

Both motor neurons and interneurons degenerate in the spinal cord of G86R SOD-1 transgenic mice (see Chapters 2 and 3). Interestingly, only half of all motor neurons and interneurons in the spinal cord have degenerated by endstage in these mice. Are there certain proteins that are primarily found within the neurons that are vulnerable to degeneration? In addition, are there specific proteins present within the neurons that are resistant to degeneration? We found that CB-containing neurons, which are a population of spinal interneurons, do not degenerate in these transgenic mice. The resistance of CB-containing neurons in SOD-1 transgenic mice suggests that this protein may protect against SOD-1 toxicity. In contrast to CB, we found that NFP is present within a vulnerable population of neurons, and that the magnitude of neuron loss in both motor neurons and interneurons is predicted by the percentage of these neuronal populations that contained nonphosphorylated NFP. The presence of nonphosphorylated NFP in the cytoplasm of neurons is therefore a marker of vulnerable neurons, just as CB is a marker of non-vulnerable neu-

rons. Although these two proteins do not account for all of the neurons that degenerate in the spinal cord, the association of vulnerability with the presence of nonphosphorylated NFP, and of resistance with the presence of CB, suggests that NFP and intracellular calcium contribute to the mechanism of degeneration that results from mutant SOD-1 expression.

Manipulations that reduce toxicity

To this point, we have discussed altered functions of mutant SOD-1, cellular dysfunctions in cells expressing mutant SOD-1, and properties of the specific cells that degenerate. The final level of research is manipulations that reduce toxicity. In many instances, these studies are critical for determining the underlying dysfunctions and mechanisms of degeneration, and if effective, provide agents for therapy in ALS patients. The manipulations reported thus far have primarily investigated excitotoxic mechanisms, but a few other potential mechanisms have also been investigated and these will be summarized as well.

The excitotoxic mechanism of degeneration has been mentioned repeatedly in this thesis, and several lines of evidence support its contribution to the mechanism of neurodegeneration. Excitotoxicity can be initiated by several events, but the overactivation of glutamate receptors is a necessary component of the mechanism (Choi, 1987; Meldrum and Garthwaite, 1990). For this reason, Roy et al. (1997) investigated non-NMDA glutamate receptor antagonists in a primary motor neuron culture that expressed mutant SOD-1. These motor neuron cultures developed intracellular aggregates of SOD-1 and NFP and had decreased survival as compared to control cultured motor neurons. In the presence of glutamate receptor antagonists, both the development of aggregates and the increased neuronal loss was attenuated. Although this study has the drawback of being conducted in a cell culture system that may or may not be fundamentally different from motor neurons *in vivo*, this study does suggest that the overactivation of non-NMDA glutamate receptors

may play an important role in the neurodegeneration caused by mutations in SOD-1. A second study investigating the role of excitotoxicity was the treatment of SOD-1 transgenic mice with riluzole (Gurney et al., 1996). Riluzole is an agent that decreases the release, and also perhaps the receptor binding, of glutamate. It has some effectiveness in sporadic ALS patients (Bensimon et al., 1994). Therefore, it was not surprising that riluzole treatment caused an 11% increase in the total life span of G93A SOD-1 transgenic mice (Gurney et al., 1996), which is approximately the same improvement as was observed in ALS patients (Bensimon et al., 1994). The similar improvement in sporadic ALS patients and SOD-1 transgenic mice suggests that riluzole interacts with a component of the mechanism of degeneration that is common to both. Although riluzole clearly reduces glutamate toxicity, it is unclear whether it is effective through its interaction with glutamate, glutamate receptors, or even perhaps glutamate transporters or mitochondria (Mu et al., 1997). A third agent investigated for its potential attenuation of degeneration in SOD-1 transgenic mice is carboxyfullerenes (Dugan et al., 1997). This agent antagonizes both NMDA and non-NMDA receptors. When infused intraperitoneally, this compound delayed the onset of symptoms and death in SOD-1 transgenic mice. Taken together, these studies suggest that reducing glutamate transmission is effective in reducing the toxicity resultant from SOD-1 mutations.

In addition to these studies in ALS models with mutations in SOD-1, reducing glutamate transmission or components of excitotoxic degeneration appear to be useful for reducing toxicity in other models of ALS. Based on the finding of reduced glutamate transporters in ALS patients (Rothstein et al., 1992; Rothstein, 1995), Rothstein et al. (1993, 1996) produced a model of degeneration by antagonizing glutamate transporters in a spinal cord slice preparation. This manipulation leads to preferential degeneration of motor neurons, which is attenuated by antagonists to non-NMDA glutamate receptors. Thus, providing further evidence that overactivation of non-NMDA glutamate receptors is an important component of the mechanism of degeneration. The final manipulation that

was aimed at reducing excitotoxic degeneration in ALS was in a motor neuron culture that had been treated with ALS serum. Due to the presence of antibodies against voltage-dependent calcium channels, the serum from ALS patients is toxic to cultured motor neurons (Smith et al., 1994). Transfection of CB, which is not normally expressed in differentiated motor neurons, protects motor neurons against this ALS serum toxicity (Ho et al., 1996). Given the importance of calcium in the mechanism of excitotoxicity, this result suggests that CB can reduce this toxicity and provides further evidence that excitotoxicity is a component of the mechanism of ALS degeneration. In light of this cell culture data, the resistance of CB-containing neurons in SOD-1 transgenic mice to degeneration appears of even greater importance (see Chapter 2). Taken together these results strongly suggest that increased intracellular calcium, perhaps secondary to excitotoxicity, is a component of the mechanism of degeneration in ALS.

Manipulations that reduce excitotoxic degeneration are not the only ones that have been effective in reducing degeneration and prolonging the life span of SOD-1 transgenic mice. SOD-1 transgenic mice mated with NFP-L knockout mice have a 12% delay in onset of symptoms and a corresponding increase in total life span (Williamson et al., 1997). These mice also have a reduced number of NFP inclusions, as compared to SOD-1 transgenic mice. This increase in survival is as large as was reported for riluzole and suggests that alterations in NFP are a component of the mechanism of degeneration in SOD-1 transgenic mice. In addition to the NFP-L knockout mice, mating SOD-1 transgenic mice with a mouse overexpressing *Bcl-2* causes a 15% increase in survival and a 19% delay in onset of symptoms (Kostic et al., 1997). *Bcl-2* is a membrane protein, localized to the mitochondria, smooth endoplasmic reticulum, and nuclear envelope, that has been demonstrated to reduce apoptotic cell death (Hale et al., 1996; Herrmann et al., 1996; Deshmukh and Johnson Jr., 1997; Rowan and Fisher, 1997). The exact mechanism by which *Bcl-2* reduces apoptosis is controversial, but it may involve a stabilization of the mitochondrial membrane, as *Bcl-2* can attenuate the loss of mitochondrial membrane

potential associated with apoptosis (Shimuzu et al., 1996). Along with the disrupted morphology of mitochondria in SOD-1 transgenic mice and the loss of mitochondrial potential in a mutant SOD-1 transfected neuroblastoma cell line, this result suggests the involvement of mitochondria. The final two manipulations that reduce toxicity are treatment with copper chelators (Hottinger et al., 1997) and vitamin E (Gurney et al., 1996). Copper is the active site metal in SOD-1, and increased exposure to copper has been proposed to account for the gains-of-function, as copper chelators completely attenuate the increased peroxidation reaction of mutant SOD-1 (Wiedau-Pazos et al., 1996). The effectiveness of copper chelators in SOD-1 transgenic mice may be by reducing this peroxidase reaction or another gain-of-function. Alternatively, copper chelation may reduce toxicity by reducing the expression of control and mutant SOD-1 in response to a limited supply of copper. The mechanism by which vitamin E reduces toxicity is also difficult to determine. It appears to reduce lipid peroxidation, and this may account for the 14% delay in symptom onset, but vitamin E can also reduce several other oxygen radical toxicities and the non-specific nature of this manipulation severely limits any conclusions about mechanism (Buettner, 1993; van Acker et al., 1993; Kamal-Eldin and Appelqvist, 1996)

.

Mechanism of Degeneration

In the previous section, we have summarized all that is currently known about the mechanism of degeneration that results from mutations in SOD-1. Many of these results suggest their own mechanism, and one could postulate that the mutations in SOD-1 are affecting glutamate neurotransmission, mitochondria, and NFP through separate mechanisms. However, it is more likely that the mechanisms suggested by these results interact as components of a single mechanism. Is there one mechanism that can be proposed to account for all of the published results? Although there are still some gaps, the following mechanism provides an explanation for most of the published results.

Figure 5-2

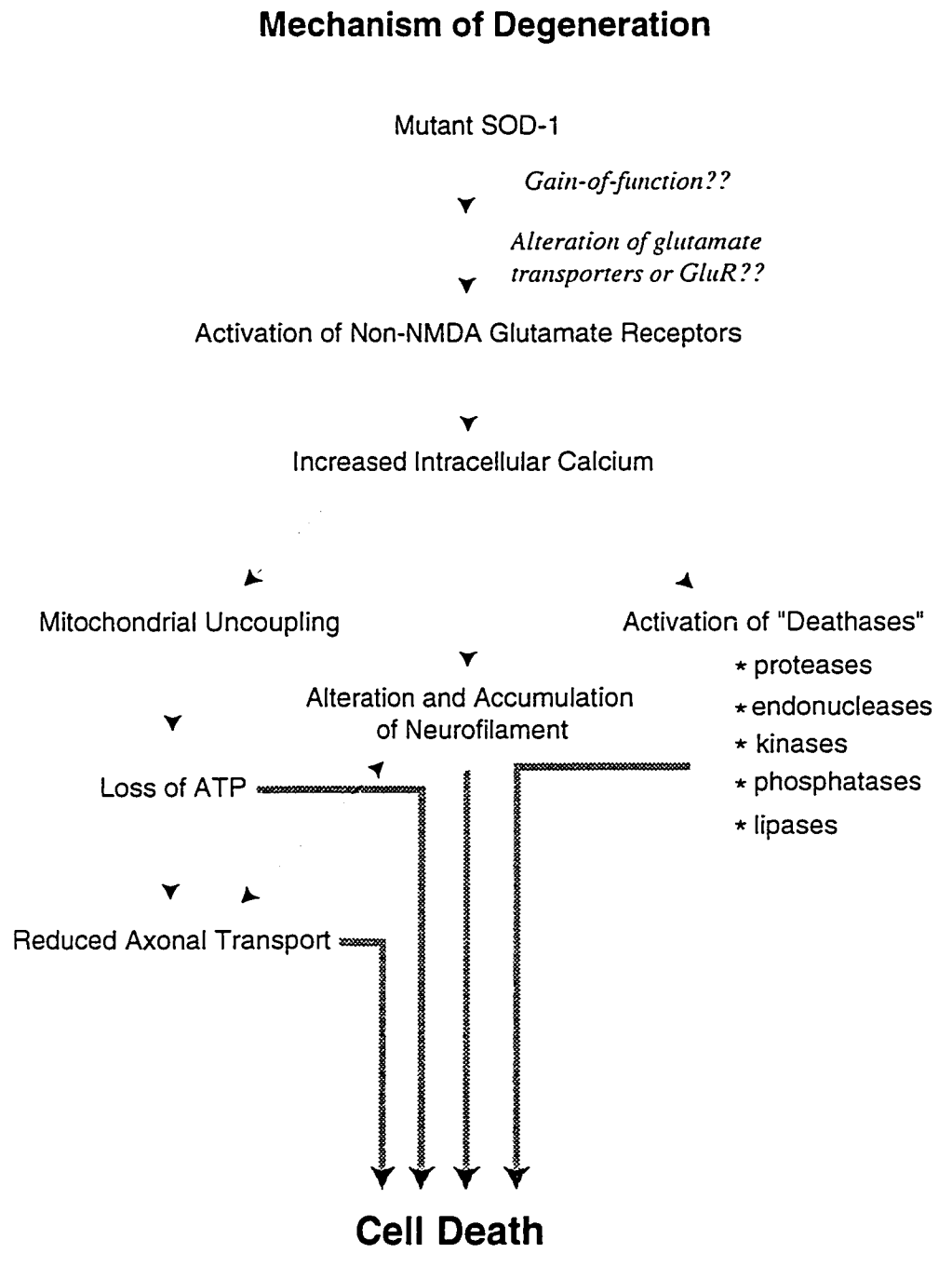

The mechanism for degeneration (see Figure 5-2) begins with the mutations in SOD-1. As discussed above, the mutant forms of SOD-1 appear to have acquired a gain-of-function. At this point, it is unclear which of the presented gains-of-function, or per-

haps one that has not yet been found, is responsible for beginning the mechanism of degeneration. This is perhaps the largest gap in the entire mechanism. At the end of this section, we will discuss potential mechanisms for filling this gap, but they are only conjecture, and this part of the mechanism remains the most mysterious.

After the gains-of-function, the proposed mechanism skips to increased activation of non-NMDA glutamate receptors. Antagonists of non-NMDA glutamate receptors attenuate the development of NFP aggregates and neurodegeneration in a motor neuron culture expressing a mutant form of SOD-1 (Durham et al., 1997; Roy et al., 1997), reduce the degeneration in a spinal cord slice preparation treated with glutamate transporter antagonists (Rothstein and Kuncl, 1995), and delay the onset of symptoms and death in SOD-1 transgenic mice (Dugan et al., 1997). In addition, infusion of kainate, which is a non-NMDA receptor agonist, into the spinal cord produces a similar pathologic profile and pattern of degeneration as was observed in SOD-1 transgenic mice (Ikonomidou et al., 1996). In addition to vulnerability of motor neurons, infusing acromelic acid, which is also a non-NMDA glutamate receptor agonist, produces degeneration of interneurons in the spinal cord (Kwak and Nakamura, 1995). Thus, the vulnerability of interneurons in SOD-1 transgenic mice can also be explained by non-NMDA glutamate receptor activation. Given that overactivation of non-NMDA glutamate receptors appears to be a component of the mechanism of degeneration, what is the cause of this overactivation? There are several possible explanations that have been investigated, and several others that have not. First, there is evidence that the glial glutamate transporter GLT-1 may be reduced in SOD-1 transgenic mice (Bruijn et al., 1997b), as it is in sporadic ALS patients (Rothstein et al., 1995). If this is true, then alterations of glutamate transporters may be the initiating event for the excitotoxic degeneration, and investigators should search for connections between mutant forms of SOD-1 and GLT-1. The study by Roy et al. (1997), however, suggests that alterations in the glial glutamate transporter cannot alone account for the excitotoxic degeneration. In this study, mutant SOD-1 transfected into motor neuron cul-

tures induced degeneration, and it is difficult to envision a mechanism by which mutated SOD-1 in neurons disrupts glutamate transporters in glia. In fact, the reduction in GLT-1, which has only been reported in endstage SOD-1 transgenic mice and ALS patients, may actually occur secondary to motor neuron degeneration, as GLT-1 is selectively down-regulated in astrocytes cultured in the absence of neurons (Swanson et al., 1997). A second explanation for the overactivation of glutamate receptors is that glutamate receptors, themselves, may be disrupted, leading to receptors that produce a greater response to glutamate binding. Given the importance of calcium flux in the excitotoxic mechanism, we hypothesized that altered incorporation of GluR2 into the AMPA glutamate receptor might contribute to excitotoxicity, but this does not appear to be the case (see Chapter 4). We did not investigate subunits of kainate receptors, and future research should focus on this subclass of glutamate receptors as potential contributors to ALS excitotoxicity.

Either through alterations in the glutamate receptor or increased glutamate activation, the overactive non-NMDA glutamate receptor leads to an increase in intracellular calcium. Intracellular calcium may be increased directly by activation of calcium-permeable non-NMDA receptors, or indirectly by depolarization and subsequent activation of voltage-dependent calcium channels. Increased intracellular calcium was reported in the neuroblastoma cell line transfected with mutant SOD-1 (Carri et al., 1997). In addition, CB-containing spinal neurons were resistant to degeneration in SOD-1 transgenic mice (see Chapter 2), and motor neurons in culture transfected with CB were protected against the toxicity of ALS serum (Ho et al., 1996). In addition to being buffered by calcium-binding proteins like CB, intracellular calcium is reduced by sequestration in mitochondria and endoplasmic reticulum, and transport out of the cell by Na^{+}/Ca^{2+} exchangers or Ca^{2+}-ATPases (Carafoli, 1987). It is important that these mechanisms are functional because increased intracellular calcium can activate numerous proteases, endonucleases, kinases, phosphatases, and other enzymes that are damaging to cells when their activity is not tightly regulated (Krieger et al., 1994). Unfortunately, the mechanisms in place to

remove calcium are vulnerable to large increases in intracellular calcium. Sequestration of intracellular calcium in mitochondria, which appears to be the most effective method for removing cytoplasmic calcium in cortical pyramidal cell cultures (White and Reynolds, 1995), causes uncoupling of ATP synthesis from respiratory oxidation (Wang et al., 1994b; Werth and Thayer, 1994). Without active mitochondria, the efficiency of ATP production is greatly reduced. Reduced ATP results in decreased activity of the Ca^{2+}-ATPases, which leads directly to increased intracellular calcium, and the Na^{+}/K^{+} ATPases, which may cause greater calcium flux indirectly through activated voltage-dependent calcium channels. This leads to greater elevation of intracellular calcium, further reduces mitochondrial function, and initiates a potentially devastating positive feedback loop.

Besides lacking the ability to further sequester calcium and reducing energy-dependent mechanisms for calcium-extrusion, mitochondrial damage and the resultant energy-deficient state could greatly reduce other cellular functions that require ATP like axonal transport. Axonal transport, which is dependent on cellular energy, is disrupted in SOD-1 transgenic mice (Zhang et al., 1997). Although this disruption could be due to the dysfunction of a protein required for transport, the equal disruption of both fast and slow axonal transport, which utilize different transport machinery, suggests that the altered transport may be due to reduced cellular energy. The reduction in axonal transport could account for both the accumulation of NFP in somata of motor neurons and the reduced NFP in motor neuron axons that have been observed in SOD-1 transgenic mice (Morrison et al., 1996; Tu et al., 1996; Zhang et al., 1997; Morrison et al., 1998).

In addition to being altered secondary to axonal transport disruption, NFP can be abnormally phosphorylated or subject to increased proteolysis directly by mitochondrial uncoupling or increased intracellular calcium. Treatment of rat pheochromocytoma cells with a mitochondrial uncoupler leads to both a decrease in ATP levels and an increase in phosphorylation of the medium and heavy subunits of NFP (Bush et al., 1995). In addi-

tion, calcium activates an endogenous protease, calpain, that degrades NFP (Glass et al., 1994; Raabe et al., 1995). Through either of these mechanisms, NFP can be altered directly, and the observed disruptions of NFP in SOD-1 transgenic mice and motor neuron cell cultures could be dependent on these mechanisms rather than the decrease in axonal transport. In fact, alterations in NFP may lead to disruptions in axonal transport, rather than *vice versa*. Collard et al. (1995) reported a defect in anterograde axonal transport in transgenic mice that overexpress human NFP-H. Therefore, whether altered axonal transport leads to NFP disruption, or NFP disruption causes a reduction in axonal transport is unclear, and future experiments should be directed at distinguishing between these two possibilities.

What exactly causes cell death in this mechanism of degeneration? The answer to this important question is not known. Reductions in axonal transport or the accumulation of NFP could disrupt the delivery of critical factors to axon terminals, causing a dying-back neuropathy. Alternatively, the increase in intracellular calcium may activate certain enzymes, such as proteases, endonucleases, kinases, and phosphatases, that lead to cell death. The true mechanism is probably a combination of these mechanisms, because a neuron with impaired ATP production, high intracellular calcium, reduced axonal transport, and accumulation of NFP is vulnerable to degeneration from an innumerable number of mechanisms.

We suggest in this putative mechanism that NFP alteration is secondary to excitotoxic degeneration. We come to this conclusion because several studies have demonstrated that NFP is altered following an excitotoxic disruption, while there is no direct evidence that alterations in NFP increase the vulnerability of neurons to excitotoxicity. In the spinal cord of rodents administered intrathecal kainate, NFP accumulated in axonal swellings (Ikonomidou et al., 1996) and there was an increase in phosphorylated NFP in somata of ventral horn neurons (Hugon and Vallat, 1990). In addition, NFP degradation and alterations in phosphorylation were observed in neurons in other regions of the ner-

vous system following intraperitoneal injection of kainate (Wang et al., 1994a). Therefore, until NFP alteration can be shown to increase the vulnerability of neurons to excitotoxicity or alter a component of the excitotoxic mechanism, the changes in NFP must be presumed to be secondary to the excitotoxic mechanism. This conclusion is consistent with our finding that CB-containing neurons are resistant to degeneration regardless of whether or not they contain NFP, as this finding suggests that CB interacts with a component of the mechanism of degeneration that precedes alterations in NFP (see Chapter 2).

Our suggestion that the excitotoxic component of the mechanism precedes NFP disruption should not dissuade researchers from investigating this issue. Although there is no direct evidence that disruptions of NFP can precipitate an excitotoxic event, several lines of evidence suggest that NFP may modulate components of the excitotoxic mechanism. First, NFP has been shown to have both high and low affinity binding sites for calcium, and therefore may act to buffer free intracellular calcium levels (Lefebvre and Mushynski, 1987; Krinks et al., 1988; Lefebvre and Mushynski, 1988; Abercrombie et al., 1990). In fact, there are sequences in the rod domain of all NFP subunits that are homologous to the EF-hand sequence of calcium-binding proteins (Lefebvre and Mushynski, 1988). If NFP normally plays a role in buffering intracellular calcium, then the disruption of NFP in SOD-1 transgenic mice and ALS patients could lead to excitotoxicity by reducing the capacity of neurons to buffer the intracellular calcium loads that result from glutamate receptor activation. A second mechanism by which disruptions of NFP may create an excitotoxic environment is through direct interactions with glutamate receptors. Glutamate receptor subunits are anchored to the cellular membrane by cytoskeletal components, and recently, the interaction of NFP with specific glutamate receptor subunit splice variants has been demonstrated (Ehlers et al., 1998). The specificity of this interaction suggests that disruptions of NFP may lead to a loss of anchoring for some, but not all, glutamate receptor subunits. This alteration in glutamate receptor subunit composi-

tion may dramatically alter glutamate receptor function, as has been demonstrated in vitro, and may provide a mechanism by which alterations in NFP can induce excitotoxicity in a neuronal population. At this time, however, these mechanisms are speculation. Transgenic mice or cell cultures with alterations in NFP should be investigated for their sensitivity to glutamate toxicity, as they would provide a more definitive answer to this hypothesized mechanism for inducing excitotoxicity.

The major gap in this proposed mechanism is obviously the one that connects the mutations in SOD-1 with the increased activity of non-NMDA glutamate receptors. The simplest mechanism by which the activity of glutamate receptors can be increased is by elevated levels of synaptic glutamate, either by increased synaptic release of glutamate or decreased uptake of glutamate from synapses. Thus far, there has been no evidence for increased synaptic release of glutamate in ALS. In contrast, Rothstein and colleagues have demonstrated that glutamate transporters are reduced in ALS patients and SOD-1 transgenic mice (Rothstein et al., 1992; Rothstein et al., 1995; Bruijn et al., 1997b). Interestingly, the activity and protein levels of glutamate transporters are disrupted, while the mRNA levels are unaltered (Bristol and Rothstein, 1996), suggesting a post-transcriptional mechanism for disrupting glutamate transporters. Any of the proposed gains-of-function could disrupt glutamate transporters. Increased nitrotyrosines or oxidation could result in less functional protein and perhaps greater protein degradation, and thus reduced transporter activity. In fact, peroxynitrite, the substrate necessary for nitrotyrosines, inhibits glutamate transport in purified or recombinant glutamate transporters (Trotti et al., 1996). The investigators did not evaluate whether the transporters had increased nitration of tyrosines, but the finding of reduced activity is quite interesting and suggests that these transporters should be investigated in depth. In addition to altered enzymatic activity, the abnormal binding to KARS and TRAP could alter the function of the endoplasmic reticulum or protein synthesis, either of which might disrupt the translation of glutamate transporters.

In addition to increased extracellular glutamate, a second possibility for increased non-NMDA glutamate receptor-dependent excitotoxicity is a direct alteration of the glutamate receptor. In the context of the entire mechanism, increased activity of glutamate receptors is not strictly required, but rather increased permeability to calcium without a change in activity would be sufficient for this mechanism. The properties of glutamate receptors, including calcium permeability, are dependent on their receptor subunits (Hollmann and Heinemann, 1994). The calcium permeability of AMPA receptors is determined by the presence or absence of RNA edited GluR2, while RNA edited GluR5 and GluR6 appear to determine the calcium permeability of kainate receptors (Burnashev et al., 1995; Geiger et al., 1995). The presence of RNA edited GluR2 in the AMPA subunit prevents calcium flux, and RNA edited GluR5 and GluR6 appear to have a similar function in the kainate receptor. GluR2 does not appear to be altered in SOD-1 transgenic mice, but whether RNA editing of GluR2 was disrupted was not determined (see Chapter 4). The distribution of GluR5 and GluR6 have not been examined in SOD-1 transgenic mice or ALS patients. Reduced presence of GluR5 or GluR6 in the kainate receptor, or reduced RNA editing of glutamate receptor subunits, would produce glutamate receptors that respond to normal glutamate activation with abnormally high influx of calcium. Glutamate receptor subunits or enzymes important in RNA editing could be targets of oxidative damage by mutations in SOD-1, or be disrupted by the abnormal binding of mutant SOD-1 to KARS or TRAP.

A third possible mechanism for increasing calcium permeability is an alteration in the voltage-dependent calcium channel. These channels normally respond to depolarization, which can be produced by the activation of glutamate or other ligand-dependent ion channels, with increased permeability to calcium (Hofmann et al., 1994; McCleskey, 1994). The function of these calcium channels can be modified by phosphorylation, and therefore it would not be surprising if nitration or oxidation of channel subunits alters their calcium permeability properties. An alteration in these voltage-dependent calcium chan-

nels such that the channel is permeable to calcium with reduced or no depolarization would increase intracellular calcium levels and produce excitotoxic degeneration.

The mechanism for degeneration resultant from mutations in SOD-1 is by no means complete, but compared to our knowledge just a few years ago, great strides have been made toward understanding the pathogenesis of degeneration. In this chapter, we have restricted ourselves to the ALS mechanism initiated by mutations in SOD-1. This obviously would only be pertinent in a small percentage of ALS patients, as the vast majority of patients do not have mutations in SOD-1. Examining this mechanism, however, it appears likely that most of the mechanism will apply to sporadic ALS patients, as well. Sporadic ALS patients also show a reduction in glutamate transporter activity that could increase synaptic glutamate and produce an excitotoxic degeneration by the mechanism described. In addition, alterations in intracellular calcium, either mediated by an excitotoxic activation of glutamate receptors or by an autoimmune response against voltage-dependent calcium channels, are involved in some cases of sporadic ALS. The alterations in NFP, which may be near the endpoint of the proposed mechanism, are also clearly apparent in sporadic ALS as well. Therefore, it appears that the mechanism of degeneration detailed in this chapter will be applicable to all ALS patients, despite perhaps dramatic differences in the initiating events.

Appendix

List of Publications

Peer-reviewed reports:

Morrison, B.M., J.W. Gordon, M.E. Ripps, and J.H. Morrison (1996) Quantitative immunocytochemical analysis of the spinal cord in G86R superoxide dismutase transgenic mice: neurochemical correlates of selective vulnerability. J. Comp. Neurol. *373 (4):* 619-631.

Morrison, B.M., W.G. Janssen, J.W. Gordon, and J.H. Morrison (1998) Time course of neuropathology in the spinal cord of G86R superoxide dismutase transgenic mice. J. Comp. Neurol. *391 (1):* 64-77.

Morrison, B.M., W.G.M. Janssen, J.W. Gordon, and J.H. Morrison (1998) Light and electron microscopic distribution of the AMPA receptor subunit, GluR2, in the spinal cord of control and G86R mutant superoxide dismutase transgenic mice. J. Comp. Neurol. *395:* 523-534.

Review articles:

Morrison, B.M., J.H. Morrison, and J.W. Gordon (1998) Superoxide dismutase and neurofilament transgenic models of amyotrophic lateral sclerosis. J. Exp. Zoology *(in press).*

Morrison, B.M., P.R. Hof, and J.H. Morrison (1998) Determinants of neuronal vulnerability in neurodegenerative diseases. Ann. Neurol. *(in press).*

Abstracts:

Morrison, B.M., J.W. Gordon, P.R. Hof, M.E. Ripps, and J.H. Morrison (1995) Immunohistochemical characterization of degenerating neurons in the spinal cord of mutant superoxide dismutase transgenic mice. Society for Neuroscience Abstract 21, 387.14.

Morrison, B.M., J.W. Gordon, and J.H. Morrison (1996) Neurochemical Markers of Vulnerability and Protection in Mutant Superoxide Dismutase Transgenic Mice. Society for Neuroscience Abstract 22, 648.6.

Morrison, B.M., J.W. Gordon, W.G. Janssen, and J.H. Morrison (1997) Distribution of the AMPA Receptor Subunit, GluR2, in the Spinal Cord of Control and Mutant Superoxide Dismutase Transgenic Mice. Society for Neuroscience Abstract 23, 742.7

Bibliography

Abe, K., L.-H. Pan, M. Watanabe, T. Kato, and Y. Itoyama (1995) Induction of nitrotyrosine-like immunoreactivity in the lower motor neuron of amyotrophic lateral sclerosis. Neurosci. Lett. *199:*152-154.

Abercrombie, R.F., N.F. Al-Baldawi, and J. Jackson (1990) Ca^{2+} binding by Myxicola neurofilament proteins. Cell Calcium *11:*361-370.

Adams, R.D., M. Victor, and A.H. Ropper (1997) Principles of Neurology. New York: McGraw-Hill.

Alexianu, M.E., B.-K. Ho, A.H. Mohamed, V. La Bella, R.G. Smith, and S.H. Appel (1994) The role of calcium-binding proteins in selective motoneuron vulnerability in amyotrophic lateral sclerosis. Ann. Neurol. *36:*846-858.

Andressen, C., I. Blümcke, and M.R. Celio (1993) Calcium-binding proteins: Selective markers of nerve cells. Cell Tissue Res. *271:*181-208.

Antal, M., T.F. Freund, and E. Polgar (1990) Calcium-binding proteins, parvalbumin- and calbindin-D28k-immunoreactive neurons in the rat spinal cord and dorsal root ganglia: A light and electron microscopic study. J. Comp. Neurol. *295:*467-484.

Appel, S.H., R.G. Smith, J.I. Engelhardt, and E. Stefani (1993) Evidence for autoimmunity in amyotrophic lateral sclerosis. J. Neurol. Sci. *118:*169-174.

Arvidsson, U., B. Ulfhake, S. Cullheim, V. Ramirez, O. Shupliakov, and T. Hökfelt (1992) Distribution of calbindin D28k-like immunoreactivity (LI) in the monkey ventral horn: Do Renshaw cells contain calbindin D28k-LI? J. Neurosci. *12:*718-728.

Avraham, K.B., M. Schickler, D. Sapoznikov, R. Yarom, and Y. Groner (1988) Down's syndrome: Abnormal neuromuscular junction in tongue of transgenic mice with elevated levels of human Cu/Zn-superoxide dismutase. Cell *54:*823-829.

Baimbridge, K.G., M.R. Celio, and J.H. Rogers (1992) Calcium-binding proteins in the nervous system. Trends Neurosci. *15:*303-308.

Bar-Peled, O., J. Vornov, A. Thomas, R.J. O'Brien, J.H. Morrison, C.M. Knudson, S.J. Korsmeyer, and J.D. Rothstein (1997) Enhanced susceptibility of motor neurons to excitotoxicity is dependent on Ca^{2+}-permeable AMPA/kainate receptors and BAX expression. Soc. Neurosci. Abstr. *23:*2305.

Beal, M.F., R.J. Ferrante, S.E. Browne, R.T. Matthews, N.W. Kowall, and R.H. Brown Jr. (1997) Increased 3-nitrotyrosine in both sporadic and familial amyotrophic lateral sclerosis. Ann. Neurol. *42:*646-654.

Beckman, J.S., M. Carson, C.D. Smith, and W.H. Koppenol (1993) ALS, SOD and peroxynitrite. Nature *364:*584.

Beckman, J.S., and J.P. Crow (1993) Pathological implications of nitric oxide, superoxide and peroxynitrite formation. Biochem. Soc. Trans. *21:*330-334.

Beckman, J.S., H. Ischiropoulos, L. Zhu, M. van der Woerd, C. Smith, J. Chen, J. Harrison, J.C. Martin, and M. Tsai (1992) Kinetics of superoxide dismutase- and iron-catalyzed nitration of phenolics by peroxynitrite. Arch. Biochem. Biophys. *298:*438-445.

Bensimon, G., L. Lacomblez, V. Meininger, and A.S. Group (1994) A controlled trial of riluzole in amyotrophic lateral sclerosis. N. Engl. J. Med. *330:*585-591.

Bjugn, R. (1993) The use of the optical disector to estimate the number of neurons, glial and endothelial cells in the spinal cord of the mouse - with a comparative note on the rat spinal cord. Brain Res. *627:*25-33.

Bjugn, R., and H.J.G. Gundersen (1993b) Estimate of the total number of neurons and glial and endothelial cells in the rat spinal cord by means of the optical disector. J. Comp. Neurol. *328:*406-414.

Blaustein, M.P. (1988) Calcium transport and buffering in neurons. Trends Neurosci. *11:*438-443.

Bloom, F.E., W.G. Young, E.A. Nimchinsky, P.R. Hof, and J.H. Morrison (1997) Neuronal vulnerability and informatics in human disease. In S. H. Koslow, M. F. Huerta (eds): Progress in Neuroinformatics Research Vol. 1, Neuroinformatics - An Overview of the Human Brain Project. Mahwah: Lawrence Erlbaum, pp. 83-123.

Bonnot, A., M. Corio, G. Tramu, and D. Viala (1996) Immunocytochemical distribution of ionotropic glutamate receptor subunits in the spinal cord of the rabbit. J. Chem. Neuroanat. *11:*267-278.

Borchelt, D.R., M.K. Lee, H.S. Slunt, M. Guarnieri, Z.-S. Xu, P.C. Wong, R.H. Brown Jr., D.L. Price, S.S. Sisodia, and D.W. Cleveland (1994) Superoxide dismutase 1 with mutations linked to familial amyotrophic lateral sclerosis possesses significant activity. Proc. Natl. Acad. Sci. USA *91:*8292-8296.

Boulter, J., M. Hollmann, A. O'Shea-Greenfield, M. Hartley, E. Deneris, C. Maron, and S. Heinemann (1990) Molecular cloning and functional expression of glutamate receptor subunit genes. Science *249:*1033-1037.

Brady, S.T. (1993) Motor neurons and neurofilaments in sickness and in health. Cell *73:*1-3.

Bristol, L.A., and J.D. Rothstein (1996) Glutamate transporter gene expression in amyotrophic lateral sclerosis motor cortex. Ann. Neurol. *39:*676-679.

Brose, N., G.W. Huntley, Y. Stern-Bach, G. Sharma, J.H. Morrison, and S.F. Heinemann (1994) Differential assembly of coexpressed glutamate receptor subunits in neurons of rat cerebral cortex. J. Biol. Chem. *269:*16780-16784.

Bruijn, L.I., M.F. Beal, M.W. Becher, J.B. Schulz, P.C. Wong, D.L. Price, and D.W. Cleveland (1997a) Elevated free nitrotyrosine levels, but not protein-bound nitrotyrosine or hydroxyl radicals, throughout amyotrophic lateral sclerosis (ALS)-like disease implicate tyrosine nitration as an aberrant in vivo property of one familial ALS-linked superoxide dismutase 1 mutant. Proc. Natl. Acad. Sci. USA *94:*7606-7611.

Bruijn, L.I., M.W. Becher, M.K. Lee, K.L. Anderson, N.A. Jenkins, N.G. Copeland, S.S. Sisodia, J.D. Rothstein, D.R. Borchelt, D.L. Price, and D.W. Cleveland (1997b) ALS-linked SOD1 mutant G85R mediates damage to astrocytes and promotes rapidly progressive disease with SOD1-containing inclusions. Neuron *18:*327-338.

Buettner, G.R. (1993) The pecking order of free radicals and antioxidants: lipid peroxidation, a-tocopherol, and ascorbate. Arch. Biochem. Biophys. *300:*535-543.

Burnashev, N., H. Monyer, P.H. Seeburg, and B. Sakmann (1992) Divalent ion permeability of AMPA receptor channels is dominated by the edited form of a single subunit. Neuron *8:*189-198.

Burnashev, N., Z. Zhou, E. Neher, and B. Sakmann (1995) Fractional calcium currents through recombinant GluR channels of the NMDA, AMPA and kainate receptor subtypes. J. Physiol. *485.2:*403-418.

Burstein, R., R.J. Dado, and G.J. Giesler Jr. (1990) The cells of origin of the spinothalamic tract of the rat: a quantitative reexamination. Brain Res. *511:*329-337.

Bush, M.L., J.S. Miyashiro, and V.M. Ingram (1995) Activation of a neurofilament kinase, a tau kinase, and a tau phosphatase by decreased ATP levels in nerve growth factor-differentiated PC-12 cells. Proc. Natl. Acad. Sci. USA *92:*1861-1865.

Campbell, M.J., and J.H. Morrison (1989) Monoclonal antibody to neurofilament protein (SMI-32) labels a subpopulation of pyramidal neurons in the human and monkey neocortex. J Comp Neurol *282:*191-205.

Carafoli, E. (1987) Intracellular calcium homeostasis. Annu. Rev. Biochem. *56:*395-433.

Carri, M.T., A. Ferri, A. Battistoni, L. Famhy, R. Gabbianelli, F. Poccia, and G. Rotilio (1997) Expression of a Cu,Zn superoxide dismutase typical of familial amyotrophic lateral sclerosis induces mitochondrial alteration and increase of cytosolic Ca2+ concentration in transfected neuroblastoma SH-SY5Y cells. FEBS Lett. *414:*365-368.

Carriedo, S.G., H.-Z. Yin, R. Lamberta, and J.H. Weiss (1995) In vitro kainate injury to large, SMI-32(+) spinal neurons is Ca^{2+} dependent. NeuroReport *6:*945-948.

Carriedo, S.G., H.Z. Yin, and J.H. Weiss (1996) Motor neurons are selectively vulnerable to AMPA/kainate receptor-mediated injury in vitro. J. Neurosci. *16:*4069-4079.

Celio, M.R. (1990) Calbindin D-28k and parvalbumin in the rat nervous system. Neuroscience *35:*375-475.

Chard, P.S., D. Bleakman, S. Christakos, C.S. Fullmer, and R.J. Miller (1993) Calcium buffering properties of calbindin D-28k and parvalbumin in rat sensory neurones. J. Physiol. *472:*341-357.

Chiu, A.Y., P. Zhai, M.C. Dal Canto, T.M. Peters, Y.W. Kwon, S.M. Prattis, and M.E. Gurney (1995) Age-dependent penetrance of disease in a transgenic mouse model of familial amyotrophic lateral sclerosis. Mol. Cell. Neurosci. *6:*349-362.

Choi, D.W. (1987) Ionic dependence of glutamate neurotoxicity. J. Neurosci. *7:*369-379.

Choi, D.W., J. Koh, and S. Peters (1988) Pharmacology of glutamate neurotoxicity in cortical cell culture: attenuation by NMDA antagonists. J. Neurosci. *8:*185-196.

Collard, J.-F., F. Côté, and J.-P. Julien (1995) Defective axonal transport in a transgenic mouse model of amyotrophic lateral sclerosis. Nature *375:*61-64.

Côté, F., J.-F. Collard, and J.-P. Julien (1993) Progressive neuronopathy in transgenic mice expressing the human neurofilament heavy gene: A mouse model of amyotrophic lateral sclerosis. Cell *73:*35-46.

Coyle, J.T., and P. Puttfarcken (1993) Oxidative stress, glutamate, and neurodegenerative disorders. Science *262:*689-695.

Crow, J.P., J.B. Sampson, Y. Zhuang, J.A. Thompson, and J.S. Beckman (1997a) Decreased zinc affinity of amyotrophic lateral sclerosis-associated superoxide dismutase mutants leads to enhanced catalysis of tyrosine nitration by peroxynitrite. J. Neurochem. *69:*1936-1944.

Crow, J.P., Y. Zu Ye, M. Strong, M. Kirk, S. Barnes, and J.S. Beckman (1997b) Superoxide dismutase catalyzes nitration of tyrosines by peroxynitrite in the rod and head domains of neurofilament-L. J. Neurochem. *69:*1945-1953.

Dahl, D., B. Labkovsky, and A. Bignami (1988) Neurofilament phosphorylation in axons and perikarya: immunofluorescence study of the rat spinal cord and dorsal root ganglia with monoclonal antibodies. J. Comp. Neurol. *271:*445-450.

Dal Canto, M.C., and M.E. Gurney (1994) Development of central nervous system pathology in a murine transgenic model of human amyotrophic lateral sclerosis. Am. J. Pathol. *145:*1271-1279.

Dal Canto, M.C., and M.E. Gurney (1995) Neuropathological changes in two lines of mice carrying a transgene for mutant human Cu, Zn SOD, and in mice overexpressing wild type human SOD: A model of familial amyotrophic lateral sclerosis (FALS). Brain Res. *676:*25-40.

Dal Canto, M.C., and M.E. Gurney (1997) A low expressor line of transgenic mice carrying a mutant human Cu,Zn superoxide dismutase (SOD1) gene develops pathological changes that most closely resemble those in human amyotrophic lateral sclerosis. Acta Neuropathol. *93:*537-550.

Dawson, V.L., T.M. Dawson, E.D. London, D.S. Bredt, and S.H. Snyder (1991) Nitric oxide mediates glutamate neurotoxicity in primary cortical cultures. Proc. Natl. Acad. Sci. USA *88:*6368-6371.

DeFelipe, J., F. Conti, S.L. Van Eyck, and T. Manzoni (1988) Demonstration of glutamate-positive axon terminals forming asymmetric synapses in cat neocortex. Brain Res. *455:*162-165.

Deng, H.-X., A. Hentati, J.A. Tainer, Z. Iqbal, A. Cayabyab, W.-Y. Hung, E.D. Getzoff, P. Hu, B. Herzfeldt, R.P. Roos, C. Warner, G. Deng, E. Soriano, C. Smyth, H.E. Parge, A. Ahmed, A.D. Roses, R.A. Hallewell, M.A. Pericak-Vance, and T. Siddique (1993) Amyotrophic lateral sclerosis and structural defects in Cu,Zn superoxide dismutase. Science *261:*1047-1051.

Deshmukh, M., and E.M. Johnson Jr. (1997) Programmed cell death in neurons: Focus on the pathway of nerve growth factor deprivation-induced death of sympathetic neurons. Mol. Pharmacol. *51:*897-906.

Dugan, L.L., D.M. Turetsky, C. Du, D. Lobner, M. Wheeler, C.R. Almli, C.K.-F. Shen, T.-Y. Luh, D.W. Choi, and T.-S. Lin (1997) Carboxyfullerenes as neuroprotective agents. Proc. Natl. Acad. Sci. USA *94:*9434-9439.

Durham, H.D., J. Roy, L. Dong, and D.A. Figlewicz (1997) Aggregation of mutant Cu/Zn superoxide dismutase proteins in a culture model of ALS. J. Neuropathol. Exp. Neurol. *56:*523-530.

Eddleston, M., and L. Mücke (1993) Molecular profile of reactive astrocytes - implications for their role in neurologic disease. Neuroscience *54:*15-36.

Ehlers, M.D., E.T. Fung, R.J. O'Brien, and R.L. Huganir (1998) Splice variant-specific interaction of the NMDA receptor subunit NR1 with neuronal intermediate filaments. J. Neurosci. *18:*720-730.

Eyer, J., and A. Peterson (1994) Neurofilament-deficient axons and perikaryal aggregates in viable transgenic mice expressing a neurofilament-ß-galactosidase fusion protein. Neuron *12:*389-405.

Ferrante, R.J., L.A. Shinobu, J.B. Schulz, R.T. Matthews, C.E. Thomas, N.W. Kowall, M.E. Gurney, and M.F. Beal (1997) Increased 3-nitrotyrosine and oxidative damage in mice with a human copper/zinc superoxide dismutase mutation. Ann. Neurol. *42:*326-334.

Ferrer, I., E. Soriano, T. Tuñon, M. Fonseca, and N. Guionnet (1991) Parvalbumin immunoreactive neurons in normal human temporal neocortex and in patients with Alzheimer's disease. J. Neurol. Sci. *106:*135-141.

Ferrer, I., T. Tuñon, M.T. Serrano, R. Casas, S. Alcantara, M.J. Zujar, and R.M. Rivera (1993) Calbindin D-28k and parvalbumin immunoreactivity in the frontal cortex in patients with frontal lobe dementia of non-Alzheimer type associated with amyotrophic lateral sclerosis. J. Neurol. Neurosurg. Psychiatry *56:*257-261.

Figlewicz, D.A., A. Krizus, M.G. Martinoli, V. Meininger, M. Dib, G.A. Rouleau, and J.-P. Julien (1994) Variants of the heavy neurofilament subunit are associated with the development of amyotrophic lateral sclerosis. Hum. Mol. Genet. *3:*1757-1761.

Fisher, S.K., and B.B. Boycott (1974) Synaptic connexions made by horizontal cells within the outer plexiform layer of the retina of the cat and the rabbit. Proc. R. Soc. Lond. B. *186:*317-331.

Fonseca, M., and E. Soriano (1995) Calretinin-immunoreactive neurons in the normal human temporal cortex and in Alzheimer's disease. Brain Res. *691:*83-91.

Fonseca, M., E. Soriano, I. Ferrer, A. Martinez, and T. Tuñon (1993) Chandelier cell axons identified by parvalbumin-immunoreactivity in the normal human temporal cortex and in Alzheimer's disease. Neuroscience *55:*1107-1116.

Freist, W., and D.H. Gauss (1995) Lysyl-tRNA synthetase. Biol. Chem. Hoppe-Seyler *376:*451-472.

Fridovich, I. (1974) Superoxide dismutases. Adv. Enzymol. Relat. Areas Mol. Biol. *41:*35-97.

Fujii, J., T. Myint, H.G. Seo, Y. Kayanoki, Y. Ikeda, and N. Taniguchi (1995) Characterization of wild-type and amyotrophic lateral sclerosis-related mutant Cu,Zn-superoxide dismutases overproduced in baculovirus-infected insect cells. J. Neurochem. *64:*1456-1461.

Furuyama, T., H. Kiyama, K. Sato, H.T. Park, H. Maeno, H. Takagi, and M. Tohyama (1993) Region-specific expression of subunits of ionotropic glutamate receptors (AMPA-type, KA-type and NMDA receptors) in the rat spinal cord with special reference to nociception. Mol. Brain Res. *18:*141-151.

Garcia-Segura, L.M., D. Baetens, J. Roth, A.W. Norman, and L. Orci (1984) Immunohistochemical mapping of calcium-binding protein immunoreactivity in the rat central nervous system. Brain Res. *296:*75-86.

Geiger, J.R.P., T. Melcher, D.-S. Koh, B. Sakmann, P.H. Seeburg, P. Jonas, and H. Monyer (1995) Relative abundance of subunit mRNAs determines gating and Ca^{2+} permeability of AMPA receptors in principal neurons and interneurons in rat CNS. Neuron *15:*193-204.

Glass, J.D., B.L. Schryer, and J.W. Griffen (1994) Calcium-mediated degeneration of the axonal cytoskeleton in the Ola mouse. J. Neurochem. *62:*2472-2475.

Gorter, J.A., J.J. Petrozzino, E.M. Aronica, D.M. Rosenbaum, T. Opitz, M.V.L. Bennett, C. J.A., and R.S. Zukin (1997) Global ischemia induces downregulation of Glur2 mRNA and increases AMPA receptor-mediated Ca^{2+} influx in hippocampal CA1 neurons of gerbil. J. Neurosci. *17:*6179-6188.

Granum, S.L. (1986) The spinothalamic system of the rat. I. Location of cells of origin. J. Comp. Neurol. *247:*159-180.

Griffin, J.W., A.C. Clark, I. Parhad, D.F. Watson, and P.N. Hoffman (1991) The neuronal cytoskeleton in disorders of the motor neuron. In L. P. Rowland (eds): Amyotrophic Lateral Sclerosis and Other Motor Neuron Diseases. Raven Press, Ltd., pp. 103-113.

Gu, J.G., C. Albuquerque, C.J. Lee, and A.B. MacDermott (1996) Synaptic strengthening through activation of Ca^{2+}-permeable AMPA receptors. Nature *381:*793-796.

Gurney, M.E., F.B. Cuttings, P. Zhai, A. Doble, C.P. Taylor, P.K. Andrus, and E.D. Hall (1996) Benefit of vitamin E, riluzole, and gabapentin in a transgenic model of familial amyotrophic lateral sclerosis. Ann. Neurol. *39:*147-157.

Gurney, M.E., H. Pu, A.Y. Chiu, M.C. Dal Canto, C.Y. Polchow, D.D. Alexander, J. Caliendo, A. Hentati, Y.W. Kwon, H.-X. Deng, W. Chen, P. Zhai, R.L. Sufit, and T. Siddique (1994) Motor neuron degeneration in mice that express a human Cu,Zn superoxide dismutase mutation. Science *264:*1772-1775.

Hale, A.J., C.A. Smith, L.C. Sutherland, V.E.A. Stoneman, V.L. Longthorne, A.C. Culhane, and G.T. Williams (1996) Apoptosis: Molecular regulation of cell death. Eur. J. Biochem. *236:*1-26.

Halliwell, B., J.M.C. Gutteridge, and C.E. Cross (1992) Free radicals, antioxidants, and human disease: Where are we now? J. Lab. Clin. Med. *119:*598-620.

Hartmann, E., D. Gorlich, S. Kostka, A. Otto, R. Kraft, S. Knespel, E. Burger, T.A. Rapoport, and S. Prehn (1993) A tetrameric complex of membrane proteins in the endoplasmic reticulum. Eur. J. Biochem. *214:*375-381.

Hendrickson, A.E., S.P. Hunt, and J.Y. Wu (1981) Immunocytochemical localization of glutamic acid decarboxylase in monkey striate cortex. Nature *292:*605-607.

Hendry, S.H., E.G. Jones, P.C. Emson, D.E. Lawson, C.W. Heizmann, and P. Streit (1989) Two classes of cortical GABA neurons defined by differential calcium binding protein immunoreactivities. Exp. Brain Res. *76:*467-72.

Hendry, S.H.C., C.R. Houser, E.G. Jones, and J.E. Vaughn (1983) Synaptic organization of immunocytochemically identified GABA neurons in the monkey sensory-motor cortex. J. Neurocytol. *12:*639-660.

Herrmann, J.L., E. Bruckheimer, and T.J. McDonnell (1996) Cell death signal transduction and Bcl-2 function. Biochem. Soc. Trans. *24:*1059-1065.

Hirano, A. (1991) Cytopathology of amyotrophic lateral sclerosis. In L. P. Rowland (eds): Amyotrophic Lateral Sclerosis and Other Motor Neuron Diseases. New York: Raven Press, pp. 91-101.

Hirano, A., H. Donnenfeld, S. Sasaki, and I. Nakano (1984) Fine structural observations of neurofilamentous changes in amyotrophic lateral sclerosis. J. Neuropathol. Exp. Neurol. *43:*461-470.

Hirano, A., L.T. Kurland, and G.P. Sayre (1967) Familial amyotrophic lateral sclerosis. Arch. Neurol. *16:*232-243.

Hirokawa, N., M.A. Glicksman, and M.B. Willard (1984) Organization of mammalian neurofilament polypeptides within the neuronal cytoskeleton. J. Cell Biol. *98:*1523-1536.

Ho, B.-K., M.E. Alexianu, L.V. Colom, A.H. Mohamed, F. Serrano, and S.H. Appel (1996) Expression of calbindin-D28k in motoneuron hybrid cells after retroviral infection with calbindin-D28k cDNA prevents amyotrophic lateral sclerosis IgG-mediated toxicity. Proc. Natl. Acad. Sci. USA *93:*6796-6801.

Hof, P.R., K. Cox, and J.H. Morrison (1990) Quantitative analysis of a vulnerable subset of pyramidal neurons in Alzheimer's disease: I. Superior frontal and inferior temporal cortex. J. Comp. Neurol. *301:*44-54.

Hof, P.R., K. Cox, W.G. Young, M.R. Celio, J. Rogers, and J.H. Morrison (1991) Parvalbumin-immunoreactive neurons in the neocortex are resistant to degeneration in Alzheimer's disease. J. Neuropathol. Exp. Neurol. *50:*451-462.

Hof, P.R., and J.H. Morrison (1991) Neocortical neuronal subpopulations labeled by a monoclonal antibody to calbindin exhibit differential vulnerability in Alzheimer's disease. Exp. Neurol. *111:*293-301.

Hof, P.R., and J.H. Morrison (1994) The cellular basis of cortical disconnection in Alzheimer disease and related dementing conditions. In R. Terry, R. Katzman, K. Bick (eds): Alzheimer Disease. New York: Raven Press, pp. 197-229.

Hof, P.R., and J.H. Morrison (1995) Neurofilament protein defines regional patterns of cortical organization in the Macaque monkey visual system: A quantitative immunohistochemical analysis. J. Comp. Neurol. *352:*161-186.

Hof, P.R., E.A. Nimchinsky, M.R. Celio, C. Bouras, and J.H. Morrison (1993) Calretinin-immunoreactive neocortical interneurons are unaffected in Alzheimer's disease. Neurosci. Lett. *152:*145-149.

Hoffman, E.K., A.G. Reaume, H. Wilcox, D.G. Flood, Y.-G. Lin, and R.W. Scott (1995) Establishment and characterization of mice lacking Cu/Zn superoxide dismutase. Soc. Neurosci. Abstr. *21:*980.

Hoffman, P.N., D.W. Cleveland, J.W. Griffin, P.W. Landes, N.J. Cowan, and D.L. Price (1987) Neurofilament gene expression: A major determinant of axonal caliber. Proc. Natl. Acad. Sci. USA *84:*3472-3476.

Hoffman, P.N., J.W. Griffin, and D.L. Price (1984) Control of axonal caliber by neurofilament transport. J Cell Biol. *99:*705-714.

Hoffman, P.N., and R.J. Lasek (1975) The slow component of axonal transport. J. Cell Biol. *66:*351-366.

Hoffman, P.N., G.W. Thompson, J.W. Griffin, and D.L. Price (1985) Changes in neurofilament transport coincide temporally with alterations in the caliber of axons in regenerating motor fibers. J. Cell Biol. *101:*1332-1340.

Hofmann, F., M. Biel, and V. Flockerzi (1994) Molecular basis for Ca2+ channel diversity. Annu. Rev. Neurosci. *17:*399-418.

Hollmann, M., and S.F. Heinemann (1994) Cloned glutamate receptors. Annu. Rev. Neurosci. *17:*31-108.

Hollmann, M., A. O'Shea-Greenfield, S.W. Rogers, and S. Heinemann (1989) Cloning by functional expression of a member of the glutamate receptor family. Nature *342:*643-648.

Hottinger, A.F., E.G. Fine, M.E. Gurney, A.D. Zurn, and P. Aebischer (1997) The copper chelator d-penicillamine delays onset of disease and extends survival in a transgenic mouse model of familial amyotrophic lateral sclerosis. Eur. J. Neurosci. *9:*1548-1551.

Hugon, J., and J.M. Vallat (1990) Abnormal distribution of phosphorylated neurofilaments in neuronal degeneration induced by kainic acid. Neurosci. Lett. *119:*45-48.

Ikonomidou, C., Y. Qin Qin, J. Labruyere, and J.W. Olney (1996) Motor neuron degeneration induced by excitotoxin agonists has features in common with those seen in the SOD-1 transgenic mouse model of amyotrophic lateral sclerosis. J. Neuropathol. Exp. Neurol. *55:*211-224.

Inano, H., and B.-I. Tamaoki (1986) Purification of NADPH-cytochrome P-450 reductase from microsomal fraction of rat testes, and its chemical modification by tetranitromethane. J. Steroid Biochem. *25:*21-28.

Ince, P., N. Stout, P. Shaw, J. Slade, W. Hunziker, C.W. Heizmann, and K.G. Baimbridge (1993) Parvalbumin and calbindin D-28k in the human motor system and in motor neuron disease. Neuropathol. Appl. Neurobiol. *19:*291-299.

Ischiropoulos, H., L. Zhu, J. Chen, M. Tsai, J.C. Martin, C.D. Smith, and J.S. Beckman (1992) Peroxynitrite-mediated tyrosine nitration catalyzed by superoxide dismutase. Arch. Biochem. Biophys. *298:*431-437.

Jakowec, M.W., A.J. Fox, L.J. Martin, and R.G. Kalb (1995a) Quantitative and qualitative changes in AMPA receptor expression during spinal cord development. Neuroscience *67:*893-907.

Jakowec, M.W., L. Yen, and R.G. Kalb (1995b) In situ hybridization analysis of AMPA receptor subunit gene expression in the developing rat spinal cord. Neuroscience *67:*909-920.

Jonas, P., C. Racca, B. Sakmann, P.H. Seeburg, and H. Monyer (1994) Differences in Ca2+ permeability of AMPA-type glutamate receptor channels in neocortical neurons caused by differential GluR-B subunit expression. Neuron *12:*1281-1289.

Kamal-Eldin, A., and L.-A. Appelqvist (1996) The chemistry and antioxidant properties of tocopherols and tocotrienols. Lipids *31:*671-701.

Keinanen, K., W. Wisden, B. Sommer, P. Werner, A. Herb, T.A. Verdoorn, B. Sakmann, and P.H. Seeburg (1990) A family of AMPA-selective glutamate receptors. Science *249:*556-560.

Kimura, F., R.G. Smith, O. Delbono, O. Nyormoi, T. Schneider, W. Nastainczyk, F. Hofmann, E. Stefani, and S.H. Appel (1994) Amyotrophic lateral sclerosis patient antibodies label Ca^{2+} channel alpha1 subunit. Ann. Neurol. *35:*164-171.

Kong, S.-K., M.B. Yim, E.R. Stadtman, and P.B. Chock (1996) Peroxynitrite disables the tyrosine phosphorylation regulatory mechanism: Lymphocyte-specific tyrosine kinase fails to phosphorylate nitrated cdc2(6-20)NH2 peptide. Proc. Natl. Acad. Sci. USA *93:*3377-3382.

Kostic, V., V. Jackson-Lewis, F. de Bilbao, M. Dubois-Dauphin, and S. Przedborski (1997) BCL-2: Prolonging life in a transgenic mouse model of familial amyotrophic lateral sclerosis. Science *277:*559-562.

Krieger, C., K. Jones, S.U. Kim, and A.A. Eisen (1994) The role of intracellular free calcium in motor neuron disease. J. Neurol. Sci. *124 (Suppl):*27-32.

Krinks, M.H., C.B. Klee, H.C. Pant, and H. Gainer (1988) Identification and quantification of calcium-binding proteins in squid axoplasm. J. Neurosci. *8:*2172-2182.

Kunst, C.B., E. Mezey, M.J. Brownstein, and D. Patterson (1997) Mutations in SOD1 associated with amyotrophic lateral sclerosis cause novel protein interactions. Nature Genet. *15:*91-94.

Kwak, S., and R. Nakamura (1995) Selective degeneration of inhibitory interneurons in the rat spinal cord induced by intrathecal infusion of acromelic acid. Brain Res. *702:*61-71.

Kyrozis, A., P.A. Goldstein, M.J.S. Heath, and A.B. MacDermott (1995) Calcium entry through a subpopulation of AMPA receptors desensitized neighbouring NMDA receptors in rat dorsal horn. J. Physiol. *485.2:*373-381.

Lafon-Cazal, M., S. Pietri, M. Culcasi, and J. Bockaert (1993) NMDA-dependent superoxide production and neurotoxicity. Nature *364:*535-537.

Lee, M.K., and D.W. Cleveland (1996) Neuronal intermediate filaments. Annu. Rev. Neurosci. *19:*187-217.

Lee, M.K., J.R. Marszalek, and D.W. Cleveland (1994) A mutant neurofilament subunit causes massive, selective motor neuron death: Implication for the pathogenesis of human motor neuron disease. Neuron *13:*975-988.

Lee, M.K., Z. Xu, P.C. Wong, and D.W. Cleveland (1993) Neurofilaments are obligate heteropolymers in vivo. J. Cell Biol. *122:*1337-1350.

Lee, V.M.-Y., M.J. Carden, W.W. Schlaepfer, and J.Q. Trojanowski (1987) Monoclonal antibodies distinguish several differentially phosphorylated states of the two largest rat neurofilament subunits (NF-H and NF-M) and demonstrate their existence in the normal nervous system of adult rats. J. Neurosci. *7:*3474-3488.

Lee, V.M.-Y., L. Otvos Jr., M.J. Carden, M. Hollosi, B. Dietzschold, and R.A. Lazzarini (1988) Identification of the major multiphosphorylation site in mammalian neurofilaments. Proc. Natl. Acad. Sci. USA *85:*1998-2002.

Lefebvre, S. and W.E. Mushynski (1987) Calcium binding to untreated and dephosphorylated porcine neurofilaments. Biochem. Biophys. Res. Comm. *145:*1006-1011.

Lefebvre, S. and W.E. Mushynski (1988) Characterization of the cation-binding properties of porcine neurofilaments. Biochemistry *27:*8503-8508.

Leigh, P.N., A. Dodson, M. Swash, J.-P. Brion, and B.H. Anderton (1989) Cytoskeletal abnormalities in motor neuron disease. Brain *112:*521-535.

Leigh, P.N., and K. Ray-Chaudhuri (1994) Motor neuron disease. J. Neurol. Neurosurg. Psychiatry *57:*886-896.

Leigh, P.N., and M. Swash (1991) Cytoskeletal pathology in motor neuron disease. In L. P. Rowland (eds): Amyotrophic Lateral Sclerosis and Other Motor Neuron Diseases. New York: Raven Press, pp. 115-124.

Levitan, I.B. (1994) Modulation of ion channels by protein phosphorylation and dephosphorylation. Annu. Rev. Physiol. *56:*193-212.

Lledo, P.-M., B. Somasundaram, A.J. Morton, P.C. Emson, and W.T. Mason (1992) Stable transfection of calbindin-D28k into the GH3 cell line alters calcium currents and intracellular calcium homeostasis. Neuron *9:*943-954.

Lukas, W., and K.A. Jones (1994) Cortical neurons containing calretinin are selectively resistant to calcium overload and excitotoxicity in vitro. Neuroscience *61:*307-316.

Luque, J.M., Z. Bleuel, P. Malherbe, and J.G. Richards (1994) Alternatively spliced isoforms of the N-Methyl-D-Aspartate receptor subunit 1 are differentially distributed within the rat spinal cord. Neuroscience *63:*629-635.

Maas, S., T. Melcher, and P.H. Seeburg (1997) Mammalian RNA-dependent deaminases and edited mRNAs. Curr. Opin. Cell. Biol. *9:*343-349.

Manetto, V., N.H. Sternberger, G. Perry, L.A. Sternberger, and P. Gambetti (1988) Phosphorylation of neurofilaments is altered in amyotrophic lateral sclerosis. J. Neuropathol. Exp. Neurol. *47:*642-653.

Margulies, J.E., R.W. Cohen, M.S. Levine, and J.B. Watson (1993) Decreased GluR2(B) receptor subunit mRNA expression in cerebellar neurons at risk for degeneration. Dev. Neurosci. *15:*110-120.

Marszalek, J.R., T.L. Williamson, M.K. Lee, Z. Xu, P.N. Hoffman, M.W. Becher, T.O. Crawford, and D.W. Cleveland (1996) Neurofilament subunit NF-H modulates axonal diameter by selectively slowing neurofilament transport. J. Cell Biol. *135:*711-724.

Martin, L.J., C.D. Blackstone, A.I. Levey, R.L. Huganir, and D.L. Price (1993) AMPA glutamate receptor subunits are differentially distributed in rat brain. Neuroscience *53:*327-358.

Mattson, M.P., B. Rychlik, C. Chu, and S. Christakos (1991) Evidence for calcium-reducing and excitoprotective roles for the calcium-binding protein calbindin-D28k in cultured hippocampal neurons. Neuron *6:*41-51.

Matus, A. (1988) Neurofilament protein phosphorylation- where, when and why. Trends Neurosci. *11:*291-292.

McCleskey, E.W. (1994) Calcium channels: Cellular roles and molecular mechanisms. Curr. Opin. Neurobiol. *4:*304-312.

McHanwell, S., and T.J. Biscoe (1981) The localization of motoneurons supplying the hindlimb muscles of the mouse. Philos. Trans. R. Soc. Lond. (B) *293:*477-508.

Meldrum, B., and J. Garthwaite (1990) Excitatory amino acid neurotoxicity and neurodegenerative disease. Trends Pharmacol. Sci. *11:*379-387.

Miyasaka, H., S. Okabe, K. Ishiguro, T. Uchida, and N. Hirokawa (1993) Interaction of the tail domain of high molecular weight subunits of neurofilaments with the COOH-terminal region of tubulin and its regulation by tau protein kinase II. J. Biol. Chem. *268:*22695-22702.

Mizusawa, H., S. Matsumoto, S.-H. Yen, A. Hirano, R.R. Rojas-Corona, and H. Donnenfeld (1989) Focal accumulation of phosphorylated neurofilaments within anterior horn cell in familial amyotrophic lateral sclerosis. Acta Neuropathol. *79:*37-43.

Mockel, V., and G. Fischer (1994) Vulnerability to excitotoxic stimuli of cultured rat hippocampal neurons containing the calcium-binding proteins calretinin and calbindin D-28k. Brain Res. *648:*109-120.

Montgomery, D.L. (1994) Astrocytes: Form, functions, and roles in disease. Vet. Pathol. *31:*145-167.

Morrison, B.M., J.W. Gordon, M.E. Ripps, and J.H. Morrison (1996) Quantitative immunocytochemical analysis of the spinal cord in G86R superoxide dismutase transgenic mice: neurochemical correlates of selective vulnerability. J. Comp. Neurol. *373:*619-631.

Morrison, B.M., W.G. Janssen, J.W. Gordon, and J.H. Morrison (1998) Time course of neuropathology in the spinal cord of G86R superoxide dismutase transgenic mice. J. Comp. Neurol. *391:*64-77.

Morrison, B.M., W.G.M. Janssen, J.W. Gordon, and J.H. Morrison (1998) Light and electron microscopic distribution of the AMPA receptor subunit, GluR2, in the spinal cord of control and G86R superoxide dismutase transgenic mice. J. Comp. Neurol. *395:*523-534.

Morrison, J.H., D.A. Lewis, and M.J. Campbell (1987) The distribution of neurofibrillary tangles and non-phosphorylated neurofilament protein-immunoreactive neurons in cerebral cortex: Implications for loss of corticocortical circuits in Alzheimer's disease. In P. Davies, C. Finch (eds): Molecular Neuropathology of Aging. New York: Cold Spring Harbor Laboratory, pp. 109-124.

Mourelatos, Z., N.K. Gonatas, A. Stieber, M.E. Gurney, and M.C. Dal Canto (1996) The Golgi apparatus of spinal cord motor neurons in transgenic mice expressing mutant Cu,Zn superoxide dismutase becomes fragmented in early, preclinical stages of the disease. Proc. Natl. Acad. Sci. USA *93:*5472-5477.

Mu, X., R.D. Azbill, and J.E. Springer (1997) Riluzole treatment following spinal cord injury improves mitochondrial function and increases glutamate and glucose uptake. Soc. Neurosci. Abstr. *23:*541.16.

Munoz, D.G., C. Greene, D.P. Perl, and D.J. Selkoe (1988) Accumulation of phosphorylated neurofilaments in anterior horn motoneurons of amyotrophic lateral sclerosis patients. J. Neuropathol. Exp. Neurol. *47:*9-18.

Nakanishi, S. (1992) Molecular diversity of glutamate receptors and implications for brain function. Science *258:*597-603.

Nicolopoulos-Stournaras, S., and J.F. Iles (1983) Motor neuron columns in the lumbar spinal cord of the rat. J. Comp. Neurol. *217:*75-85.

Nishida, C.R., E.B. Gralla, and J.S. Valentine (1994) Characterization of three yeast copper-zinc superoxide dismutase mutants analogous to those coded for in familial amyotrophic lateral sclerosis. Proc. Natl. Acad. Sci. USA *91:*9906-9910.

Nixon, R.A., and R.K. Sihag (1991) Neurofilament phosphorylation: a new look at regulation and function. Trends Neurosci. *14:*501-506.

Ohara, O., Y. Gahara, T. Miyake, H. Teraoka, and T. Kitamura (1993) Neurofilament deficiency in quail caused by nonsense mutation in neurofilament-L gene. J. Cell Biol. *121:*387-395.

Olanow, C.W., and G.W. Arendash (1994) Metals and free radicals in neurodegeneration. Curr. Opin. Neurol. *7:*548-558.

Orrenius, S., M.J. Burkitt, G.E.N. Kass, J.M. Dypbukt, and P. Nicotera (1992) Calcium ions and oxidative cell injury. Ann. Neurol. *32:*S33-S42.

Oyanagi, K., F. Ikuta, and Y. Horikawa (1989) Evidence for sequential degeneration of the neurons in the intermediate zone of the spinal cord in amyotrophic lateral sclerosis: A topographic and quantitative investigation. Acta Neuropathol. *77:*343-349.

Pardo, C.A., Z. Xu, D.R. Borchelt, D.L. Price, S.S. Sisodia, and D.W. Cleveland (1995) Superoxide dismutase is an abundant component in cell bodies, dendrites, and axons of motor neurons and in a subset of other neurons. Proc. Natl. Acad. Sci. USA *92:*954-958.

Paschen, W., J. Schmitt, C. Gissel, and E. Dux (1997) Developmental changes of RNA editing of glutamate receptor subunits GluR5 and GluR6: In vivo versus in vitro. Dev. Brain Res. *98:*271-280.

Pellegrini-Giampietro, D.E., R.S. Zukin, M.V.L. Bennett, S. Cho, and W.A. Pulsinelli (1992) Switch in glutamate receptor subunit gene expression in CA1 subfield of hippocampus following global ischemia in rats. Proc. Natl. Acad. Sci. USA *89:*10499-10503.

Perry, G., D. Stewart, R. Friedman, V. Manetto, L. Autilio-Gambetti, and P. Gambetti (1987a) Filament's of Pick's bodies contain altered cytoskeletal elements. Am. J. Pathol. *127:*559-568.

Perry, T.L., S. Hansen, and K. Jones (1987b) Brain glutamate deficiency in amyotrophic lateral sclerosis. Neurology *37:*1845-1848.

Peters, A., and K.M. Harriman (1992) Different kinds of axon terminals forming symmetric synapses with the cell bodies and initial axon segments of layer II/III pyramidal cells. III. Origins and frequency of occurrence of the terminals. J. Neurocytol. *21:*679-692.

Petralia, R.S., Y.-X. Wang, E. Mayat, and R.J. Wenthold (1997) Glutamate receptor subunit 2-selective antibody shows a differential distribution of calcium-impermeable AMPA receptors among populations of neurons. J. Comp. Neurol. *385:*456-476.

Petralia, R.S., Y.-X. Wang, and R.J. Wenthold (1994a) Histological and ultrastructural localization of the kainate receptor subunits, KA2 and GluR6/7, in the rat nervous system using selective antipeptide antibodies. J. Comp. Neurol. *349:*85-110.

Petralia, R.S., N. Yokotani, and R.J. Wenthold (1994b) Light and electron microscope distribution of the NMDA receptor subunit NMDAR1 in the rat nervous system using a selective anti-peptide antibody. J. Neurosci. *14:*667-696.

Phend, K.D., A. Rustioni, and R.J. Weinberg (1995) An osmium free method of epon embedment that preserves both ultrastructure and antigenicity for post-embedding immunohistochemistry. J. Histochem. Cytochem. *43:*283-292.

Phend, K.D., R.J. Weinberg, and A. Rustioni (1992) Techniques to optimize post-embedding single and double staining for amino acid neurotransmitters. J. Histochem. Cytochem. *40:*1011-1020.

Plaitakis, A. (1991) Altered glutamatergic mechanisms and selective motor neuron degeneration in amyotrophic lateral sclerosis. In L. P. Rowland (eds): Amyotrophic Lateral Sclerosis and Other Motor Neuron Diseases. Raven Press, Ltd., pp. 319-326.

Plaitakis, A., and J.T. Caroscio (1987) Abnormal glutamate metabolism in amyotrophic lateral sclerosis. Ann. Neurol. *22:*575-579.

Plaitakis, A., E. Constantakakis, and J. Smith (1988) The neuroexcitotoxic amino acids glutamate and aspartate are altered in the spinal cord and brain in amyotrophic lateral sclerosis. Ann. Neurol. *24:*446-449.

Pogun, S., V. Dawson, and M.J. Kuhar (1994) Nitric oxide inhibits ^{3}H-glutamate transport in synaptasomes. Synapse *18:*21-26.

Puchalski, R.B., J.-C. Louis, N. Brose, S.F. Traynelis, J. Egebjerg, V. Kukekov, R.J. Wenthold, S.W. Rogers, F. Lin, T. Moran, J.H. Morrison, and S.F. Heinemann (1994) Selective RNA editing and subunit assembly of native glutamate receptors. Neuron *13:*131-147.

Raabe, T.D., T. Nguyen, and G.D. Bittner (1995) Calcium-activated proteolysis of neurofilament proteins in goldfish Mauthner axons. J. Neurobiol. *26:*253-261.

Rabizadeh, S., E.B. Gralla, D.R. Borchelt, R. Gwinn, J.S. Valentine, S. Sisodia, P. Wong, M. Lee, H. Hahn, and D.E. Bredesen (1995) Mutations associated with amyotrophic lateral sclerosis convert superoxide dismutase from an antiapoptotic gene to a proapoptotic gene: studies in yeast and neural cells. Proc. Natl. Acad. Sci. USA *92:*3024-3028.

Reaume, A.G., J.L. Elliott, E.K. Hoffman, N.W. Kowall, R.J. Ferrante, D.F. Siwek, H.M. Wilcox, D.G. Flood, M.F. Beal, R.H. Brown, R.W. Scott, and W.D. Snider (1996) Motor neurons in Cu/Zn superoxide dismutase-deficient mice develop normally but exhibit enhanced cell death after axonal injury. Nature Genet. *13:*43-47.

Ren, K., and M.A. Ruda (1994) A comparative study of the calcium-binding proteins calbindin-D28k, calretinin, calmodulin and parvalbumin in the rat spinal cord. Brain Res. Rev. *19:*163-179.

Resibois, A., and J.H. Rogers (1992) Calretinin in rat brain: an immunohistochemical study. Neuroscience *46:*101-134.

Riordan, J.F., M. Sokolovsky, and B.L. Vallee (1966) Tetranitromethane. A reagent for the nitration of tyrosine and tyrosyl residues of proteins. J. Am. Chem. Soc. *88:*4104-4105.

Ripps, M.E., G.W. Huntley, P.R. Hof, J.H. Morrison, and J.W. Gordon (1995) Transgenic mice expressing an altered murine superoxide dismutase gene provide an animal model of amyotrophic lateral sclerosis. Proc. Natl. Acad. Sci. USA *92:*689-693.

Rooke, K., D.A. Figlewicz, F.-Y. Han, and G.A. Rouleau (1996) Analysis of the KSP repeat of the neurofilament heavy subunit in familial amyotrophic lateral sclerosis. Neurology *46:*789-790.

Rosen, D.R., T. Siddique, D. Patterson, D.A. Figlewicz, P. Sapp, A. Hentati, D. Donaldson, J. Goto, J.P. O'Regan, H.-X. Deng, Z. Rahmani, A. Krizus, D. McKenna-Yasek, A. Cayabyab, S.M. Gaston, R. Berger, R.E. Tanzi, J.J. Halperin, B. Herzfeldt, R. Van den Bergh, W.-Y. Hung, T. Bird, G. Deng, D.W. Mulder, C. Smyth, N.G. Laing, E. Soriano, M.A. Pericak-Vance, J. Haines, G.A. Rouleau, J.S. Gusella, H.R. Horvitz, and R.H. Brown Jr. (1993) Mutations in Cu/Zn superoxide dismutase are associated with familial amyotrophic lateral sclerosis. Nature *362:*59-62.

Rothstein, J.D. (1995) Excitotoxic mechanisms in the pathogenesis of Amyotrophic Lateral Sclerosis. In G. Serratrice, T. Munsat (eds): Pathogenesis and Therapy of Amyotrophic Lateral Sclerosis. Philadelphia: Lippincott-Raven Publishers, pp. 7-20.

Rothstein, J.D., M. Dykes-Hoberg, C.A. Pardo, L.A. Bristol, L. Jin, R.W. Kuncl, Y. Kanai, M.A. Hediger, Y. Wang, J.P. Schielke, and D.F. Welty (1996) Knockout of glutamate transporters reveals a major role for astroglial transport in excitotoxicity and clearance of glutamate. Neuron *16:*675-686.

Rothstein, J.D., L. Jin, M. Dykes-Hoberg, and R.W. Kuncl (1993) Chronic inhibition of glutamate uptake produces a model of slow neurotoxicity. Proc. Natl. Acad. Sci. USA *90:*6591-6595.

Rothstein, J.D., and R.W. Kuncl (1995) Neuroprotective strategies in a model of chronic glutamate-mediated motor neurons toxicity. J. Neurochem. *65:*643-651.

Rothstein, J.D., R.W. Kuncl, L. Clawson, D.R. Cornblath, D.B. Drachman, and A. Pestronk (1989) Cerebrospinal fluid excitatory amino acids in amyotrophic lateral sclerosis. Ann. Neurol. *26:*144.

Rothstein, J.D., L.J. Martin, and R.W. Kuncl (1992) Decreased glutamate transport by the brain and spinal cord in amyotrophic lateral sclerosis. N. Engl. J. Med. *326:*1464-1468.

Rothstein, J.D., G. Tsai, R.W. Kuncl, L. Clawson, D.R. Cornblath, D.B. Drachman, A. Pestronk, B.L. Stauch, and J.T. Coyle (1990) Abnormal excitatory amino acid metabolism in amyotrophic lateral sclerosis. Ann. Neurol. *28:*18-25.

Rothstein, J.D., M. Van Kammen, A.I. Levey, L.J. Martin, and R.W. Kuncl (1995) Selective loss of glial glutamate transporter GLT-1 in amyotrophic lateral sclerosis. Ann. Neurol. *38:*73-84.

Rowan, S., and D.E. Fisher (1997) Mechanisms of apoptotic cell death. Leukemia *11:*457-465.

Roy, J., S. Minotti, L. Dong, D.A. Figlewicz, and H.D. Durham (1997) Blockade of non-NMDA glutamate receptors protects motor neurons from toxicity of SOD-1 mutants linked to familial ALS. Soc. Neurosci. Abstr. *23:*742.9.

Rutka, J.T., M. Murakami, P.B. Dirks, S.L. Hubbard, L.E. Becker, K. Fukuyama, S. Jung, A. Tsuga, and K. Matsuzawa (1997) Role of glial filament in cells and tumors of glial origin: A review. J. Neurosurg. *87:*420-430.

Sakaguchi, T., M. Okada, T. Kitamura, K. Kawasaki (1993) Reduced diameter and conduction velocity of myelinated fibers in the sciatic nerve of neurofilament-deficient mutant quail. Neurosci. Lett. *153:*65-68.

Sakla, F.B. (1969) Quantitative studies of the postnatal growth of the spinal cord and the vertebral column of the albino mouse. J. Comp. Neurol. *136:*237-252.

Sato, K., H. Kiyama, and M. Tohyama (1993) The differential expression patterns of messenger RNAs encoding non-N-methyl-D-aspartate glutamate receptor subunits (GluR1-4) in the rat brain. Neuroscience *52:*515-539.

Schmitt, J., E. Dux, C. Gissel, and W. Paschen (1996) Regional analysis of developmental changes in the extent of GluR6 mRNA editing in rat brain. Dev. Brain Res. *91:*153-157.

Seeburg, P.H. (1993) The molecular biology of mammalian glutamate receptor channels. Trends Neurosci. *16:*359-365.

Sharp, G.A., G. Shaw, and K. Weber (1982) Immunoelectronmicroscopical localization of the three neurofilament triplet proteins along neurofilaments of cultured dorsal root ganglion neurones. Exp. Cell Res. *137:*403-413.

Shaw, G. (1991) Neurofilament Proteins. In R.D. Burgoyne (ed): The Neuronal Cytoskeleton. New York: Wiley-Liss, pp. 185-214.

Shetty, K.T., W.T. Link, and H.C. Pant (1993) cdc2-like kinase from rat spinal cord specifically phosphorylates KSPXK motifs in neurofilament proteins: Isolation and characterization. Proc. Natl. Acad. Sci. USA *90:*6844-6848.

Shimokawa, T., R.J. Kulmacz, D.L. DeWitt, and W.L. Smith (1990) Tyrosine 385 of prostaglandin endoperoxide synthase is required for cyclooxygenase catalysis. J. Biol. Chem. *265:*20073-20076.

Shimuzu, S., Y. Eguchi, W. Kamiike, S. Waguri, Y. Uchiyama, H. Matsuda, and Y. Tsujimoto (1996) Bcl-2 blocks loss of mitochondrial membrane potential while ICE inhibitors act at a different step during inhibition of death induced by respiratory chain inhibitors. Oncogene *13:*21-29.

Siddique, T., and H.-X. Deng (1996) Genetics of amyotrophic lateral sclerosis. Hum. Mol. Genet. *5:*1465-1470.

Sidman, R.L., J.B. Angevine Jr., and E. Taber Pierce (1971) Atlas of the Mouse Brain and Spinal Cord. Cambridge, MA: Harvard University Press.

Smith, R.G., M.E. Alexianu, G. Crawford, O. Nyormoi, E. Stefani, and S.H. Appel (1994) Cytotoxicity of immunoglobulins from amyotrophic lateral sclerosis patients on a hybrid motoneuron cell line. Proc. Natl. Acad. Sci. USA *91:*3393-3397.

Smith, R.G., S. Hamilton, F. Hofmann, T. Schneider, W. Nastainczyk, L. Birnbaumer, E. Stefani, and S.H. Appel (1992) Serum antibodies to L-type calcium channels in patients with amyotrophic lateral sclerosis. N. Engl. J. Med. *327:*1721-1728.

Sokolovsky, M., J.F. Riordan, and B.L. Vallee (1966) Tetranitromethane. A reagent for the nitration of tyrosyl residues in proteins. Biochemistry *5:*3582-3589.

Sommer, B., M. Kohler, R. Sprengel, and P.H. Seeburg (1991) RNA editing in brain controls a determinant of ion flow in glutamate-gated channels. Cell *67:*11-19.

Sternberger, L.A., and N.H. Sternberger (1983) Monoclonal antibodies distinguish phosphorylated and nonphosphorylated forms of neurofilaments in situ. Proc. Natl. Acad. Sci. USA *80:*6126-6130.

Straube-West, K., P.A. Loomis, P. Opal, and R.D. Goldman (1996) Alterations in neural intermediate filament organization: functional implications and the induction of pathological changes related to motor neuron disease. J. Cell Sci. *109:*2319-2329.

Swanson, R.A., J. Liu, J.W. Miller, J.D. Rothstein, K. Farrell, B.A. Stein, and M.C. Longuemare (1997) Neuronal regulation of glutamate transporter subtype expression in astrocytes. J. Neurosci. *17:*932-940.

Switzer, R.C., III (1993) Silver staining methods: their role in detecting neurotoxicity. Ann. NY Acad. Sci. *679:*341-348.

Tachibana, M., R.J. Wenthold, H. Morioka, and R.S. Petralia (1994) Light and electron microscopic immunocytochemical localization of AMPA-selective glutamate receptors in the rat spinal cord. J. Comp. Neurol. *344:*431-454.

Takeda, S., F. Arisaka, S.-I. Ishii, and Y. Kyogoku (1990) Structural studies of the contractile tail sheath protein of bacteriophage T4. Conformational change of the tail sheath upon contraction as probed by differential chemical modification. Biochemistry *29:*5050-5056.

Tandan, R. (1994) Clinical features and differential diagnosis of classical motor neuron disease. In A. C. Williams (eds): Motor Neuron Disease. London: Chapman and Hall, pp. 3-28.

Temkin, R., D. Lowe, P. Jensen, H. Hatt, and D.O. Smith (1997) Expression of glutamate receptor subunits in alpha-motoneurons. Mol. Brain. Res. *52:*38-45.

Terao, S., G. Sobue, Y. Hashizume, T. Mitsuma, and A. Takahashi (1994) Disease-specific patterns of neuronal loss in the spinal ventral horn in amyotrophic lateral sclerosis, multiple system atrophy and X-linked recessive bulbospinal neuronopathy, with special reference to the loss of small neurons in the intermediate zone. J. Neurol. *241:*196-203.

Tolle, T.R., A. Berthele, W. Zieglgansberger, P.H. Seeberg, and W. Wisden (1993) The differential expression of 16 NMDA and non-NMDA receptor subunits in the rat spinal cord and in periaqueductal gray. J. Neurosci *13:*5009-5028.

Tolle, T.R., A. Berthele, W. Zieglgansberger, P.H. Seeburg, and W. Wisden (1995) Flip and flop variants of AMPA receptors in the rat lumbar spinal cord. Eur. J. Neurosci. *7:*1414-1419.

Tomiyama, M., R. Rodriguez-Puertas, R. Cortes, A. Christnacher, B. Sommer, A. Pazos, J.M. Palacios, and G. Mengod (1996) Differential regional distribution of AMPA receptor subunit messenger RNAs in the human spinal cord as visualized by in situ hybridization. Neuroscience *75:*901-915.

Trojanowski, J.Q., M.L. Schmidt, R.-W. Shin, G.T. Bramblett, D. Rao, and V.M.-Y. Lee (1993) Altered tau and neurofilament proteins in neurodegenerative diseases: Diagnostic implications for Alzheimer's disease and Lewy body dementias. Brain Pathol. *3:*45-54.

Trojanowski, J.Q., N. Walkenstein, and V.M.-Y. Lee (1986) Expression of neurofilament subunits in neurons of the central and peripheral nervous system: An immunohistochemical study with monoclonal antibodies. J. Neurosci. *6:*650-660.

Troost, D., P.A.E. Sillevis Smitt, J.M.B.V. de Jong, and D.F. Swaab (1992) Neurofilament and glial alterations in the cerebral cortex in amyotrophic lateral sclerosis. Acta Neuropathol. *84:*664-673.

Trotti, D., D. Rossi, O. Gjesda, L.M. Levy, G. Racagni, N.C. Danbolt, and A. Volterra (1996) Peroxynitrite inhibits glutamate transporter subtypes. J. Biol. Chem. *271:*5976-5979.

Tsuda, T., S. Munthasser, P.E. Fraser, M.E. Percy, I. Rainero, G. Vaula, L. Pinessi, L. Bergamini, G. Vignocchi, D.R. Crapper McLachlan, W.G. Tatton, and P. St George-Hyslop (1994) Analysis of the functional effects of a mutation in SOD1 associated with familial amyotrophic lateral sclerosis. Neuron *13:*727-736.

Tu, P.-H., P. Raju, K.A. Robinson, M.E. Gurney, J.Q. Trojanowski, and V.M.-Y. Lee (1996) Transgenic mice carrying a human mutant superoxide dismutase transgene develop neuronal cytoskeletal pathology resembling human amyotrophic lateral sclerosis lesions. Proc. Natl. Acad. Sci. USA *93:*3155-3160.

Tu, P.-H., K.A. Robinson, F. de Snoo, J. Eyer, A. Peterson, V.M.-Y. Lee, and J.Q. Trojanowski (1997) Selective degeneration of Purkinje cells with Lewy body-like inclusions in aged NFHLACZ trasngenic mice. J. Neurosci. *17:*1064-1074.

Tymianski, M., M.C. Wallace, I. Spigelman, M. Uno, P.L. Carlen, C.H. Tator, and M.P. Charlton (1993) Cell-permeant Ca^{2+} chelators reduce early excitotoxic and ischemic neuronal injury in vitro and in vivo. Neuron *11:*221-235.

Ulrich, J., M. Haugh, B.H. Anderton, A. Probst, C. Lautenschlager, and B. His (1987) Alzheimer dementia and Pick's disease: neurofibrillary tangles and Pick bodies are associated with identical phosphorylated neurofilament epitopes. Acta Neuropathol. *73:*240-246.

van Acker, S.A.B.E., L.M.H. Koymans, and A. Bast (1993) Molecular pharmacology of vitamin E: Structural aspects of antioxidant activity. Free Rad. Biol. Med. *15:*311-328.

van der Vliet, A., J.P. Eiserich, C.A. O'Neill, B. Halliwell, and C.E. Cross (1995) Tyrosine modification by reactive nitrogen species: A closer look. Arch. Biochem. Biophys. *319:*341-349.

Vechio, J.D., L.I. Bruijn, Z. Xu, R.H. Brown Jr., and D.W. Cleveland (1996) Sequence variants in human neurofilament proteins: Absence of linkage to familial amyotrophic lateral sclerosis. Ann. Neurol. *40:*603-610.

Vickers, J.C., and M. Costa (1992) The neurofilament triplet is present in distinct subpopulations of neurons in the central nervous system of the guinea-pig. Neuroscience *49:*73-100.

Vickers, J.C., A. Delacourte, and J.H. Morrison (1992) Progressive transformation of the cytoskeleton associated with normal aging and Alzheimer's disease. Brain Res. *594:*273-278.

Vickers, J.C., R.A. Lazzarini, B.M. Riederer, and J.H. Morrison (1995a) Intraperikaryal neurofilamentous accumulations in a subset of retinal ganglion cells in aged mice that express a human neurofilament gene. Exp. Neurol. *136:*266-269.

Vickers, J.C., J.H. Morrison, V.L. Friedrich Jr., G.A. Elder, D.P. Perl, R.N. Katz, and R.A. Lazzarini (1994) Age-associated and cell-type-specific neurofibrillary pathology in transgenic mice expressing the human mid-sized neurofilament subunit. J. Neurosci. *14:*5603-5612.

Vickers, J.C., R.A. Schumer, S.M. Podos, R.F. Wang, B.M. Riederer, and J.H. Morrison (1995b) Differential vulnerability of neurochemically identified subpopulations of retinal neurons in a monkey model of glaucoma. Brain Res. *680:*23-35.

Virgo, L., S. Samarasinghe, and J. de Belleroche (1996) Analysis of AMPA receptor subunit mRNA expression in control and ALS spinal cord. NeuroReport *7:*2507-2511.

Vissavajjhala, P., W.G.M. Janssen, Y. Hu, A.H. Gazzaley, T. Moran, P.R. Hof, and J.H. Morrison (1996) Synaptic distribution of the AMPA-GluR2 subunit and its colocalization with calcium-binding proteins in rat cerebral cortex: An immunohistochemical study using a GluR2-specific monoclonal antibody. Exp. Neurol. *142:*296-312.

Volterra, A., D. Trotti, C. Tromba, S. Floridi, and G. Racagni (1994) Glutamate uptake inhibition by oxygen free radicals in rat cortical astrocytes. J. Neurosci. *14:*2924-2932.

Wang, G.J., R.D. Randall, and S.A. Thayer (1994a) Glutamate-induced intracellular acidification of cultured hippocampal neurons demonstrates altered energy metabolism resulting from Ca^{2+} loads. J. Neurophysiol. *72:*2563-2569.

Wang, S., A. Hamberger, Q. Yang, and K.G. Haglid (1994b) Changes in neurofilament protein NF-L and NF-H immunoreactivity following kainic acid-induced seizures. J. Neurochem. *62:*739-748.

Weiss, J.H., and D.W. Choi (1991) Slow non-NMDA receptor mediated neurotoxicity and amyotrophic lateral sclerosis. In L. P. Rowland (eds): Amyotrophic Lateral Sclerosis and Other Motor Neuron Diseases. Raven Press, Ltd., pp. 311-318.

Werth, J.L., and S.A. Thayer (1994) Mitochondria buffer physiological calcium loads in cultured rat dorsal root ganglion neurons. J. Neurosci. *14:*348-356.

West, M.J. (1993) New stereological methods for counting neurons. Neurobiol. Aging *14:*275-285.

West, M.J., L. Slomianka, and H.J.G. Gundersen (1991) Unbiased stereological estimation of the total number of neurons in the subdivisions of the rat hippocampus using the optical fractionator. Anat. Rec. *231:*482-497.

White, R.J., and I.J. Reynolds (1995) Mitochondria and Na^{+}/Ca^{2+} exchange buffer glutamate-induced calcium loads in cultured cortical neurons. J. Neurosci. *15:*1318-1328.

Wiedau-Pazos, M., J.J. Goto, S. Rabizadeh, E.B. Gralla, J.A. Roe, M.K. Lee, J.S. Valentine, and D.E. Bredesen (1996) Altered reactivity of superoxide dismutase in familial amyotrophic lateral sclerosis. Science *271:*515-518.

Williams, T.L., N.C. Day, P.G. Ince, R.K. Kamboj, and P.J. Shaw (1997) Calcium-permeable amino-3-hydroxy-5-methyl-4-isoxazole propionic acid receptors: A molecular determinant of selective vulnerability in amyotrophic lateral sclerosis. Ann. Neurol. *42:*200-207.

Williams, T.L., P.G. Ince, A.E. Oakley, and P.J. Shaw (1996) An immunocytochemical study of the distribution of AMPA selective glutamate receptor subunits in the normal human motor system. Neuroscience *74:*185-198.

Williamson, T.L., L.I. Bruijn, K. Anderson, J.-P. Julien, and D.W. Cleveland (1997) Are neurofilaments necessary for the pathogenesis of SOD1 mediated ALS in mice? Soc. Neurosci. Abstr. *23:*870.3.

Wong, P.C., C.A. Pardo, D.R. Borchelt, M.K. Lee, N.G. Copeland, N.A. Jenkins, S.S. Sisodia, D.W. Cleveland, and D.L. Price (1995) An adverse property of a familial ALS-linked SOD1 mutation causes motor neuron disease characterized by vacuolar degeneration of mitochondria. Neuron *14:*1105-1116.

Xu, Z., L.C. Cork, J.W. Griffin, and D.W. Cleveland (1993) Increased expression of neurofilament subunit NF-L produces morphological alterations that resemble the pathology of human motor neuron disease. Cell *73:*23-33.

Yamasaki, H., G.S. Bennett, C. Itakura, and M. Mizutani (1992) Defective expression of neurofilament protein subunits in hereditary hypotrophic axonopathy of quail. Lab. Invest. *66:*734-743.

Yim, M.B., P.B. Chock, and E.R. Stadtman (1990) Copper, zinc superoxide dismutase catalyzes hydroxyl radical production from hydrogen peroxide. Proc. Natl. Acad. Sci. USA *87:*5006-5010.

Yim, M.B., J.-H. Kang, H.-S. Yim, H.-S. Kwak, P.B. Chock, and E.R. Stadtman (1996) A gain-of-function of an amyotrophic lateral sclerosis-associated Cu,Zn-superoxide dismutase mutant: An enhancement of free radical formation due to a decrease in Km for hydrogen peroxide. Proc. Natl. Acad. Sci. USA *93:*5709-5714.

Young, W.G., E.A. Nimchinsky, P.R. Hof, F.E. Bloom, and J.H. Morrison (1995) NeuroZoom: Computer software for quantitative neuroanatomic mapping and stereology. Soc. Neurosci. Abstr. *19:*1078.

Zhang, B., P.-H. Tu, F. Abtahian, J.Q. Trojanowski, and V.M.-Y. Lee (1997) Neurofilaments and orthograde transport are reduced in ventral root axons of transgenic mice that express human SOD1 with a G93A mutation. J. Cell Biol. *139:*1307-1315.

IMAGE EVALUATION TEST TARGET (QA-3)

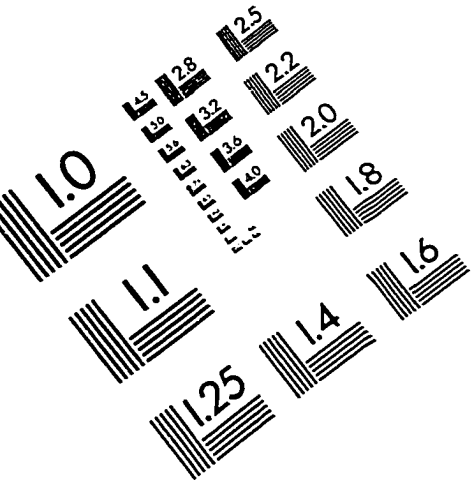

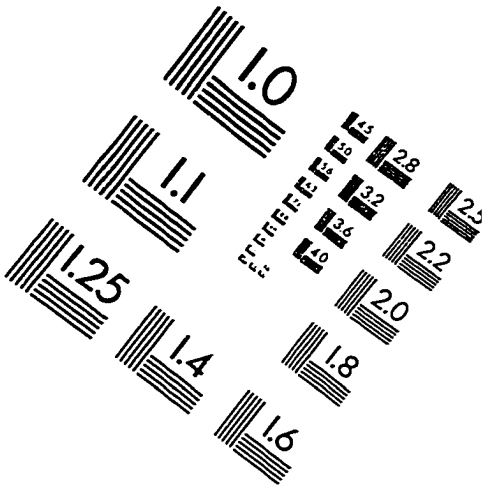

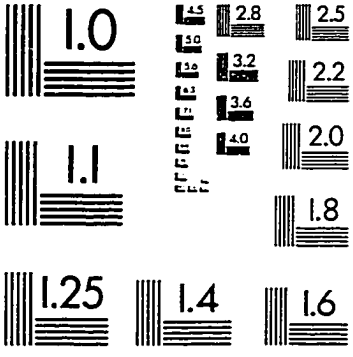

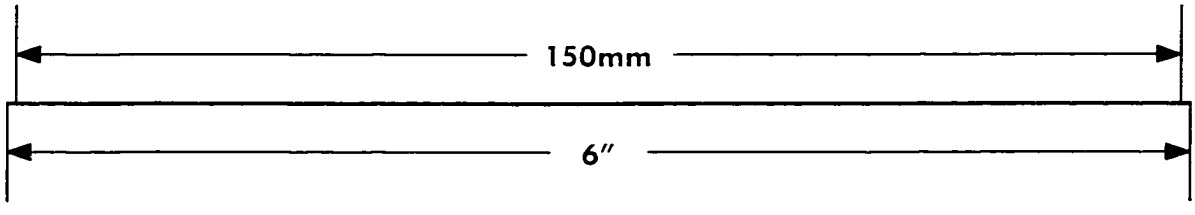

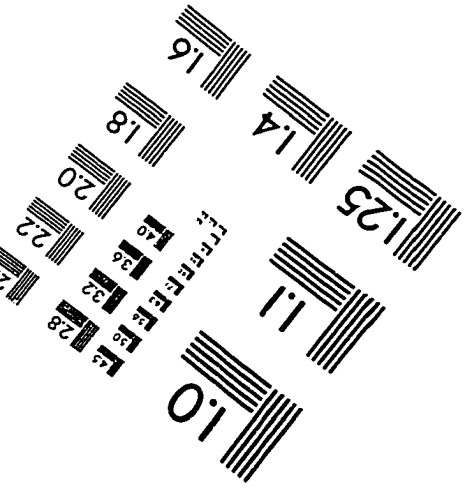

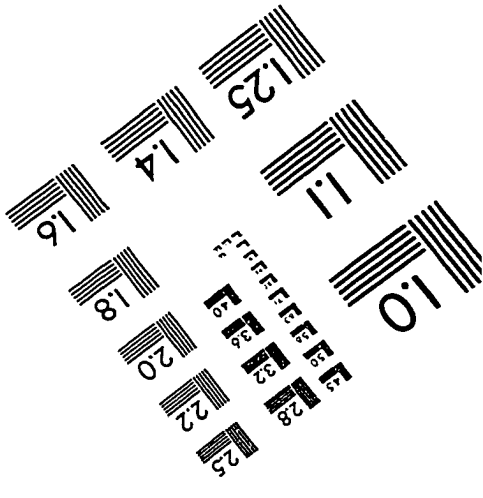

APPLIED IMAGE, Inc
1653 East Main Street
Rochester, NY 14609 USA
Phone: 716/482-0300
Fax: 716/288-5989